

STUDY OF HIGHLY EFFICIENT CORROSION INHIBITORS FOR METALS

THESIS

Submitted in fulfillment of the requirement of degree of

DOCTOR OF PHILOSOPHY

to

The Faculty of Sciences

by

RAJNI NARANG

(Registration No.: 19-YMCA-901003)

Under the Supervision of

Dr. BINDU MANGLA



Department of Chemistry

J.C. Bose University of Science and Technology, YMCA, Faridabad
Sec-6, Mathura Road, Faridabad-121006, Haryana, INDIA

April 2024

DEDICATION

In humble reverence and profound gratitude, I dedicate this thesis to God, the source of all wisdom, inspiration, and strength. Through every challenge and triumph, His guidance has been my steadfast compass, His grace has been my unfailing source of hope. His mercy has always been my unwavering wellspring of optimism. May this work be a testament to His divine wisdom and a reflection of the gifts He has bestowed upon me.

CANDIDATE DECLARATION

I hereby declare that this thesis entitled **STUDY OF HIGHLY EFFICIENT CORROSION INHIBITORS FOR METALS** by **RAJNI NARANG**, being submitted in fulfillment of the requirements for the Degree of Doctor of Philosophy in **CHEMISTRY** under Faculty of Sciences of J.C Bose University of Science & Technology, YMCA Faridabad during the academic year 2023-24, is a bonafide record of my original work carried out under guidance and supervision of **Dr. BINDU MANGLA, ASSOCIATE PROFESSOR, CHEMISTRY** and has not been presented elsewhere.

I further declare that the thesis does not contain any part of any work which has been submitted for the award of any degree either in this university or in any other university.

(Rajni Narang)

Registration No.- 19-YMCA-901003

CERTIFICATE

This is to certify that this Thesis entitled **STUDY OF HIGHLY EFFICIENT CORROSION INHIBITORS FOR METALS** by **RAJNI NARANG**, submitted in fulfillment of the requirement for the Degree of Doctor of Philosophy in **CHEMISTRY** under Faculty of Sciences, J. C Bose University of Science & Technology, YMCA, Faridabad during the academic year 2023-24, is a bonafide record of work carried out under my guidance and supervision.

I further declare that to the best of my knowledge, the thesis does not contain any part of any work which has been submitted for the award of any degree either in this university or in any other university.

Dr. Bindu Mangla
Associate Professor
Department of Chemistry
Faculty of Sciences
J.C. Bose University of Science and Technology, YMCA
Faridabad, Haryana

Dated:

Acknowledgments

First of all, I want to express special debt of gratitude to my supervisor, **Dr. Bindu Mangla**, whose unwavering guidance, mentorship, and scholarly expertise have been the cornerstones of my academic journey. Her commitment to my growth as a researcher has been a profound influence on my work.

I wish to express my gratitude to Prof. Sushil Kumar, Vice Chancellor for the visionary leadership and commitment to academic excellence at JC Bose University. His dedication to providing resources and opportunities for scholarly endeavors has been a driving force behind my academic growth. I am deeply honored to have been a part of JC Bose University, an institution that has provided me with the platform and resources to pursue knowledge and innovation.

I would like to acknowledge the diligent lab staff at CIL, JC Bose University, for their technical expertise and support. Your assistance ensured the smooth execution of experiments and contributed significantly to the quality of my research.

I am indebted to research scholars especially Priya Vasishisth, Himanshi Bairagi and Rashmi whose insightful discussions, feedback, and diverse perspectives have shaped the depth and breadth of my research. Their willingness to engage in intellectual exchanges has been a source of inspiration.

I owe my deep sense of gratitude to my husband, Mr. Manish Sachdeva, for his valuable suggestions and co-operation during the course of work. I extend my heartfelt appreciation to my dear son and daughter, who dedicated their childhood years to support my research endeavors. I would be failing in my duty if I do not express my deep sense of regards to my parents, my brothers, my sisters, my in-laws for their constant co-operation, moral and emotional support they provided me during many stressful and demanding time.

I would also like to extend my appreciation to my colleagues and friends for their unwavering support, encouragement, and belief in my abilities throughout this challenging journey.

I cannot finish without acknowledging the omnipresent and omnipotent, who guided me in my life's journey. Thank you, Dear Lord.

(Rajni Narang)

Registration No. 19-YMCA-901003

ABSTRACT

The inhibitory performance of an antibiotic drug in 0.5 M H₂SO₄ and psychotherapeutic drugs in 1M HCl for mild steel protection has been investigated in the temperature range of 303K-333K and variable concentration range by using gravimetric studies, linear polarization studies, potentiodynamic measurements, electrochemical impedance studies and atomic force microscopic studies. The inhibition efficiency was found to increase with increase in concentration of the drug and decreased with increase in temperature whereas corrosion rate was decreased with increase in drug concentration and increased with increase in temperature. The thermodynamic, kinetic and adsorption parameters were evaluated using weight loss method. Change in enthalpy(ΔH) of corrosion process for all concentrations was found to be positive at all temperatures for all the experimental drugs indicating endothermic nature of corrosion process. Free energy Change (ΔG) values for corrosion phenomenon was found to be positive indicating instability of activation complex formed during corrosion process. Langmuir adsorption isotherm was followed and revealed adsorption of inhibitor as monolayer on mild steel surface for all the drugs. Adsorption of inhibitor on mild steel was physisorption or chemisorption depending upon ΔG_{ads} as computed from Langmuir adsorption isotherm. All the experimental drugs showed physical as well as chemical adsorption on metal surface. Polarization resistance was increased and corrosion current was decreased with increase in concentration for all the drugs which shows effectiveness of drugs for protecting metal. As per the electrochemical impedance spectroscopy data, the charge transfer resistance (R_{ct}) increased with a rise in inhibitor concentration, indicating a decrease in charge transfer between metal and aggressive medium thereby showing decrease in corrosion rate. Increases in drug concentration resulted in a drop in double layer capacitance (C_{dl}), which may have been caused by increases in the thickness of the double layer showing the adsorption of drug on the mild steel surface. The results obtained from potentiodynamic polarization analysis (Tafel plot) demonstrated that all the studied corrosion inhibitors function as mixed type inhibitors. It shows inhibition of corrosion has occurred at cathodic as well as anodic site. Surface roughness reduction of mild steel after application of inhibitor as calculated from Atomic Force Microscope indicates effectiveness of the drug in inhibiting the corrosion. Quantum chemical analysis was done to compute energy of highest occupied molecular orbital (HOMO), energy of lowest molecular orbital (LUMO), ionization energy(I), electron affinity(A), fraction of transferred electrons(ΔN), dipole moment (μ), electronegativity(χ) and global hardness(h). The study helped to examine how the molecular structure of each corrosion inhibitor influenced the percentage of inhibition efficiency and values obtained from theoretical calculations were in agreement with experiment results. The study revealed strong interaction between metal and inhibitor molecule via chemical adsorption by donation of

electron from inhibitor to mild steel.

Four drugs (Ethambutol, Sertraline, Paroxetine and Escitalopram) were recognized as effective corrosion inhibitors owing to the presence of heteroatoms and pi electrons and donation of electrons occurred from inhibitor to vacant orbital of metal thereby forming strong interaction among them as protective coating of inhibitor was developed over the surface of mild steel. Among four inhibitors, inhibition efficiency was found to be maximum for Paroxetine due to presence of large number of heteroatoms along with aromatic ring.

LIST OF ABBREVIATIONS

Arrhenius Pre Exponential Factor	A
Double Layer Capacitance	C_{dl}
Concentration	Conc.
Common Phase Element	CPE
Corrosion Rate	Cr
Density	D
Activation Energy of Corrosion	E_a
Ethambutol	EBT
Corrosion Potential	E_{corr}
Escitalopram	EST
Fourier Transform Infrared	FTIR
Plank's Constant	h
Corrosion current Density	I_{corr}
Inhibition Efficiency	IE
mils per year	mpy
Avogadro's Number	N
Paroxetine	PAX
parts per million	ppm
Universal Gas Constant	R
Polarization Resistance	R_p
Solution Resistance	R_s
Sertraline	SRT
Time	t
Absolute Temperature	T
Impedance of the AC Circuit	Z
Anodic Tafel Slope	β_a
Cathodic Tafel Slope	β_c
Free Energy of Adsorption	ΔG_{ads}
Enthalpy Of Activation	ΔH
Entropy Of Activation	ΔS
Angular Frequency	ω
Adsorption Constant	K_{ads}

CONTENTS

Dedication	ii
Declaration	iii
Certificate	iv
Acknowledgements	v
Abstract	vi
Abbreviation	viii
List of Tables	xiii
List of Figures	xv
1 INTRODUCTION AND LITERATURE REVIEW	1
1.1 Overview of Corrosion	1
1.2 Educational pursuit	2
1.2.1 Material loss	3
1.2.2 Economic Loss	3
1.2.3 Impact on Environment	3
1.2.4 Human life and safety	4
1.3 Factors influencing the rate of corrosion	4
1.3.1 Nature of metal	4
1.3.2 Nature of Environment	6
1.4 Mechanism/Electrochemical Theory of Corrosion	6
1.5 Types of Corrosion	8
1.5.1 Intergranular Corrosion	8
1.5.2 Concentration cell corrosion	9
1.5.3 Crevice Corrosion	9
1.5.4 Pitting Corrosion	10
1.5.5 Selective Corrosion	10
1.5.6 Erosion Corrosion	11

1.5.7	Cavitation Corrosion	11
1.5.8	Stress Corrosion	12
1.6	Approaches to inhibit or control the corrosion	13
1.6.1	Corrosion inhibitors	13
1.6.2	Organic and Inorganic Compounds as Corrosion Inhibitors	18
1.6.3	Natural/Green Inhibitors	19
1.6.4	Nanomaterials as Inhibitors	19
1.6.5	Drugs as corrosion inhibitors	20
1.7	Different Variety of Drugs as Corrosion Inhibitor	21
1.7.1	Corrosion protection by analgesic drugs	21
1.7.2	Corrosion protection by Antibiotic drugs	21
1.7.3	Corrosion protection by Antihistamine drugs	25
1.7.4	Corrosion protection by antipyretic drugs	26
1.7.5	Corrosion protection by antidepressant /Psychotherapeutic drugs	26
1.8	General Mechanism of action of Drug inhibitor	27
1.9	Considerations to apply drugs as corrosion inhibitors	28
1.9.1	Selection of material for the study	29
1.9.2	Selection of Acids for the Study	29
1.10	Objectives of the study	29
1.11	Methodology adopted	30
1.11.1	Weight loss method	30
1.11.2	Electrochemical study	31
1.11.3	Quantum Chemical Study	32
1.11.4	Surface study	33
2	Anti-Tuberculosis Drug Ethambutol as Effective Corrosion Inhibitor	35
2.1	Introduction	35
2.2	Experimental and Methods	37
2.2.1	Preparation of metal sample and test solutions	37
2.2.2	Weight Loss Study	38
2.2.3	Electrochemical Study	38
2.2.4	Quantum Chemical Study	39
2.2.5	Surface Study	40
2.3	Result and Discussions	40
2.3.1	Characterization	40
2.3.2	Weight Loss Study	41
2.3.3	Electrochemical Study	48
2.3.4	Quantum Chemical Study	51

2.3.5	Surface Study: Atomic Force Microscopy (AFM)	53
2.4	Mechanism of Inhibition	54
2.5	Conclusion	54
3	Antidepressant drug Sertraline as an Efficient Corrosion Inhibitor for Mild Steel	56
3.1	Introduction	56
3.2	Experimental and Methods	58
3.2.1	Preparation of metal sample and test solution	58
3.2.2	Weight Loss Study	58
3.2.3	Electrochemical Study	59
3.2.4	Quantum Chemical Study	60
3.2.5	Surface Study	61
3.3	Results and Discussion	61
3.3.1	Characterization	61
3.3.2	Weight Loss Study	62
3.3.3	Electrochemical Study	68
3.3.4	Quantum Chemical Study	72
3.3.5	Surface Study: Atomic Force Microscopy (AFM)	74
3.4	Mechanism of Inhibition	74
3.5	Conclusion	75
4	Anti-depressant drug Paroxetine as efficient corrosion inhibitor for mild steel	77
4.1	Introduction	77
4.2	Experimental and Methods	79
4.2.1	Preparation of metal sample and test solutions	79
4.2.2	Weight Loss Study	79
4.2.3	Electrochemical Study	80
4.2.4	Quantum Chemical Study	81
4.2.5	Surface Study	82
4.3	Result and Discussions	82
4.3.1	Characterization	82
4.3.2	Weight Loss Study	83
4.3.3	Electrochemical Study	89
4.3.4	Surface Study: Atomic Force Microscope (AFM)	93
4.3.5	Quantum Chemical Study	94
4.4	Mechanism of Inhibition	96
4.5	Conclusion	97

5	Anti-depressant drug Escitalopram as efficient corrosion inhibitor for mild steel	98
5.1	Introduction	98
5.2	Experimental and Methods	100
5.2.1	Preparation of metal sample and test solutions	100
5.2.2	Weight Loss Study	101
5.2.3	Electrochemical Study	101
5.2.4	Quantum Chemical Study	102
5.2.5	Surface Study	103
5.3	Result and Discussions	103
5.3.1	Characterization	103
5.3.2	Weight Loss Study	104
5.3.3	Electrochemical Study	111
5.3.4	Quantum Chemical Study	115
5.3.5	Surface Study: Atomic Force Microscopy (AFM)	118
5.4	Mechanism of inhibiton	119
5.5	Conclusion	120
6	Conclusion	122
	Publications	128
	References	131

LIST OF TABLES

1.1	Analgesic drugs for the protection of various metals in various media . . .	22
1.2	Antibiotic drugs for the protection of various metals in various media . . .	22
1.3	Anti-histamine drugs for the protection of various metals in various media.	25
1.4	Antipyretic drugs for the protection of various metals in various media . . .	26
1.5	Antidepressant drugs for the protection of various metals in various media	27
2.1	IE, C_r , and θ of EBT with mild steel at 303K and 313K temperature with different concentration range	43
2.2	IE, C_r , and θ of EBT with mild steel at 323K and 333K temperature with different concentration range	43
2.3	Kinetic and Thermodynamic parameters of EBT with MS at different temperatures and inhibitor concentration range	44
2.4	EBT Langmuir adsorption isotherm parameters at 303-333 K.	47
2.5	Linear polarization resistance variables of MS with EBT in 0.5M H ₂ SO ₄	48
2.6	Tafel polarization variables of MS with EBT in 0.5M H ₂ SO ₄	49
2.7	EIS Parameters for Mild Steel with EBT in 0.5M H ₂ SO ₄	51
2.8	Quantum Chemical parameters for EBT	52
3.1	IE, C_r , and θ of Sertraline with mild steel at 303K and 313K temperature with different concentration range	63
3.2	IE, C_r , and θ of Sertraline with mild steel at 323K and 333K temperature with different concentration range	64
3.3	Activation and thermodynamic parameters of corrosion in different sertraline concentrations in 1 M HCl	65
3.4	Free energy of activation of Sertraline with MS at different temperatures and inhibitor concentration range	65
3.5	Parameters of adsorption computed from Langmuir isotherm of adsorption	67
3.6	Linear polarization resistance variables of mild steel in blank and in the presence of Sertraline inhibitor at various concentrations in 1 M HCl.	68
3.7	Tafel polarization parameters of mild steel in the presence of Sertraline in 1M HCl	69

3.8	Electrochemical Impedance Variables of Mild Steel in blank and in presence of variable concentrations of Sertraline in 1M HCl	72
3.9	Quantum Chemical parameters for Sertraline	73
4.1	IE, C_r , and θ of Paroxetine with mild steel at 303K and 313K temperature with different concentration range	85
4.2	IE, C_r , and θ of Paroxetine with mild steel at 323K and 33K temperature with different concentration range	85
4.3	Kinetic and Thermodynamic parameters of Paroxetine with MS at different temperatures and inhibitor concentration range	86
4.4	Parameters of adsorption computed from Langmuir isotherm of adsorption	89
4.5	Linear polarization resistance data for mild steel in blank and in the presence of Paroxetine inhibitor at various concentrations.	89
4.6	Tafel polarization parameters of mild steel in the presence of Paroxetine in 1M HCl.	90
4.7	Electrochemical Impedance Variables of Mild Steel in blank and in presence of variable concentrations of Paroxetine	92
4.8	Quantum Chemical parameters for Paroxetine for gas and aqueous phase	94
4.9	Mulliken Charges for gas(g) and aqueous phase(aq) Paroxetine	95
5.1	IE, C_r , and θ of Escitalopram with mild steel at 303K and 313K temperature with different concentration range	106
5.2	IE, C_r , and θ of Escitalopram with mild steel at 323K and 333K temperature with different concentration range	106
5.3	Kinetic and Thermodynamic parameters of Escitalopram with MS at different temperatures and inhibitor concentration range	107
5.4	Parameters of adsorption as computed from Langmuir isotherm of adsorption.	111
5.5	Linear polarization resistance characteristics of mild steel with Escitalopram.	112
5.6	Tafel polarization characteristics of mild steel when exposed to Escitalopram in a 1M HCl environment	113
5.7	EIS Characteristics of Mild Steel in the varying concentrations of Escitalopram	115
5.8	Quantum Chemical parameters for Escitalopram for gas and aqueous phase	116
5.9	Mulliken Charges for gas(g) and aqueous phase(aq) Escitalopram.	118
6.1	Effectiveness of experimental drugs against corrosion	125

LIST OF FIGURES

1.1	Corrosion and Extraction of metal	2
1.2	Corrosion Effects	2
1.3	Factors influencing the rate of corrosion	5
1.4	Corrosion Mechanism	8
1.5	Intergranular Corrosion	8
1.6	Concentration Cell Corrosion	9
1.7	Crevice Corrosion	10
1.8	Pitting Corrosion	10
1.9	Selective Corrosion	11
1.10	Erosion Corrosion	11
1.11	Cavitation Corrosion	12
1.12	Stress Corrosion	12
1.13	Different Corrosion Prevention Methods	13
1.14	Different Classification of Corrosion Inhibitor	14
1.15	Types of Corrosion Inhibitors on the basis of electrochemical reaction	15
1.16	Types of Corrosion Inhibitors on the basis of Application	16
1.17	Different types of Corrosion Inhibitor	18
1.18	Mechanism of Adsorption of Inhibitor	28
1.19	System for Quantum Chemical Study	33
1.20	Bruker Atomic Force Microscope	33
2.1	Structural information of EBT	37
2.2	FT-IR spectrum of EBT	41
2.3	Rate of Corrosion of MS in 0.5M H ₂ SO ₄ with 200-1000 ppm of EBT at 303-333 K	42
2.4	IE of EBT against MS in 0.5M H ₂ SO ₄ at 303-333K with 200-1000 ppm of EBT	42
2.5	Arrhenius plot: log C _r vs $\frac{1}{T}$ at varying EBT concentrations.	44
2.6	Plot of log C _r /T vs 1/T at different concentrations of EBT	45
2.7	Plot of activation parameters, E _a and ΔH vs. concentration of EBT	46
2.8	Langmuir adsorption isotherm for EBT.	47

2.9	Curves of Potentiodynamic polarization for MS in 0.5M H ₂ SO ₄ solution with 200-1000 ppm of EBT	49
2.10	Nyquist plots for MS in 0.5M H ₂ SO ₄ solution containing 200-1000 ppm of EBT	50
2.11	Equivalent Circuit Scheme	50
2.12	Optimized Structure(a) and the corresponding HOMO (b) and LUMO (c) for EBT	52
2.13	(a) & (b) are 2D, 3D images of polished metal (reference); (c) & (d) are 2D, 3D images of MS surface immersed in 0.5M H ₂ SO ₄ (blank); (e) & (f) are 2D, 3D images of MS immersed in 0.5M H ₂ SO ₄ with EBT	53
3.1	Structural information of Sertraline	57
3.2	FT-IR Spectrum of SRT	62
3.3	Corrosion Rate (mpy) of mild steel surface in 1 M HCl at 10-50ppm concentration of SRT and 303-333K temperature	62
3.4	Inhibition efficiency (%) of mild steel surface in 1 M HCl at 10-50ppm concentration and 303-333K temperature	63
3.5	Arrhenius Plot in blank and with different concentrations of SRT in 1 M HCl for mild steel corrosion.	64
3.6	Transition state plot in blank and with different concentrations of Sertraline in 1 M HCl for mild steel corrosion.	65
3.7	SRT adsorption on mild steel surface using the Langmuir isotherm in 1 M HCl	67
3.8	Tafel plot for mild steel in 1N HCl solution containing various Concentrations of SRT	69
3.9	Nyquist plot of the EIS for mild steel in 1M HCl solution containing various concentrations of SRT	70
3.10	Equivalent Circuit model of the EIS for mild steel in 1M HCl solution containing various concentrations of SRT	71
3.11	Optimized Structure(a) and the corresponding HOMO(b) and LUMO(c) for SRT	73
3.12	(a) & (b) - 2D and 3D scan of reference material (polished metal), (c) & (d) - 2D and 3D scan of 1M HCl immersed metal surface (blank), (e) & (f) - 2D and 3D scan of 50 ppm SRT in 1 M HCl immersed metal surface.	74
4.1	Structural information of Paroxetine	78
4.2	UV spectrum of Paroxetine	82
4.3	FT-IR spectrum of Paroxetine	83
4.4	Effect of Paroxetine concentration on rate of corrosion of mild steel in 1 M HCl at various temperatures (303-333K).	84

4.5	Inhibition Efficiency of Paroxetine versus concentrations (5-20 ppm) at different temperatures	84
4.6	Arrhenius Plot in blank and with different concentrations of Paroxetine in 1 M HCl for mild steel corrosion.	86
4.7	Transition state plot in blank and with different concentrations of Paroxetine in 1 M HCl for mild steel corrosion.	87
4.8	Variation of activation energy and enthalpy versus concentration of Paroxetine	87
4.9	Adsorption isotherm of drug Paroxetine on mild steel surface in 1 M HCl at various temperatures.	88
4.10	Tafel plot for mild steel in 1M HCl solution containing various Concentrations of Paroxetine	90
4.11	Nyquist plots for mild steel in 1M HCl solution with various concentrations of Paroxetine	91
4.12	Equivalent Circuit Model of the EIS	92
4.13	(a) and (b) are 2D and 3D scan of polished metal (reference), (c) and (d) are 2D and 3D scan of MS surface immersed in 1 M HCl (blank), (e) and (f) are 2D and 3D scan of MS immersed in 20 ppm Paroxetine in 1 M HCl.	93
4.14	Optimized Structure and the corresponding HOMO and LUMO for Paroxetine in Gas (a,c,e) and Aqueous phase (b,d,f)	95
5.1	Structural information of Escitalopram	99
5.2	UV spectrum of Escitalopram	104
5.3	FT-IR Spectrum of Escitalopram	104
5.4	Rate of Corrosion of MS in 1M HCl with 5-20 ppm of EST at 303-333K	105
5.5	Inhibition Efficiency of Escitalopram for mild steel protection in 1 M HCl at 303-333K with 5-20 ppm of EST.	105
5.6	Arrhenius plot for $\log C_r$ vs $1/T$ for mild steel variable concentrations of Escitalopram.	107
5.7	Transition state plot for mild steel protection in blank and at variable concentrations of Escitalopram in 1 M HCl.	108
5.8	Variation of activation energy and enthalpy versus concentration of Escitalopram.	109
5.9	Langmuir Isotherm of adsorption for Escitalopram.	110
5.10	Tafel graph depicting mild steel in a 1M HCl with varying concentration of Escitalopram.	113
5.11	Nyquist Diagrams depicting mild steel in a 1 M HCl with varying concentration of Escitalopram.	114

5.12	Equivalent Circuit model of the EIS	114
5.13	Optimized Structure and the corresponding HOMO and LUMO for Escitalopram in the Gas phase (a, c, e) and Aqueous phase (b, d, f).	117
5.14	(a) & (b) are 2D and 3D scan of polished metal (reference), (c) & (d) are 2D and 3D scan of MS surface immersed in 1 M HCl(blank), (e) & (f) are 2D and 3D scan of MS immersed in 20 ppm Escitalopram in 1 M HCl	119
6.1	Plot showing % Inhibition efficiency versus drug used under study . . .	125

CHAPTER 1

INTRODUCTION AND LITERATURE REVIEW

1.1 OVERVIEW OF CORROSION

Advanced materials science offers a wide array of construction materials, encompassing metals, alloys, plastics, ceramics, wood, and more. While many metals commonly employed in construction may initially appear to possess remarkable strength, it is important to recognize that, except noble metals, they are inherently chemically unstable when exposed to various environmental conditions. In practically every environment where metals find application, the feasibility of their use in buildings, bridges, and other applications depends on protective measures. In certain metal-environment systems, metals achieve protection through passivation, while in others, the metallic surface remains active, necessitating the implementation of appropriate design strategies. This is especially relevant in the case of mild steels, which represent a cost economical and versatile metallic material. Corrosion refers to the degradation and consequent loss of solid materials due to exposure to chemical or electrochemical surrounding[1]. This process is the opposite of metal extraction (Figure 1.1). Initially, metal exists as minerals or ores, maintaining a stable state according to thermodynamics. Metallurgical processes transform it into metal, causing it to become thermodynamically unstable as it stores a significant amount of energy. When metal interacts with a compatible environment, it forms corresponding oxides, carbonates, sulfates, or sulfides, achieving a state of stability. This occurrence is irreversible. The prevalent form of corrosion seen in iron is rusting. While the methodology may appear elementary, it is essential to recognize that the manifestations and impacts of this response exhibit significant variation when applied to different metals in diverse environmental conditions. Metals and their alloys represent the foremost applicant materials for construction and manufacturing endeavors, thus interpreting the issue of material deterioration due to corrosion as a global concern of supreme importance. The corrosion-induced degradation of these metals entails the deterioration of their mechanical properties, resulting in substantial material losses. The economic toll exacted by corrosion is indeed substantial and exerts a pronounced impact on national economies. To safeguard the economic stability and industrial progress of nations, corrosion protection has emerged as a dynamically

evolving field of research, witnessing concerted efforts aimed at thwarting corrosion.

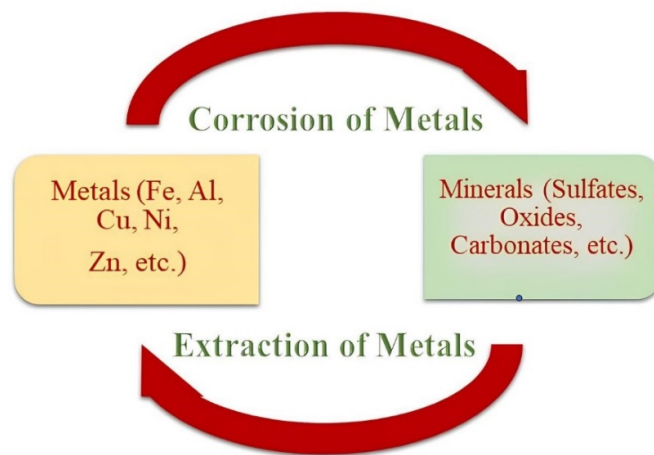


Figure 1.1: Corrosion and Extraction of metal

Despite the extensive body of research dedicated to comprehending the multifaceted facets of corrosion, numerous practical scenarios involving metal degradation remain subjects of contention and unresolved inquiries. Consequently, substantial research endeavors are currently directed toward the comprehensive investigation of the corrosion process and the enhancement of materials' durability.

1.2 EDUCATIONAL PURSUIT

Corrosion causes several problems related to economic loss, material conservation, human life and safety, and environmental safety and this forms the basis for the study of corrosion and its methods of prevention (Figure 1.2).

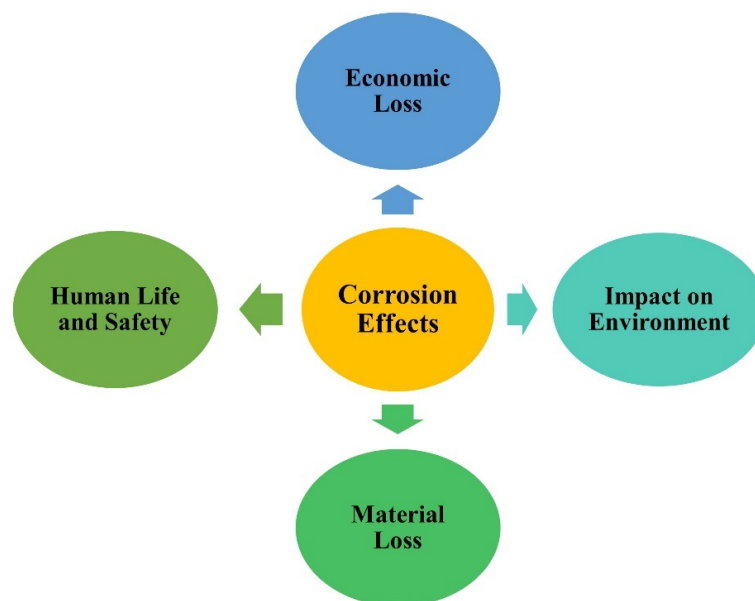


Figure 1.2: Corrosion Effects

1.2.1 Material loss

Corrosion leads to significant material loss, causing a reduction in mechanical strength and thinning of materials, ultimately leading to the failure of machines. It damages electronic equipment, buildings, bridges, and monuments. Monuments and statues which are tourist attractions, are susceptible to environmental attacks, leading to substantial deterioration, and eventually, they lose their original appearance. Damage to a turbine engine occurred in England and a large amount of crude oil spilled in California due to corrosion cracks in 2015[2].

1.2.2 Economic Loss

Corrosion incurs substantial expenses and significantly impacts the economies of nations. The costs associated with corrosion can be categorized as direct or indirect. Direct costs encompass infrastructure, utilities, transportation, production, and manufacturing. On the other hand, indirect costs consist of expenses related to labor involved in corrosion management, the equipment required to address corrosion-related issues, and the revenue loss due to disruptions in product supply[3]. As per estimates, the cost of corrosion globally is US\$2.5 trillion, or 3.4% of the global GDP (2013). It is more than Rs. 2.0 lakh crores per annum in India[4]. In the United States alone, corrosion generates a direct cost of about \$276 billion annually, equivalent to 3.1% of the nation's gross domestic product (GDP). When factoring in the indirect costs, the total expense of corrosion is estimated to reach \$552 billion or potentially more. To tackle this issue and reduce corrosion-related expenses, it is crucial to employ effective corrosion inhibition methods to minimize the damage caused by corrosion[5].

1.2.3 Impact on Environment

The ecosystem is significantly harmed by corrosion. It results in the production of a variety of corrosion byproducts, including metals and chemical compounds, which pollute the air, soil, and water, producing pollution and possible risks to ecosystems and species. The quality of human drinking water may be compromised because aquatic life is particularly vulnerable. Additionally, corrosion-related failures in infrastructure, such as pipes and storage tanks, can lead to spills and leaks that disturb the natural habitats of plants and animals as well as destroy ecosystems and contaminate the soil. Corrosion also increases the amount of energy needed for industrial processes, particularly for pumping and other tasks. As a result of this increased energy use, greenhouse gas emissions have increased.

1.2.4 Human life and safety

Due to its impact on many industries and infrastructure, corrosion poses several risks to human life and safety. Buildings, bridges, and pipelines that have deteriorated can have structural failures. People who are inside or close to these structures may face a risk to their lives if this causes collapses. Corrosion on trains, planes, ships, and automobiles can jeopardize their mechanical systems, compromising their structural integrity, potentially resulting in injuries or fatalities. Consuming contaminated drinking water poses a health concern to consumers due to corrosion in water distribution networks. Pipelines carrying gas and oil can corrode, leading to leaks that might result in fires, explosions, and environmental concerns that could be harmful to the populations nearby. Corroded machinery can malfunction in industrial environments, causing mishaps that could damage nearby people and the employees themselves.

1.3 FACTORS INFLUENCING THE RATE OF CORROSION

The corrosivity magnitude is fundamentally contingent upon the intrinsic properties of the metals involved and the ambient conditions to which they are exposed. Key determinants include the structural attributes of the metallic substrate, the characteristics of the immediate environment, and the specific electrochemical processes transpiring at the metal-environment interface, all of which essential effect on the corrosion phenomenon. The extent of corrosion predominantly axes upon a constellation of factors elucidated in Figure 1.3 and subsequently expounded upon below.

1.3.1 Nature of metal

- i) **Position in galvanic series:** The galvanic series gives information on the electrode potential of various elements. Corrosion is more to occur in metals with negative electrode potential. For example, magnesium ($E^{\circ} = -2.37$ V) corrodes faster than iron ($E^{\circ} = -0.44$).and that's why magnesium serves as a sacrificial anode during the protection of underground iron pipes. The corrosion rate upsurges with the magnitude of the potential gap among the metals. The difference in potential give impetus for the electrochemical reaction to take place.
- ii) **Physical state:** The amount of corrosion is mostly determined by the physical condition of the deteriorating metal. Metals that are exposed to a corrosive environment and have a larger surface area tend to corrode more quickly. Powdered metal corrodes to a larger extent as a consequence of higher surface area.
- iii) **Anodic and cathodic area:** The degree of corrosion and cathodic to anodic area proportion (Z) are intimately correlated. This relationship can also be expressed as $Z = \text{cathode area}/\text{anode area}$. When Z is greater than one, the corrosion rate

intensifies since all of the electrons produced at the anode are used at the cathode. This causes the anodic reaction rate to accelerate, which in turn causes a metal's outer region to corrode more severely. Higher corrosion rates are associated with greater cathodic areas than anodic areas.

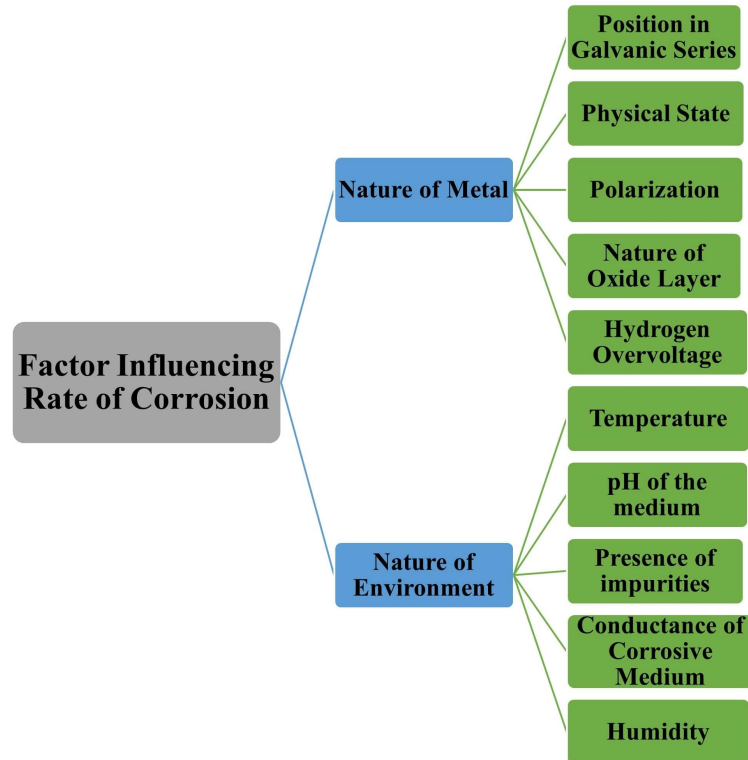


Figure 1.3: Factors influencing the rate of corrosion

- iv) **Polarization:** It is worth emphasizing that corrosion involves the simultaneous occurrence of anodic and cathodic reactions, leading to electrode polarization. The occurrence of corrosion is significantly impacted by the polarization of the cathode or anode. Introducing complexing agents near the anode or employing oxidizing substances around the cathode can diminish the impact of polarization, resulting in an accelerated corrosion rate. Depolarizers are utilized to counter the polarization effect and enhance the rate of corrosion.
- v) **Nature of protective layer formed after corrosion:** Virtually all metals develop a thin layer of metal oxide on their surfaces after corrosion when exposed to air. The volume of this oxide layer varies based on the metal's susceptibility to corrosion and the surrounding conditions. The specific volume ratio refers to the correlation between the quantities of metal oxide and the quantities of metal. In general, a higher volume ratio results in an oxide layer that is impermeable, serving as a protective barrier against corrosion. Conversely, with a lower volume ratio, this protective effect diminishes. The protective layer formed after the cor-

rosion predicts the further rate of corrosion. A stable protective layer formed over aluminum prevents its further corrosion. The formation of an unstable protective layer in noble metals does not allow the metal to corrode. A volatile layer of molybdenum dioxide formed after corrosion accelerates further corrosion.

- vi) **Hydrogen overvoltage:** As the hydrogen gas is released at the cathode, low hydrogen overvoltage metals are more at risk of corrosion.

1.3.2 Nature of Environment

- i) **Temperature:** Metal corrosion is significantly influenced by the temperature. As a result of an increase in temperature, the medium's ionization or the reaction gaining activation energy rises, speeding up the process of corrosion. A passive metal transition into an active state takes place at excessive temperatures, and corrosion accelerates with rising ambient temperature. As an illustration, let's examine the scenario of caustic brittle fracture occurring in high-pressure boilers.
- ii) **pH of the medium:** The kind of cathode process that will occur depends on the pH of the solutions. In most situations, acidic media tend to be more corrosive than alkaline/neutral media. Iron corrodes slowly until the pH of the water reaches an acidic range, but when oxygen is present, the corresponding corrosion rate increases considerably. Increasing the pH of the immediate surroundings reduces the corrosion of metals that are vulnerable to acid attack.
- iii) **Presence of impurities in the environment:** The air around industrial facilities may contain corrosive gases such as SO_2 , CO_2 , H_2S , and vapors of HCl , H_2SO_4 and other acidic gases. These gases cause a rise in the liquid concentrations, electrical conductivity, and corrosive current. In the marine atmosphere, ions make seawater more conductive and increase the rate of corrosion.
- iv) **Conductance of corrosive medium:** The internal cell resistance, which in turn depends on the conductance of the corrosive media, determines the corrosion current. In a more conductive medium, there is severe to the age of material due to corrosion.
- v) **Humidity:** Humidity gives the metal's substrate enough moisture to create conductive electrolytes and accelerate ion mobility, which speeds up the process of corrosion.

1.4 MECHANISM/ELECTROCHEMICAL THEORY OF CORROSION

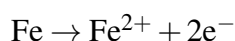
The electrochemical theory suggests that the following modification occur when a metal gets in touch with its surroundings(Figure 1.4).

- The metal's substrate forms tiny electrochemical cells with anodic and cathodic regions.
- Presence of impurities within the metallic substance create anodic and cathodic zones.
- The anode experiences oxidation, while the cathode undergoes reduction.
- Consequently, the anode corrodes, whereas the cathode remains unaffected.

At the anode, a process of oxidation occurs, where metals are transformed into metal

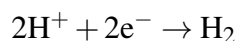


In the case of iron (Fe):

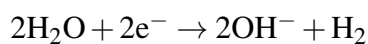


At the cathode, reduction reactions take place by different ways, under different conditions:

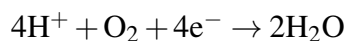
Case i) In an acidic medium and lack of oxygen:



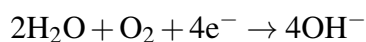
Case ii) In neutral and alkaline medium and absence of oxygen:



Case iii) In an acidic medium and presence of oxygen:



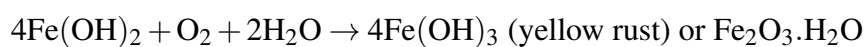
Case iv) In the neutral and alkaline medium and the presence of oxygen:



In general, Fe^{2+} from the anode and OH^{-} from the cathode diffuse and react to form $2\text{Fe}(\text{OH})_2$ as precipitate



In the excess of oxygen $2\text{Fe}(\text{OH})_3$ is formed



In a limited supply of oxygen black anhydrous magnetite (Fe_3O_4) is formed. The acidic solutions, particularly HCl and H_2SO_4 are used for pickling and etching processes, particularly corrosive and pose challenges when they come into contact with MS (mild steel). When equipment or apparatus are exposed to these corrosive media, they are susceptible to damage and lead to reduced efficiency and decreased lifespan of the original metal as a consequence of corrosion.

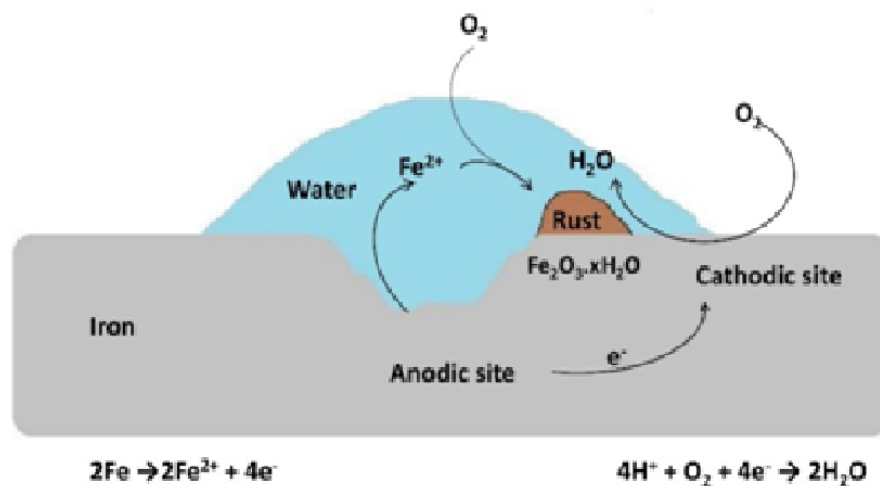


Figure 1.4: Corrosion Mechanism

1.5 TYPES OF CORROSION

There are various types of degradation in different environments which are given below

1.5.1 Intergranular Corrosion

It is a kind of localized degradation that mostly attacks nearby regions or grain borders, with only mild or no assault on the grains (Figure 1.5).



Figure 1.5: Intergranular Corrosion

Passive alloys subjected to certain aggressive environments experience the same

type of localized degradation as in other types corrosion. Intergranular corrosion occurs when certain metals and alloys attain high temperatures during heat treatment or welding. The intergranular corrosion in austenitic stainless steel 316L was determined with the use of electrolytic etching in oxalic acid and potent kinetic reactivation tests along with analysis by electron microscopy armed with energy dispersive X-ray spectroscopy after annealing at 650°C[6].

1.5.2 Concentration cell corrosion

A specific type of corrosion known as a concentration cell happens when two different sections of metal have varying species concentrations (Figure 1.6). When corrosive solutions of varying concentrations come into contact with two or more portions of the same metal surface, corrosion takes place. In the presence of a range of concentrations of the same electrolyte, the same metal exhibits various electrical characteristics. Differences in dissolved oxygen concentration cause localized corrosion of metal in areas with differing polarities, such as anodic and cathodic zones, which are produced by oxygen concentration cells, also known as differential aeration. The corrosion current is determined using the oxygen concentration cell by polarizing the cathode and anode, measuring the resistance of the transporting medium and metal, and figuring out the circuit's open-circuit potential[7].

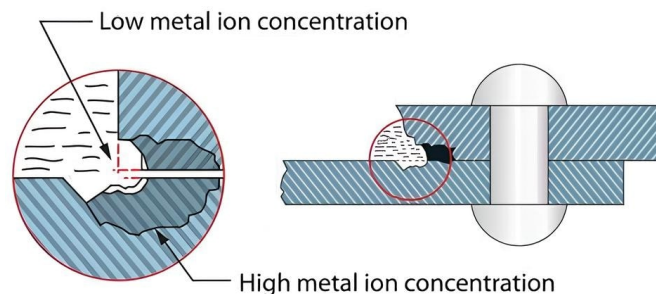


Figure 1.6: Concentration Cell Corrosion

1.5.3 Crevice Corrosion

A metal surface is the target of crevice corrosion, which happens right where or very close to the fissures created when two surfaces are linked (Figure 1.7). This kind of corrosion happens when an electrolyte that is stationary and has little oxygen exposure is exposed to the crevice. As water builds up inside the fissure, the process progresses, possibly resulting in a differential in oxygen content between the lower and upper regions of the crevice. Consequently, the corrosion process is started when the base of crevice turns into an anodic area relative to the higher region [8].



Figure 1.7: Crevice Corrosion

1.5.4 Pitting Corrosion

It refers to a kind of confined degradation that produces pits in smaller locations (Figure 1.8). It mainly affects passive metals and alloys like stainless steel, aluminium alloys and other materials whereas their protective oxide film is either chemically or mechanically compromised and fails to re-form. This leads to the formation of narrow and deep pits, which quickly penetrate the metal's wall thickness. The extent of pitting can be assessed by pitting potentials through measurement[9].

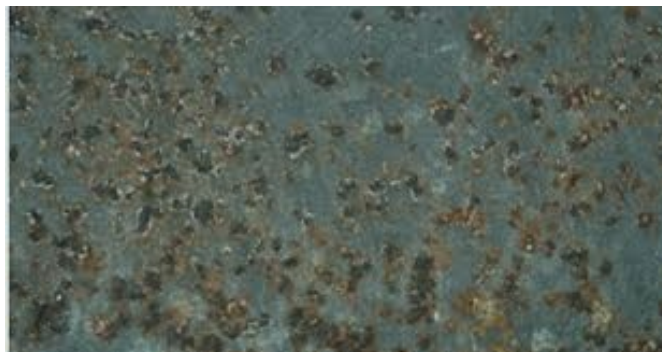


Figure 1.8: Pitting Corrosion

1.5.5 Selective Corrosion

The way metals and alloys corrode can be influenced by their inherent arrangement, potentially leading to specific elements dissolving. This process of dissolution mainly takes place due to tiny galvanic corrosion processes, leading to the extraction of the less resistant metal from the alloy in appropriate conditions (Figure 1.9). Alloys with a notable divergence between the metals they consist of in the galvanic hierarchy, like brass composed of copper and zinc, are especially prone to this occurrence, as seen in cases like dezincification[10].



Figure 1.9: Selective Corrosion

1.5.6 Erosion Corrosion

Disintegration of materials which is caused by the interaction of metal surfaces with corrosive media while undergoing relative movement is referred as Erosion corrosion (Figure 1.10). The extent of erosion-corrosion varies depending upon the speed of this movement, leading to abrasion in some cases. This form of corrosion is recognizable by the presence of grooves and surface irregularities. It is also related to the composition and microstructure of the material[11]. To mitigate erosion corrosion and abrasion-corrosion, one can decide on more resistant materials and enhance the design of the components involved.

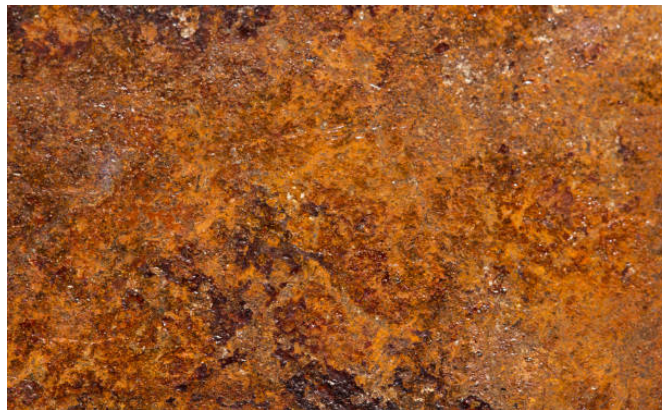


Figure 1.10: Erosion Corrosion

1.5.7 Cavitation Corrosion

When gas bubbles burst on a metal substrate, a specific type of erosion known as cavitation corrosion occurs, leaving pits in its wake. (Figure 1.11). This phenomenon is frequently linked to sudden pressure fluctuations in water brought on by hydrodynamic elements like propeller blades time. Pitting brought on by cavity collapses causes severe wear on parts and can drastically reduce the lifespan of pumps or propellers. Although

cathodic protection can slightly reduce cavitation, maintaining appropriate surface conditions and ensuring proper water flow are the major strategies to counteract cavitation erosion.



Figure 1.11: Cavitation Corrosion

1.5.8 Stress Corrosion

When a metal is subjected to both a corrosive environment and tensile stress at the same time, stress corrosion cracking is the sort of failure that results (Figure 1.12). Stress corrosion is characterized by highly localized attacks, even when overall corrosion is minimal. Different corrosive agents, such as caustic alkalis and storing nitrate for mild steel, traces of ammonia for brass, and acid chloride solutions for stainless steel, can induce this type of corrosion.

Stress corrosion is frequently seen in fabricated items made of certain alloys like high zinc brasses and nickel brasses, particularly when these materials are subjected to stresses caused by processes like drawing, rolling, or insufficient annealing. However, pure metals are relatively resistant to stress corrosion.



Figure 1.12: Stress Corrosion

The prevailing belief is that stress corrosion involves localized electrochemical corrosion occurring along narrow paths, where certain areas become anodic compared to

the larger cathodic areas of the metal surface. The presence of stress leads to strain, resulting in localized areas of higher electrical potential. These areas become highly chemically active and are susceptible to attack even by mild corrosive environments, ultimately leading to the formation of cracks. Under sufficiently high tensile stress and specific environmental conditions, almost all alloys are vulnerable to stress corrosion.

1.6 APPROACHES TO INHIBIT OR CONTROL THE CORROSION

The imperative to employ construction materials in a secure, cost-efficient manner, while concurrently addressing the challenges arising from corrosion, has become a topic of widespread deliberation across diverse industries. Corrosion and its amelioration constitute global concerns, and the repercussions stemming from inadequate attention to this domain are acutely discernible. From a global economic standpoint, it is imperative to institute effective methodologies and strategies to curtail the losses inflicted by corrosion. Compared to some recent reviews, articles, and prevention techniques, the present study offers up-to-date knowledge of the different types of protective coatings on metals (Figure 1.13).

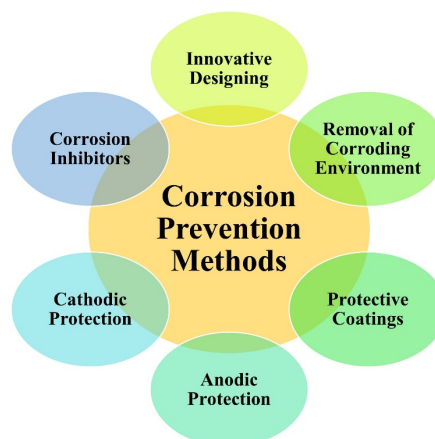


Figure 1.13: Different Corrosion Prevention Methods

Among all the methods, using corrosion inhibitors is the best method for corrosion prevention as it does not require any special equipment for its application.

1.6.1 Corrosion inhibitors

Some chemical compounds act as corrosion inhibitors that are added to the medium and are capable of reducing corrosion. These serve as the most practicable, cost-effective, and efficient approach to managing deterioration on the surface of the metal in different mediums by preventing metal dissolution and acid consumption. These inhibitors operate through the mechanism of molecular adsorption, wherein the compound exerts corrosion inhibition by regulating both anodic and cathodic processes. The protonated

entities adhere to cathodic sites on the surface, attenuating the liberation of hydrogen gas. Consequently, the pace of corrosion diminishes correspondingly. Inhibitory agents can be administered either in the form of solutions or as protective coatings, employing diverse methodologies. Corrosion inhibitors encompass compounds that engage with the metal surface or ambient gases in order to curtail the electrochemical reactions inherent to the corrosion process. These agents are harnessed to mitigate the impact of corrosive surroundings upon metallic substrates. In different industries, the various compounds including organic and inorganic substances are used as inhibitors. The compounds generally containing atom having lone pair of electrons such as nitrogen (N), oxygen (O), Sulphur (S) and phosphorus (P) and a mediately with an aromatic ring, unsaturation, which has been demonstrated to be a key component of highly effective inhibitors to reduce the pace at which metals corrode in harsh conditions. In general, anti-corrosive potential of inhibitor hinges upon the proclivity for establishing strong coordinate bonds with the metal substrates. Consequently, both phenomena adhere to an analogous sequence, namely $O < N < S < P$. The risk inherent with these substances is apparent during the fabrication of such products or in their utilization. Corrosion inhibitors have long been associated with stability and environmental issues that are of worldwide significance. As a consequence, it is a great juncture to gain knowledge about protection against corrosion using low-cost, readily accessible, and environment benign inhibitors. Inhibitors are broadly classified into three categories as given in the figure 1.14.

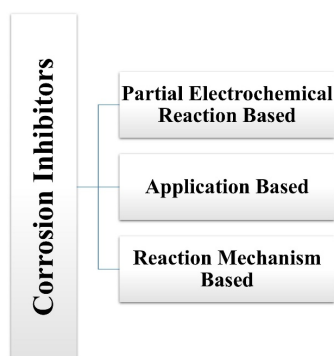


Figure 1.14: Different Classification of Corrosion Inhibitor

a) On the basis of partial electrochemical reactions occurring on cathode and anode inhibitors are of three types

- i) Anodic Inhibitor** : On anode oxidation of metal occurs to liberate metal ions. Anodic corrosion inhibitors protect the metal by suppressing anodic reaction and forming a protective oxide layer over the surface of metal (Figure 1.15 (a)). They

induce a significant anodic shift, converting the metal into a passivated region. Passivation aids in reducing the metal's susceptibility to corrosion. In hydrochloric acid, it was discovered that the drug fluconazole was an anodic inhibitor for steel protection. The E_{corr} values were shifted to positive side depicting anodic type inhibition of corrosion. Fluconazole protected the mild steel by getting adsorbed on metal surface[12]. Examples of anodic corrosion inhibitors are chromates, phosphate, nitrates, and molybdates[13].

ii) Cathodic Inhibitor : Cathodic inhibitors are employed to reduce the occurrence of the cathodic reaction. They induce a significant cathodic shift (Figure 1.15 (b)). Examples of cathodic corrosion inhibitors are sulphite and bisulphite, which react with oxygen to form sulphates. Cathodic inhibitors shift the E_{corr} toward negative side depicting cathodic type inhibition of corrosion. Amisulpride acts predominantly as cathodic inhibitor by preventing reduction reaction and evolution of hydrogen[14] .

iii) Mixed Inhibitors: Mixed corrosion inhibitors also create a thin layer of protective nature on the metal surface. They suppress reactions taking place at both oxidizing and reducing electrodes, achieved by forming a precipitate on the metal's surface. Corrosion potential values do not alter much by the addition of inhibitor (Figure 1.15 (c)). E_{corr} values shift by a factor not more than 85 mV for inhibitors that suppress both anodic and cathodic reactions. Nitrofurantoin protected mild steel at both the cathodic and anodic sites in 1 M Hydrochloric acid solution. Silicates also act as mixed inhibitors[15].

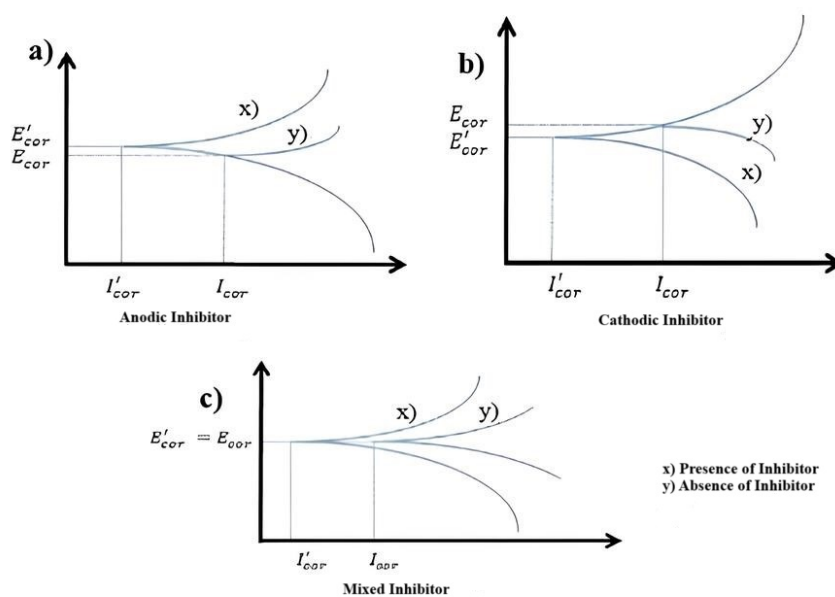


Figure 1.15: Types of Corrosion Inhibitors on the basis of electrochemical reaction

b) Inhibitors according to their method of inhibition and their surrounding applicability

On the basis of application of inhibitor in the medium, inhibitors can be categorized into various classes

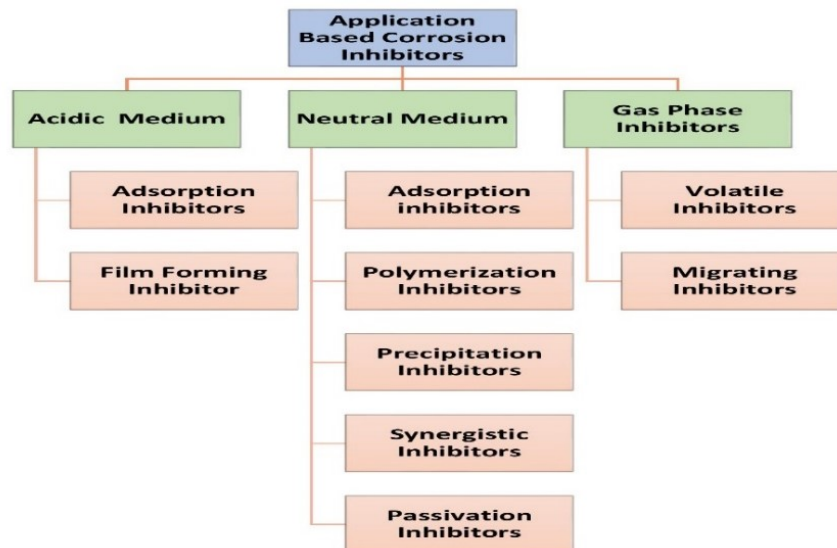


Figure 1.16: Types of Corrosion Inhibitors on the basis of Application

i) Inhibitors in Acidic Medium

- **Adsorption Inhibitors:** Corrosion inhibitors used in acidic environment are generally organic compounds as they have hetero atoms, aromatic ring, heterocyclic ring which provide electrons for the donation to vacant orbital of metal to be protected and get adsorbed. Efficiency of adsorption inhibitor depends upon functional group present in inhibitor, concentration and strength of bond between metal and inhibitor.
- **Film forming Inhibitors:** Certain inhibitors work by covering the metal substrate by a protective layer that prevents hostile substances from penetrating the metal. For example acetylenic corrosion inhibitors form protective film on iron and steel surface[16].

ii) Inhibitors in Neutral Medium

- **Precipitation Inhibitors:** Since protective surface coatings frequently develop in neutral settings and leave the metal surface coated in an insoluble

salt layer, inhibition can occur. These salt films tend to be thicker in comparison to the previously mentioned adsorbed films. Inhibitors that trigger the formation of these insoluble salt films are typically cathodic inhibitors because they restrict or block the diffusion of oxygen to the cathodic sites, which in turn leads to film formation on the surface. As an instance, the precipitation of materials like Zn, Mg, and Ni insoluble hydroxides[17].

- **Passivation Corrosion Inhibitors:** Corrosion inhibitors commonly bring into play by passivation mechanism in neutral solutions. In such instances, the metal surface's passivation can be initiated by oxidizing corrosion inhibitors such as chromates, nitrites, nitrates, and molybdates. This phenomenon is particularly relevant when dealing with a metal that undergoes passivation.
- **Adsorption Inhibitors:** Inhibitors designed for use in neutral conditions can offer adsorption as the mechanism of corrosion protection. It's important to bring to light, that in a neutral environment, oxygen reduction typically serves as the dominant cathodic process, whereas in acidic solutions, hydrogen evolution takes precedence as the dominant cathodic reaction. Additionally, in neutral environments, metals often develop an oxide layer, which is generally less stable when exposed to acidic conditions. Benzoates and salicylate are typical inhibitors that operate in neutral medium through mechanism of adsorption. The inhibition mechanism occurs by blocking the corrosion processes by preventing the electrolyte from accessing certain areas of the metal surface.
- **Synergistic Corrosion Inhibitor:** Synergistic effect occurs when mixture of inhibitors is used for corrosion inhibition. Various mechanisms occur for the protection of metal by strengthening of inhibitor metal interaction and provide barrier between metal and aggressive medium. Synergistic effect has been observed due to organic compounds, inorganic compounds and polymeric mixtures etc. Inhibitory action is more pronounced due to combined cathodic and anodic inhibition[18].
- **Film Precipitation Corrosion Inhibitors:** Precipitate forms a film of protection over the metal surface, which serves the basis for the inhibitory mechanism of precipitation inhibitors. For cathodic reactions, it serves as an obstruction. Its examples include polyphosphates and organophosphates.

iii) Gas Phase Corrosion Inhibitors

- **Volatile inhibitors:** The majority of volatile inhibitors are organic substances with a high vapor pressure and low molecular weight which include

aliphatic compounds, aromatic substances, cyclohexylamines, heteroalkylated lower amines and aminonitrobenzoates. These inhibitors reach from the source to metal surface through evaporation being volatile. Adsorption-based inhibition mechanism prevails for effective lowering of corrosion rates with such inhibitors. Furthermore, the establishment of a hydrophobic film can further enhance protection[19].

- **Migrating Corrosion Inhibitors:** These inhibitors are used to safeguard steel bars embedded in concrete constructions. These migratory materials have the capacity to permeate concrete structures and protect steel from corrosion brought on by chloride exposure. The inhibitor's migration occurs through both liquid and gas phases. Liquid diffusion happens through the moisture consistently found in concrete structures, while gaseous diffusion is a result of the inhibitor's elevated vapour pressure. Diffusion occurs due to capillary action and microstructure of concrete. Migrating corrosion inhibitors are amines and alkyl amine based with phosphorous inorganic compounds[20].

c) Inhibitors on the basis of Reaction Mechanism

Several types of molecules have been examined for their capacity to prevent corrosion. (Figure 1.17).

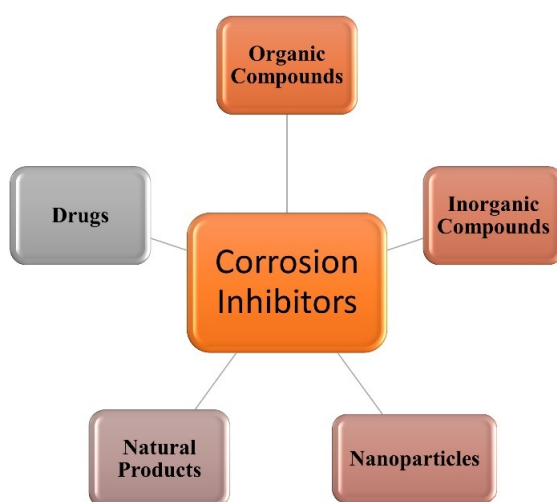


Figure 1.17: Different types of Corrosion Inhibitor

1.6.2 Organic and Inorganic Compounds as Corrosion Inhibitors

Organic inhibitors are highly effective in preventing corrosion. The inhibition process is facilitated by the presence of hetero atoms such as N, S, and O, as well as high electron density groups in the organic compounds. Compounds containing amine,

aldehyde groups, and high electron density structures exhibit exceptional corrosion-inhibiting properties for various metals[21]. Even organic polymers can serve as corrosion inhibitors[22]. Various organic substances have been studied on different materials in different media as corrosion inhibitors. Organic compounds demonstrate remarkable inhibition efficiency, as they create a protective barrier after adsorption on the metal surface, displacing water molecules. The effectiveness of organic inhibitors depends on the compound's structure, physical and chemical properties. Factors such as the size of the molecule, chain length, aromaticity, bond strength, and solubility of the inhibitor also influence its action. The inhibition efficiency is determined by the constancy of the adsorbed layer formed on surface of the metal by action of the inhibitor. The Schiff bases act as admirable corrosion inhibitors for mild steel in 0.5 M HCl. The standard techniques were employed for the investigation of Schiff bases. Surface characterization was done by SEM and IR spectroscopy.

However, a major drawback of these inhibitors is their toxicity to the environment. On the other hand, inorganic compounds are also used as corrosion inhibitors for various metals. Chromates, for instance, are efficient inhibitors as they form monoatomic or polyatomic oxide layers on the metal surface. However, these inhibitors are toxic and non-eco-friendly.

1.6.3 Natural/Green Inhibitors

Green or natural compounds are investigated to be excellent corrosion inhibitors. Green inhibitors are like synthetic corrosion inhibitors in their action[23]. They also get adsorbed on metal surfaces by physical or chemical adsorption. Natural inhibitors are not only eco-friendly but also with high inhibition efficiency. Argemone Mexicana leaf extract[24], Saraca Ashoka seed extract[25], Sida cordifolia[26], Myristica fragrans, Ginkgo leaf extract[27], Parthenium hysterophorus plant extract [28], Xanthium strumarium [29], Pineapple stem extract[30], Prosopis juliflora [31], Pongamia pinnata leaf extract[32], Ruta chalepensis [33] have been studied as corrosion inhibitors for various metals in different corrosive media by employing corrosion techniques like weight loss, electrochemical methods and surface analysis. Tulsi leaf extract can act as a corrosion inhibitor not only for the protection of zinc in sulphuric acid[34] but also for the protection of mild steel[35], tin[36] and aluminum alloy in various media [37]. Natural compounds are found to be very aggressive inhibitors but their method of extraction is difficult and they are complex in structure.

1.6.4 Nanomaterials as Inhibitors

Nano particles have a size between 1-100 nm. Nowadays Nanoparticles are widely used in various fields of science as they have unique characteristics in terms of mechan-

ical strength, greater outward area and optical activity. Nanoparticles also have their applications in the form of corrosion inhibitor coatings. Nano compounds inhibit the reaction of surface and control the corrosion rate by blocking active sites of the metal surface and also provide hardness, strength, durability, optical qualities and thermal stability. Nano compounds also give hardness, durability, strength, thermal stability and optical properties while inhibiting surface reaction and regulating corrosion rate by blocking active areas on the metal surface. Smart anticorrosive coatings can also be developed by incorporating Nano containers loaded with corrosion inhibitors into a protective layer. There is a controlled release of inhibitors depending upon stimulus such as pH change. Hybrid sol-gel coatings prepared from modified silanes and corrosion inhibitors embedded with silica nanoparticles can also be used for the protection of alloys and metals. Polymer-stabilized nanoparticles can also be used as effective corrosion inhibitors. Metal along with metal oxides e.g. Ag[38], TiO₂[39], Cu₂O[40], ZnO[41], ZrO₂[42], SiO₂[43], nanocrystals alloys e.g. Monel-type Ni–Cu nanocrystal alloy[44], nanotubes, nanofibers, nanocomposites were found to be efficient corrosion inhibitors as investigated by polarization and impedance studies. Nanocomposite is formed by organic and inorganic constituents[45]. Inorganic constituent provides adhesiveness, ductility and mechanical strength while organic component provides more flexibility, improved compatibility and porosity reduction. Commonly used organic parts are alumina polyurethanes[46] or zirconium phosphate polyurethanes[47], polystyrene[48], polyvinyl alcohol[49], while inorganic component[50] includes metal nanoparticles [51]. By forming the oxide layer, Nanocrystal alloys offer hardness, electrical resistivity, wear resistance, and high-temperature corrosion resistance. Nanotubes have hollow tubular nanostructures in shape. They are suitable for use as coating materials to inhibit corrosion. Nano containers are smart materials that release the inhibitor with respect to changes in pH. Nanofibers are efficient corrosion inhibitors as they control cathodic reactions. Nanocomposites are made up of inorganic and organic components. The organic part provides flexibility and reduction of porosity while Inorganic components provide high ductility, high mechanical strength and adhesiveness.

1.6.5 Drugs as corrosion inhibitors

Numerous methods are available to investigate the potential of drugs as corrosion-inhibitory compounds. The techniques aided with Electrochemical Impedance Spectroscopy (EIS) is useful to ascertain the inhibitory efficacy by means of polarization resistance. So as to evaluate the effectiveness of inhibition, potentiodynamic polarization (PDP) measurements are utilized for computing the corrosion potential and current using the Tafel slope. By analyzing the shift in corrosion potential (E_{corr}), the mechanism of inhibition is grouped as cathodic, anodic, or mixed type. In order to look more closely at how drugs affect the metal surface, Mass loss measurement is helpful

to find out corrosion rate and inhibition efficiency under specific conditions of temperature, concentration, and immersion time. Surface morphology of the metal before and after inhibition may be studied with latest microscopy techniques such as Transmission Electron Microscopy (TEM), Scanning Electron Microscopy (SEM), and Atomic Force Microscopy (AFM). Chemical analysis is carried out using FTIR and FTIR-ATR to determine the drug molecule's functional groups and the link between it and the metal substrate. Additionally, Kinetic and Thermodynamic parameters are used for assessing the feasibility of drug molecule. For a more in-depth understanding, Quantum Chemical Calculation Method and Density Functional Theory (DFT) with high accuracy are applied to determine the optimized structure of inhibitors, electronegativity, frontier orbitals (HOMO and LUMO), chemical hardness, and chemical softness. X-ray Fluorescence (XRF) and Energy Dispersive X-ray analysis (EDAX) are employed to identify the elemental composition of the materials under investigation. Furthermore, The sort of transition occurring in the drug molecule and the establishment of an barrier by drug are both demonstrated by UV-VIS spectroscopy. Through the utilization of these diverse techniques, drugs from various categories have been investigated and shown promise as effective corrosion inhibitors.

1.7 DIFFERENT VARIETY OF DRUGS AS CORROSION INHIBITOR

1.7.1 Corrosion protection by analgesic drugs

Analgesic drugs, primarily designed to alleviate pain, share structural properties similar to corrosion inhibitors, making them viable for corrosion control purposes. Several analgesic medications have demonstrated effectiveness in corrosion control, successfully preventing corrosion in commonly used mild steel in industrial applications. For instance, Voltaren proved to be a competent inhibitor in HCl, achieving a remarkable 96.1% performance based on weight loss, electrochemical techniques, scanning electron microscopy, and electron dispersive X-ray analysis. Similarly, Etricoxib was studied for its corrosion-inhibitory properties on carbon steel in phosphoric acid, exhibiting high efficiency. A variety of analgesic drugs are listed in Table 1.1, showcasing their potential as corrosion inhibitors.

1.7.2 Corrosion protection by Antibiotic drugs

Antibiotic medications are known for their efficacy in combating infections caused by microorganisms, particularly bacteria. Owing to their conjugated electron system and non-bonding electrons, these drugs may potentially be used as corrosion inhibitors. For instance, Streptomycin was subjected to a study to assess its ability to inhibit corrosion in mild steel when exposed to HCl-corrosive conditions.

Table 1.1: Analgesic drugs for the protection of various metals in various media

Analgesics Drug					
Drug	Material and Medium	Techniques used	Followed Isotherm and Mode of inhibition	Inhibition efficacy (%)	Ref.
Voltaren	Al in 1M HCl	Weight Loss Study, Electrochemical Study	Langmuir Mixed	89.7	[52]
Analgin	MS in 1M HCl	Quantum Chemical Study, Electrochemical Study, Weight Loss	Langmuir Mixed	96.1	[53]
Etoricoxib	Carbon Steel in 0.5M H ₃ PO ₄	Electrochemical Study, Weight Loss, SEM, EDX	Langmuir Anodic	80.6	[54]
Phenazone	Al in 1M HCl	Electrochemical Study, Gasometry, Quantum Chemical Study, SEM	Tempkin Mixed	82	[55]
Tramadol	Al in 1M HCl	Weight Loss Study, Electrochemical Study, Quantum Chemical Study	Langmuir Mixed	98	[56]

Table 1.2: Antibiotic drugs for the protection of various metals in various media

Antibiotics Drugs					
Drug	Material and Medium	Techniques used	Followed Isotherm and Mode of inhibition	Inhibition efficacy (%)	Ref.
Cefotaxime	MS in 0.1M HCl	Electrochemical study, Weight Loss	Langmuir Mixed	95.8	[57]
Amodiaquine	MS in 0.1M HCl	Electrochemical study, Weight Loss Study	Langmuir Mixed	44.33	[58]
EBT	2205 Duplex Stainless Steel in 0.5M HCl	Weight Loss Study, Electrochemical study	Langmuir Mixed	98.3	[59]
	MS in 2M HCl	Quantum Chemical, Electrochemical, SEM, Weight Loss	Langmuir Mixed	91.3	[60]
	MS in 0.5M HCl	Electrochemical study, Weight Loss study, MD simulations	Langmuir Mixed	95	[61]
Ciprofloxacin	Carbon steel in 1M HCl	Electrochemical study, Hydrogen evolution, EFM, SEM, Weight loss	Langmuir Mixed	91	[62]

Fluconazole	Al in 0.1M HCl	Quantum Chemical Study, Weight loss	Langmuir Mixed	82	[63]
Clotrimazole	Al in 1M HCl	Quantum Chemical Study, Weight loss	Langmuir Mixed	90.9	[64]
Piperacillin	MS in 1M HCl	Electrochemical Study, Weight Loss	Langmuir Mixed	93	[65]
Streptomycin	MS in 1M HCl	Electrochemical Study, Weight Loss, Atomic Force Microscopy	EI Awady Mixed	88.5	[66]
Doxycyclin	MS in 1M HCl	Weight Loss Study, Electrochemical Study, AFM	Langmuir Mixed	95	[67]
Ceftazidime	Copper in 1M HCl	Weight Loss Study, Electrochemical Study, SEM, EDX, EFM Quantum Chemical Study	Langmuir Mixed	94.2	[68]
Meropenem	Cu in 1M HNO ₃	Weight loss Study, Electrochemical Study, EFM, SEM, EDX, Quantum Chemical Study	Tempkin Mixed	98.7	[69]
Isoniazid	MS in 1M HCl	Weight loss, Electrochemical Study, Atomic Force Microscopy, XPS	Langmuir Mixed	96	[70]
Chloramphenicol	A315MS in 0.1M HCl	Weight loss Study, LPR, OCP	Langmuir Mixed	85.3	[71]
Chloroquine	Al in 1M HCl	Quantum Chemical Study, Weight Loss	Freundlich Mixed	74.99	[72]
Nitrofurantoin	MS in 1M HCl	Electrochemical Study, Weight loss, SEM, EDX	Langmuir Mixed	97.6	[73]
Paromomycin	Zn in 1M HCl	Electrochemical Study, Weight Loss	Temkin Mixed	91.96	[74]
Septazole	Cu in 0.1M HCl	Electrochemical Study, Quantum Chemical Study, Weight Loss, EFM, SEM	Langmuir Mixed	97	[75]
Ampicillin	Al in 3.5% NaCl	Electrochemical Study, Quantum Chemical Study, Weight Loss, SEM	Langmuir Mixed	85	[76]
Cloxacillin	MS in 1N HCl	Electrochemical Study, Weight Loss, Hydrogen permeation measurement, Diffused reflectance Spectroscopy	Temkin Mixed	81	[77]

Dicloxacillin	Al in 0.5M HNO ₃	Electrochemical Study, Quantum Chemical Study, Weight Loss, Optical Microscopy, SEM	Langmuir Mixed	58.9	[78]
Cefadroxil	Al in 1M HCl	Electrochemical Study, Quantum Chemical Study, Weight Loss, SEM	Adsorption Mixed	93.22	[78]
Metronidazole	MS in Aqueous	Weight Loss Study, Electrochemical Study, FTIR	Langmuir Mixed	83	[79]
Ofloxacin	MS in 1N HCl	Weight Loss Study	Langmuir	92.13	[80]
Norfloxacin	MS in 1N HCl	Weight Loss Study	Langmuir	91.54	[80]
Ciprofloxacin	304 Stainless Steel in 1.5% NaCl	Electrochemical Study	Adsorption Anodic	93	[81]
Cephalothin	API 5L X52 in 1M HCl	Weight Loss Study, Electrochemical Study, SEM	Langmuir Mixed	87	[82]
Gentamicin	MS in 1M HCl	Electrochemical Study, Weight Loss, SEM	Langmuir Mixed	89.3	[83]
Neomycin	Carbon Steel in 0.1M H ₂ SO ₄	Electrochemical Study, Weight Loss, AFM	Langmuir Mixed	76.4	[84]
Moxifloxacin	Carbon Steel in 1M HCl	Weight loss Study, Electrochemical Study, Hydrogen Evolution, SEM	Langmuir Mixed	92	[85]
Albendazole	MS in 0.1M HCl	Electrochemical Study, Weight Loss	Langmuir Mixed	96	[86]
Benzimidazole	MS in HCl	Weight Loss Study, Electrochemical Study, SEM	Langmuir Mixed	92	[81]

The investigation involved weight loss and electrochemical measurements, demonstrating an inhibition efficacy of more than 88%. The research indicated that the drug protected against corrosion by adsorbing onto the metal surface without altering the underlying corrosion mechanism. Another antibiotic, Ampicillin, was also investigated for its corrosion inhibition properties on mild steel, both in sulphuric acid and hydrochloric acid environments, exhibiting significant effectiveness. Ampicillin also displayed corrosion inhibition capabilities on zinc and stainless steel. Moreover, other antibiotics such as Cefotaxime, EBT, Fluconazole, and Clotrimazole were tested for their ability to inhibit corrosion on various materials exposed to different aggressive media. These antibiotics proved to be effective corrosion inhibitors. Table 1.2 provides information on some of the antibiotic drugs studied for their potential as corrosion inhibitors on

different materials and in various corrosive environments.

1.7.3 Corrosion protection by Antihistamine drugs

Antihistamine medications have proven to be effective in treating allergies. These drugs also demonstrate significant potential as corrosion inhibitors. For instance, Cetirizine has been extensively studied and found to be a highly efficient corrosion inhibitor, with an impressive inhibition efficacy of 95%. This effectiveness was assessed through various methods, including quantum chemical calculations, gravimetric and electrochemical analysis. Cetirizine exhibited its protective effects on mild steel at both cathodic and anodic sites, forming a monolayer on the metal surface. Similarly, Promethazine and dioxopromethaxime have also been identified as effective corrosion inhibitors for copper in sulphuric acid. Their corrosion prevention capabilities were notable, with Promethazine showing a behavior of mixed type and an efficacy of 93.43%, while dioxopromethaxime demonstrated an efficacy of 96.98%. Table 1.3 lists some of the antihistamine drugs that have been mentioned in the context of their corrosion inhibition potential.

Table 1.3: Anti-histamine drugs for the protection of various metals in various media.

Anti-Histamine Drugs					
Drug	Material and Medium	Techniques used	Followed Isotherm and Mode of inhibition	Inhibition efficacy (%)	Ref.
Cetirizine	Cu in 0.5M H ₂ SO ₄	Weight Loss Study, Electrochemical Study, Quantum Chemical Study, XPS	Langmuir Mixed	93	[87]
Promethazine	Cu in 0.5M H ₂ SO ₄	Electrochemical Study, Weight Loss, Quantum Chemical Study, SEM	Langmuir Mixed	96.98	[88]
Fexofenadine	MS in 1M HCl	Quantum Chemical Study, Electrochemical Study, Weight Loss	Langmuir Mixed	97	[89]
Diphenahy-dramine-hydrochloride	MS in 1M HCl	Electrochemical Study, Weight Loss, SEM	Langmuir Mixed	91.4	[90]
Meclizine	Al in 1M HCl	Weight Loss Study, Electrochemical Study, SEM	Langmuir Mixed	95.4	[91]
Pheniramine	MS in 1M HCl	Weight Loss Study, Electrochemical Study, SEM	Langmuir Mixed	98.1	[92]

1.7.4 Corrosion protection by antipyretic drugs

The antipyretic drugs are primarily used to bring down body temperature. Due to their environmentally benign nature and favorable structural properties, these can be used as corrosion inhibitors. Ibuprofen triazole has been investigated for its anticorrosive characteristics in sulphuric acid with an inhibition efficiency of 97% by using gravimetric, electrochemical techniques, and quantum chemical study. Paracetamol was also studied for its anticorrosive behavior and its efficiency was found to be high for carbon steel, copper and mild steel in acidic media. Aspirin is also found to be effective for mild steel, copper and aluminum corrosion inhibition. Many antipyretic drugs have been mentioned in table 1.4.

Table 1.4: Antipyretic drugs for the protection of various metals in various media

Antipyretics Drugs					
Drug	Material and Medium	Techniques used	Followed Isotherm and Mode of inhibition	Inhibition efficacy (%)	Ref.
Ibuprofen	Mild Steel in 0.5M H ₂ SO ₄	Electrochemical, Weight loss	Langmuir Mixed	63.2	[93]
	Al 6063 in 0.5M H ₂ SO ₄	Electrochemical, Weight loss	Langmuir Mixed	80.58	[94]
	430T1 Stainless Steel in 0.5M H ₂ SO ₄	Electrochemical, Weight loss	Langmuir Mixed	60.69	[95]
		Electrochemical, Weight loss, Quantum chemical study	Langmuir Mixed		
	H ₂ SO ₄ Cu in Acid Mixture	Electrochemical, Weight loss, Quantum chemical study	Langmuir Mixed	97.2	[96]
Paracetamol	Cu in Acid Mixture	Electrochemical, Weight loss, Quantum chemical study, SEM	Langmuir Mixed	96.3	[97]
		SEM, Weight loss, Electrochemical, Quantum chemical study	Langmuir Mixed		
		Electrochemical, Weight loss	Langmuir Mixed		
	Low Carbon Steel in 1M H ₂ SO ₄	Electrochemical, Weight loss	Langmuir Mixed	94	[98]
		Electrochemical, Weight loss	Langmuir Mixed		
Carbon Steel in 0.5M H ₂ SO ₄	Electrochemical, Weight loss	Langmuir Mixed	94	[99]	
Carbon Steel in 1M HCl	Electrochemical, Weight loss study	Langmuir Mixed	85	[99]	
Aspirin	MS in 1M HCl	SEM, Electrochemical, Electrochemical, Weight loss, Quantum chemical study	Langmuir Mixed	80	[100]
	Cu in 0.5M HCl	Electrochemical, Weight loss, Quantum chemical study		67	[101] [102]

1.7.5 Corrosion protection by antidepressant /Psychotherapeutic drugs

Drugs used for psychotherapy are very important in treating depression and anxiety. One such medication is Fluoxetine, which has been successfully evaluated for its capacity to prevent corrosion in hydrochloric acid when mixed with polyethylene glycol and glutathione. This combination demonstrated 85.6% corrosion inhibition efficacy, with

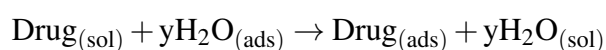
the aid of both electrochemical and weight loss methods. Additionally, SEM micrographs were employed to provide visual evidence of its inhibitory action. Another effective drug, Alprazolam, demonstrated a corrosion prevention efficiency of 86% in mild steel, as determined by weight loss and electrochemical experiments. Moreover, several other psychotherapeutic drugs, including Venlafaxine, Benzodiazepam, Lorazepam, and barbiturates, have been identified as excellent corrosion inhibitors through various corrosion testing techniques. Table 1.5 contains a list of numerous antidepressant drugs, some of which have been discussed for their potential as corrosion inhibitors.

Table 1.5: Antidepressant drugs for the protection of various metals in various media

Anti-depressants Drugs					
Drug	Material and Medium	Techniques used	Followed Isotherm and Mode of inhibition	Inhibition efficacy (%)	Ref.
Alprazolam	Al in 3M HCl	Electrochemical, Quantum Chemical Study	Langmuir Mixed	98.9	[103]
Venlafaxine	MS in 0.5M HCl	Electrochemical, Weight loss, Quantum chemical study, Atomic Force Microscopy	Langmuir Mixed	86.1	[104]
Benzodiazepine	MS in 1M HCl	Electrochemical Study, Weight Loss Study	Langmuir Mixed	91	[105]
Lorazepam	MS in 1M HCl	SEM, Electrochemical, Weight loss, Quantum chemical study	Langmuir Mixed	90	[106]
Ketosulphone	Zn in 0.1M HCl	Electrochemical study, SEM	Langmuir Mixed	96	[107]
Barbiturates	MS in 1M H ₃ PO ₄	Electrochemical Study, Weight loss Study, Quantum chemical study	Langmuir Mixed	89.3	[108]

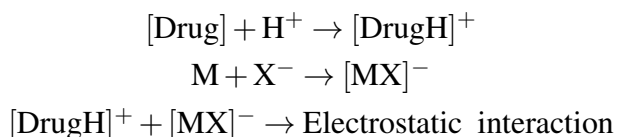
1.8 GENERAL MECHANISM OF ACTION OF DRUG INHIBITOR

The mechanism of drug as corrosion inhibitor on metal in acidic environment can be explained based on thermodynamic, electrochemical and quantum chemical studies. Inhibitor molecules get adsorbed on metal surfaces by displacing water molecules already adsorbed on metal by a displacement reaction.



Gravimetric measurements justify the physical/chemical adsorption mechanism of

inhibition. The drug molecules get protonated at active sites (N, O) having maximum charge density which in turn adsorb negative ions and generate charge in acidic media. Drug molecules get positively charged in acidic corrosive environment and metals get oppositely charged because of same corrosive solution negative ions, these oppositely charged causes interaction between the two, drug and metal, called physisorption.



The movement of electrons from a drug molecule to metal substrate in order to generate a coordinated interaction is the process of chemisorption. Electrochemical measurements suggest mixed/cathode/anodic type behavior of inhibitors for materials in acids. The inhibitor prevents corrosion at the anodic site by reducing the evolution of hydrogen and at the cathodic site by adsorbing directly on the metal surface (Figure 1.18).

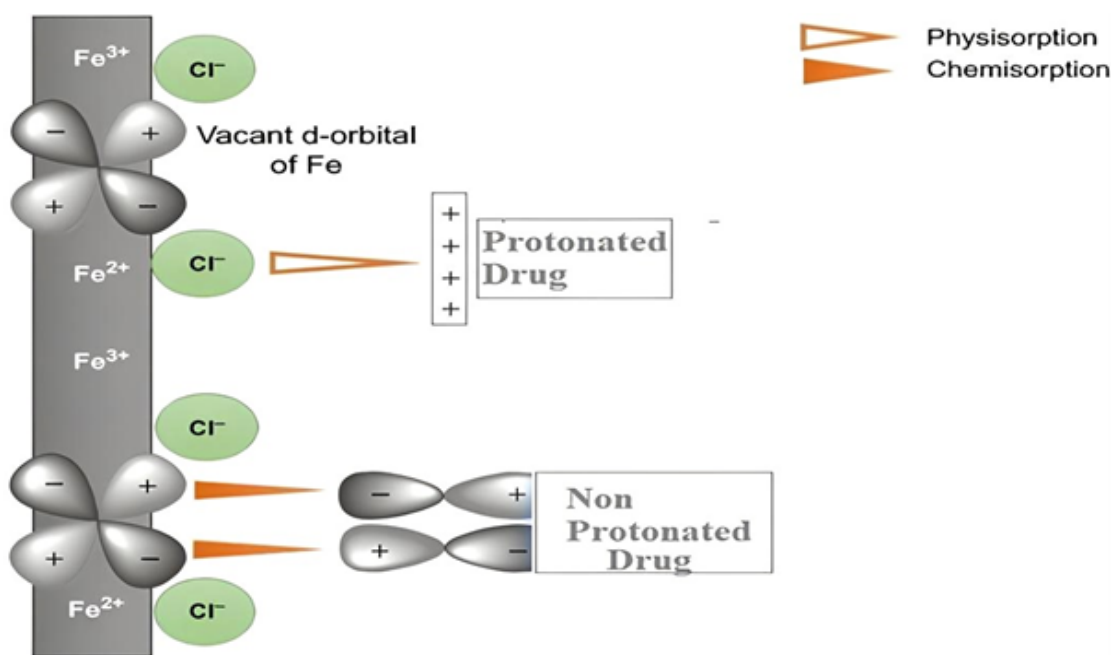


Figure 1.18: Mechanism of Adsorption of Inhibitor

1.9 CONSIDERATIONS TO APPLY DRUGS AS CORROSION INHIBITORS

Traditionally several approaches like metal coatings and cathodic protection have been used, but a highly efficient method to combat corrosion involves using corrosion inhibitors for metals and alloys. The chemical molecules that act as inhibitors comprise atoms having non-bonded electrons. Although a number of inhibitors of deterioration have been investigated, economical, innovative, and potentially effective inhibitors are

needed in order to effectively decrease the extent of corrosion and maybe prolong the lifespan of materials. So, the present work focuses on exploring new drugs and then assessing their efficiencies for corrosion control through weight loss, electrochemical, quantum chemical and surface studies.

1.9.1 Selection of material for the study

Corrosion in iron and steel which are commonly employed metals, can occur in various environments, especially outdoor settings. Their selection is often based on factors other than corrosion resistance, such as strength, ease of production, and affordability. These differences are evident in the rate at which the metals are corroded. Mild steel is extensively utilized in engineering and construction worldwide, and corrosion can be found in diverse settings, ranging from homes to workplaces. MS enables the production of various items, including vehicles, protective gear, refrigerators, cargo ships, and medical surgery tools. It is also applied in marine, chemical processing, oil refining, and metal-processing equipment, among other industries. Despite advances in corrosion science and technology, corrosion continues to pose significant challenges for global businesses. Therefore, it has become technologically significant to analyze how mild steel deteriorates in circumstances containing acid environment and how to safeguard it as a result.

1.9.2 Selection of Acids for the Study

The current effort intends to investigate the effectiveness of antibacterial and antidepressant medications as mild steel corrosion inhibitors in acidic conditions. Drugs are not utilized in the ratio of their synthesis and a major amount of drug is left without their usage.

1.10 OBJECTIVES OF THE STUDY

Drugs are not utilized in the good ratio of their synthesis and a major amount of drug is left without their usage. The present study intends to conceptualize efficient corrosion inhibitors in the form of antibacterial and antidepressant drugs for mild steel in acidic media. The objectives of the study are as follows

- i) To study of drugs as efficient corrosion inhibitors because they have required structural properties.
- ii) To assess the relationship between the concentration of the inhibitor and the rate of corrosion of metal in corrosive media.
- iii) To study the effect of temperature on corrosion rate and inhibition efficiency of metal in corrosive media.

- iv) To determine kinetic parameters of corrosion phenomenon.
- v) To determine thermodynamic parameters and adsorption isotherms of the phenomenon.
- vi) To perform the electrochemical analysis of the phenomenon.
- vii) To do the surface analysis of the metal sample

1.11 METHODOLOGY ADOPTED

The following methodology was adopted for the investigation of drugs as efficient corrosion inhibitors.

1.11.1 Weight loss method

The weight loss method is widely used for the determination of corrosion rates and corrosion inhibition efficiencies of compounds at various temperatures and with different immersion timings. This method is based on the measurement of the weight of a metal sample before and after its immersion in corrosive media for a particular immersion time at a particular temperature. Metal samples of known dimension were abraded with emery papers of various grades to remove impurities of the metal surface, cleaned using double distilled H₂O, decontaminated using (CH₃)₂CO, and then dried in hot air. The standard balance was used to weigh the metal samples before they were submerged in varying quantities of corrosive and inhibitor solutions. Then the metal samples were withdrawn after a particular immersion time, cleaned, and weighed again. We used the following formulas to compute the inhibition efficiency and corrosion rate as a proportion of the surface covering.

$$C_r(\text{mpy}) = \frac{534 \times W}{A \times t \times D}$$

$$\theta = \frac{W_o - W_i}{W_o}$$

$$\text{IE}\% = \left(\frac{W_o - W_i}{W_o} \right) \times 100$$

Where; IE- Inhibition efficiency; θ - surface coverage; C_r - Corrosion rate; W_o – weight loss of metal sample in corrosive solution without inhibitor; W_i – a weight loss of inhibited metals using the inhibitor,

W- Weight loss in mg ; A- sample surface area in cm²; t- immersion time in hours; D- sample density in gm/cm³.

Thermodynamic and kinetic parameters are important to understand corrosion phenomena. Kinetic factors involve activation energy, E_a , and corresponding pre-exponential

factor, A, of the process. Generally, low activation energy and high exponential factor accelerate the process. Arrhenius's equation helps in the calculation of kinetic factors.

$$\log C_r = \frac{-E_a}{2.303RT} + \log A$$

Thermodynamic factors involve free energy change (ΔG), enthalpy change (ΔH) and entropy change (ΔS) of the process. The transition state equation helps in the calculation of these factors.

$$C_r = \frac{RT}{Nh} \exp\left(\frac{\Delta S}{R}\right) \exp\left(\frac{-\Delta H}{RT}\right)$$

(h: Planck's constant; N: Avogadro's number; R: Molar gas constant)

1.11.2 Electrochemical study

The metal specimen under study serves as the working electrode in the corrosion cell, and the saturated calomel or Ag/AgCl electrode is the most commonly used reference electrode. The electrochemical investigations were conducted on an electrochemical workstation (Gamry Potentiostat - IFC1010E-28152) with a three-electrode system. The metal specimen was scrubbed with multiple types of emery paper to prepare it to serve as the working electrode. It was then cleaned with double-distilled H_2O , decontaminated using $(CH_3)_2CO$, and dried. Open circuit potential was stabilized for 1 hour before actual electrochemical measurements for each concentration.

- i) Linear polarization study:** Linear Polarization Resistance is the sole technique for monitoring corrosion that enables direct measurement of corrosion rates. The potential is set within a particular range and scanning rate of 1mV/s for linear polarization resistance measurements. When a metal or alloy electrode is placed in an electrolytic solution, it undergoes corrosion through an electrochemical process. This process encompasses two simultaneous cathodic and anodic reactions. The corrosion rate can be determined by employing a modified form of Faraday's Law, the degree of corrosion is calculated using the corrosion current (I_{corr}), which results from the electrons flow across the anodic and cathodic zones.

$$C_r = \frac{I_{corr} \times E}{A \times D} \times 128.67$$

The relationship between inhibition efficiency and linear polarization resistance is depicted as

$$IE\% = \frac{R_p' - R_p^o}{R_p^o} \times 100$$

Where; I_{corr} - Corrosion current, E - Equivalent weight of the metal, R_p^0 - Polarization resistance in blank solution, R_p' - Polarization resistance with inhibitor

ii) Potentiodynamic Polarization studies: Potentiodynamic polarization is an electrochemical investigative technique where a current is conducted between a specific metal specimen and an inert electrode in a provided solution. This process is carried out to modify the electrochemical potential (V) of the sample under examination, followed by the recording of the current density associated with a particular potential. To examine the impact of corrosion on metal, a Tafel plot with a scan rate of 1 mV/s was created and placed in the potential between -250 to +250 mV. It provides details on the corrosion suppression process. Greater changes imply the use of cathodic or anodic type inhibitors, whilst changes of below 85 mV indicate the usage of a mixed type inhibitor. The formula mentioned below was employed to get the corrosion inhibition efficiency (IE%) based on the corrosion current densities (I_{corr})

$$\text{IE}\% = \frac{I_{\text{corr}}^{\circ} - I_{\text{corr}}'}{I_{\text{corr}}^{\circ}} \times 100$$

Where I_{corr}° and I_{corr}' are corrosion current density in blank solution and solution with inhibitor, respectively.

iii) Electrochemical Impedance: The process of corrosion inhibition and surface characteristics were examined using Electrochemical Impedance spectroscopy. In order to generate the Nyquist plot, the EIS was performed using AC signals, employing a frequency range of 10^5 Hz to 0.2 Hz using an amplitude of 10 mV. Charge transfer resistance (R_{ct}) data were used to calculate the drug's effectiveness of inhibition. (R_{ct}) values.

$$\text{IE}\% = \frac{R_{\text{ct}}' - R_{\text{ct}}^{\circ}}{R_{\text{ct}}'} \times 100$$

Where, R_{ct}' and R_{ct}° are charge transfer resistance with inhibitor and in blank solution, respectively.

1.11.3 Quantum Chemical Study

Quantum chemical study is utilized to explore the relationship between drug molecule composition and inhibition efficacy, as well as the method of inhibition, and to characterize different quantum molecular properties. Using Spartan 20 software, theoretical calculations were carried out to assess the quantum chemical parameters[109]. The optimized structure and the corresponding highest occupied molecular orbital (HOMO) and lowest unoccupied molecular orbital (LUMO) were taken using DFT calculations

on basic set 6-31 G* with method ω B97X-D. It has been reported to provide reliable results to describe the energy of HOMO as well as of the LUMO; electronegativity (χ) and other molecular properties like electron affinity (A), Ionization potential (I), chemical hardness (η), and fraction of transferred electrons(ΔN) can be calculated from these parameters[110].

$$A = -E_{\text{LUMO}}$$

$$I = -E_{\text{HOMO}}$$

$$\chi = \frac{I+A}{2}$$

$$\eta = \frac{I-A}{2}$$

$$\Delta N = \frac{\chi_{\text{Fe}} - \chi_{\text{inh}}}{2(\eta_{\text{Fe}} + \eta_{\text{inh}})}$$

Where χ_{Fe} and η_{Fe} are electronegativity and global hardness of iron ($\chi_{\text{Fe}} = 7 \text{ eV/mol}$, $\eta_{\text{Fe}} = 0$).

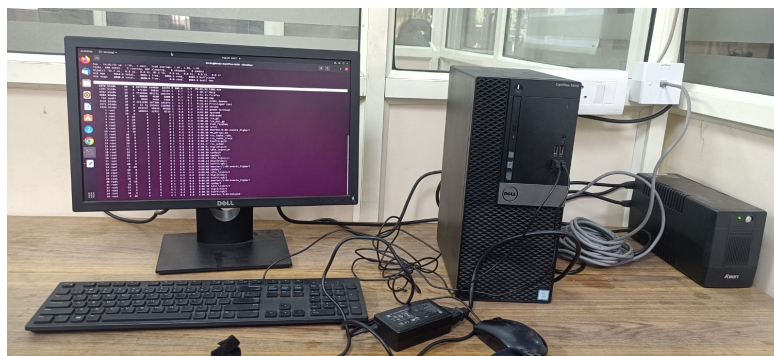


Figure 1.19: System for Quantum Chemical Study

1.11.4 Surface study

Surface study gives important information regarding the protection of metal surfaces by measuring surface roughness.



Figure 1.20: Bruker Atomic Force Microscope

Atomic force microscopy is a prevailing technique for the imaging of any type of surface including polymer, glass, metal etc. For the present study, an Atomic Force Microscopic (AFM) scan was run for the surface characterization in which the specimen was dipped

inside the blank and inhibited corrosive media separately for 4 hours before surface characterization. AFM scans have been performed using Atomic Force Microscope by Bruker and analysis was done on the area of 10 X 10 μm by using Nanoscope 7.

CHAPTER 2

ANTI-TUBERCULOSIS DRUG ETHAMBUTOL AS EFFECTIVE CORROSION INHIBITOR

2.1 INTRODUCTION

Owing to its versatility and affordability mild steel also known as carbon steel with low carbon content, finds an extensive range of applications. It is commonly used in the construction industry for structural components such as beams, columns, and reinforcement bars, thanks to its strength and durability. Mild steel is also employed in the automotive sector for the production of vehicle chassis and body panels, owing to its formability and being protected. Extensive research and testing are typically required to identify and optimized weldability. Additionally, it is used in the manufacturing of pipes, tubing, and containers due to its corrosion resistance. Its malleability makes it suitable for fabrication in various forms, including sheets and wires, making it essential in the production of consumer goods, industrial machinery, and household appliances. Overall, mild steel's adaptability makes it a fundamental material in diverse industries, contributing to its widespread use. To fight the effects of rust and corrosion, these industries frequently utilize HCl and H₂SO₄, sometimes in varying concentrations, either alone or in blends. However, corrosion is a significant concern in various industries and applications. Mild steel, while versatile and cost-effective, is vulnerable to corrosion due to its iron content. Corrosion occurs when the metal reacts with moisture, oxygen, and other environmental factors, leading to the formation of oxides of iron, commonly called as rust. This corrosion process weakens the steel's structural integrity and aesthetic appeal, making it crucial to implement preventive measures such as coatings, paints, or galvanization. In marine environments or areas with high humidity, mild steel is particularly susceptible to rapid corrosion. Regular maintenance and the use of corrosion-resistant coatings are essential to extend the lifespan and maintain the performance of mild steel components in various industries, including construction, automotive, and manufacturing. Corrosion inhibitors have emerged as a practical ecological solution, owing to their economical usage requirements, ready accessibility, and remarkable effectiveness in corrosion control. These inhibitors exhibit an inherent affinity for substantial adsorption onto the metal substrate through physicochemical interactions, thereby enhancing

their corrosion-mitigating capabilities. Notably, previously untapped pharmaceutical agents are being repurposed to address the need for solid waste containment, offering environmentally-centric alternatives for corrosion prevention.

Numerous kinds of substances have already been explored as inhibitors of corrosion for distinct metallic substrates and alloys in different environments[111]. Pharmaceutical compounds generally have one or other required structural properties like heteroatoms (N, O, S), aromatic ring, conjugation and π -electrons to show anticorrosive characteristics[112]. The area of employing such chemicals to serve as anti-corrosion agents is an emerging field and tablets, even in expired form can also be used as corrosion inhibitors, as many groups remain active sometimes even after a long time of expiry[113]. Pharmaceutical compounds of different classes such as analgesics, antibiotics, antipyretics, tranquilizers, sulfa drugs antihistamines and bronchodilators etc. have proven to be efficient and safe corrosion inhibitors[114].

Ethambutol (EBT) is 2, 2'(Ethylenediimino)-di-butanol is available in the form of dihydrochloride salt (Figure 2.1), a medication primarily used in the treatment of tuberculosis (TB) and is often included as part of a combination therapy regimen to combat the disease effectively. It works by restraining the growth of the bacteria responsible for TB, specifically *Mycobacterium tuberculosis*. EBT interferes with the synthesis of the bacterial cell wall, which weakens the cell structure and makes it more susceptible to the body's immune system and other anti-TB drugs. It is usually administered orally, and its dosage depends on factors such as the patient's age, weight, and the severity of the TB infection. EBT is typically used in combination with other anti-TB drugs, as using a combination of drugs helps reduce the risk of drug resistance and improves treatment outcomes. Using drug molecules as corrosion inhibitors is an innovative approach in the field of corrosion science and materials protection. Certain drug molecules, due to their chemical properties and structural characteristics, can exhibit corrosion inhibition properties when applied to metal surfaces in corrosive environments. These drug molecules often contain functional groups that can interact with metal surfaces, forming a protective layer which hinders the corrosion process. The choice of drug molecule as a corrosion inhibitor may depend on factors such as its chemical composition, solubility, and compatibility with the metal being protected. Extensive research and testing are typically required to identify and optimize drug molecules for use as corrosion inhibitors in practical applications. Additionally, safety considerations and environmental impacts should be thoroughly evaluated when repurposing drug molecules for industrial corrosion protection.

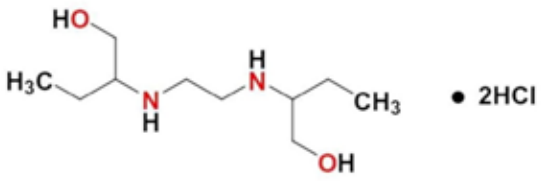
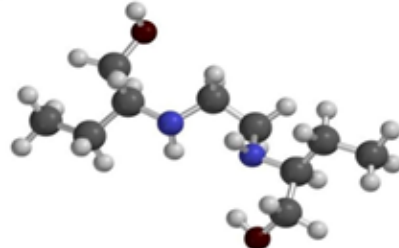
Drug name	Ethambutol Hydrochloride
Drug category	Psychotherapeutic drug
Chemical Formula	$C_{10}H_{24}N_2O_2$
IUPAC name	2, 2'-(Ethylenediimino)-di-butanol
Structural formula	
3 D structure	

Figure 2.1: Structural information of EBT

In our current study, we have undertaken a comprehensive evaluation of EBT's capacity to prevent mild steel (MS) from corroding in an acidic atmosphere containing 0.5 M H_2SO_4 . This study employs various corrosion assessment techniques, including weight loss analysis, potentiodynamic polarization methods and electrochemical impedance spectroscopy (EIS). The selection of EBT as a corrosion inhibitor is grounded in several key considerations: (i) EBT molecules possess electron-rich atoms with non-bonding electrons within their molecular structure, making them highly conducive to adsorption onto the mild steel (MS) surface; (ii) The presence of electron-donating groups like $-CH_3$ further facilitates the interaction of EBT molecules with metal. To gain insights into the impact of these inhibitors, surface analyses with Atomic Force Microscopy (AFM) were carried out. Additionally, computational studies were conducted to establish a connection among theoretical calculations and experimental results, that enhance the understanding of the corrosion inhibition mechanisms.

2.2 EXPERIMENTAL AND METHODS

2.2.1 Preparation of metal sample and test solutions

Mild steel with composition Mn (0.54%), Si (0.20%), C (0.17%), P (0.16%), and Fe (98.7%) was resized into a specimen of dimensions $2\text{ cm} \times 5\text{ cm} \times 0.02\text{ cm}$ for the

present study. Test specimens were scoured with emery papers of grades 200 to 1000 and finished to a mirror surface, cleaned by double distilled H₂O and decontaminated by CH₃(₃)₂CO and dried. For this work, double-distilled H₂O was employed for dilution of analytical grade 18 M sulfuric acid (Sigma Aldrich) to 0.5 M. EBT is a water-soluble drug and was taken in tablet form as EBT Dihydrochloride (Brand Name - Combutil 800; from Lupin Ltd.) with a molecular mass of 204.31 g/mol, purchased from the local market, extracted in pure form, and afterward used as an inhibitor. The stock solution of 1000 ppm of the inhibitor was made by dissolving 1000 mg of the drug in 1L of solution and further diluted to prepare the desired inhibitor concentrations (200-1000 ppm) for experimental study. EBT tablet was characterized by FT-IR spectrum performed on Perkin Elmer FT-IR Spectrophotometer (model: Spectrum 2) at the range 4500-500 cm⁻¹.

2.2.2 Weight Loss Study

When assessing the amount of substance loss resulting from corrosion, a basic and popular technique for the weight loss analysis is used. In this procedure, a metal or material specimen is exposed to an atmosphere that is corrosive for a predetermined amount of time, and its decrease in weight is then measured following the exposure. Standard procedures were followed while measuring weight loss using a Mettler Toledo analytical balance (ME 204) with a minimum count of 0.1 mg. MS coupons were abraded with emery paper of various grades, weighed before and after the immersion in corrosive media of 0.5M H₂SO₄ with 4 hours immersion time at 303K, 313K, 323K, and 333K.

The formula was utilized to compute the EBT inhibition efficiency, surface coverage, and rate of corrosion.

$$IE\% = \frac{W_0 - W_i}{W_0} \times 100$$

$$\theta = \frac{W_0 - W_i}{W_0}$$

$$C_r(\text{mpy}) = \frac{534 \times W}{A \times t \times D}$$

Where; IE: Inhibition efficiency; θ : Surface coverage; C_r : Corrosion rate; W_0 : Weight loss of metal coupon in blank solution; W_i : Weight loss of inhibited metals, W : Weight loss (mg); A : Sample surface area (cm²); t : Immersion time (hours), D – Sample density (g/cm³).

2.2.3 Electrochemical Study

Electrochemical studies were completed on an electrochemical workstation (Gamry Potentiostat - IFC1010E-28152) on MS sample in 0.5M H₂SO₄ with three electrode

systems using Ag/AgCl electrode as reference electrode and platinum wire as counter electrode, and metal specimen of the bare dimension of 1 cm × 1 cm was working electrode in corrosion cell. The working electrode is prepared by scrubbing the metal specimen with emery papers of grades 200-1000, was then cleaned using double distilled H₂O, decontaminated using (CH₃)₂CO and then dried in hot air to make it suitable for use as the working electrode. Open circuit potential was stabilized for 1 hour prior to actual electrochemical measurements for each concentration. The potential was set within the range of -0.02 to +0.02V with a scanning rate of 1mV/s for linear polarization resistance measurements. The relationship between inhibition efficiency and linear polarization resistance is depicted as:

$$IE\% = \frac{R_p' - R_p^\circ}{R_p^\circ} \times 100$$

Where, R_p° is the polarization resistance in blank solution, and R_p' is the polarization resistance with inhibitor.

In order to obtain Nyquist plots, EIS was carried out using AC signals with an amplitude of 10 mV and frequencies from 10⁵ – 0.2 Hz. The EBT effectiveness was assessed using the provided formula:

$$IE\% = \left(1 - \frac{R_{ct}^\circ}{R_{ct}'}\right) \times 100$$

Where, R_{ct}° and R_{ct}' represents charge transfer resistance in blank solution and inhibited respectively.

Scan rate of 1mV/s was set in a potential range of -250 to +250 mV for Tafel plot for the study of corrosion on metal. The corrosion inhibition efficiency (IE%) was assessed from the corrosion current densities (I_{corr}) using the formula: -

$$IE\% = \frac{I_{corr}^\circ - I_{corr}'}{I_{corr}^\circ} \times 100$$

Where, I_{corr}° is corrosion current density in blank solution; I_{corr}' is corrosion current density with inhibitor.

Each experiment was run in triplicate and then the mean value of corrosion parameters is reported.

2.2.4 Quantum Chemical Study

DFT was used to explore the relationship between EBT molecular framework and anti-corrosion performance as well as the way inhibition works and to characterize a variety of quantum molecular characteristics. The optimized structure and different DFT variables of EBT in different phase i.e., in both aqueous and gas phase were taken using DFT calculations on basic set 6-31 G* with method ω B97X-D in Spartan 20 software.

DFT has been reported to provides reliable results to describe some important molecular parameters like E_{HOMO} , E_{LUMO} , electronegativity (χ) and these variables may be used to derive other molecular features. Ionization potential (I) represents the tendency of a chemical species to lose electrons and related to the E_{HOMO} by the equation:

$$I = -E_{\text{HOMO}}$$

E_{LUMO} is connected with electron affinity (A), which is a chemical species proclivity for obtaining electrons.: E_{HOMO} as follows:

$$A = -E_{\text{LUMO}}$$

Electronegativity is the tendency of an atom to attract electrons and can be computed using a formula that described below:

$$\chi = (I + E)/2$$

Chemical hardness (η) is an assessment of an atom's resistance to a transfer of charge, and it may be computed using the formula:

$$\eta = (I - A)/2$$

The fraction of transferred electrons in a chemical reaction is given by the equation:

$$\Delta N = \frac{\chi_{\text{Fe}} - \chi_{\text{inh}}}{2(\chi_{\text{Fe}} + \chi_{\text{inh}})}$$

Where χ_{Fe} – electronegativity of iron (7 ev/mol), η_{Fe} – global hardness of iron (0). The values have been reported in the literature[115] .

2.2.5 Surface Study

Surface characterization was conducted through Atomic Force Microscopic (AFM) analysis, involving the immersion of the specimen in two distinct conditions: one with the presence of EBT and the other without it, both in a 0.5M H_2SO_4 solution. The immersion duration was set at 4 hours prior to the commencement of surface characterization. The AFM scan was executed employing a cutting-edge Atomic Force Microscope by Bruker.

2.3 RESULT AND DISCUSSIONS

2.3.1 Characterization

To verify that the experimental drug had specific groups, an FT-IR spectra was obtained. Based on the investigation, peaks corresponding to N-H, O-H, C-H, and C-N stretching were identified. (Figure 2.2)[59].

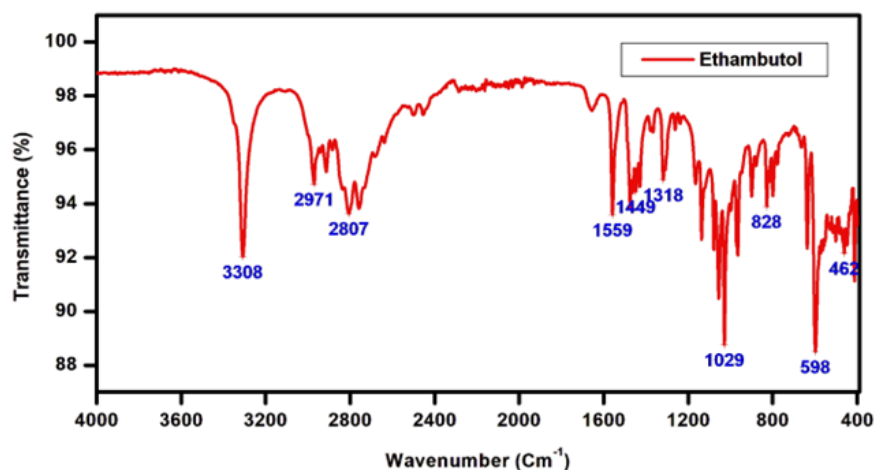


Figure 2.2: FT-IR spectrum of EBT

2.3.2 Weight Loss Study

a) Effect of inhibitor concentration on Corrosion rate and Inhibition efficiency

A crucial component of corrosion mitigation schemes is the impact of concentration of EBT drug on the extent of corrosion and its effectiveness for corrosion prevention. Generally, as the inhibitor concentration increases, corrosion rate tends to decrease, leading to higher inhibition efficiency. This trend occurs because a higher concentration of inhibitors provides more active sites for adsorption onto the metal surface, forming a protective barrier that hinders corrosion processes. However, there is often an optimal concentration range where inhibition efficiency is maximized, beyond which increasing the inhibitor concentration may yield diminishing returns. In order to conduct weight loss investigations and determine Inhibition efficiency (IE), corrosion rate (C_r), and surface coverage (θ) (Table 2.1, 2.2), a mild steel sample specimen was subjected to various inhibitor concentrations (200-1000 ppm) at temperatures 303-333 K in 0.5M H_2SO_4 . Experimental data has shown that raising the inhibitor concentration depresses the corrosion rate at all temperatures and it is because of a protective layer formed over the MS, which ultimately reduces rate of corrosion (Figure 2.3). It has also been learned from the experimental data that for all concentrations of EBT, corrosion rate increases as the temperature rises which may be attributed to active desorption with enhancing temperature. At the concentration of 1000 ppm the inhibitor showed best of its efficiency in 0.5M H_2SO_4 at 313K (Figure 2.4) and may be ascribed to the increased surface area covered by the adsorbed molecules over the metal surface[116].

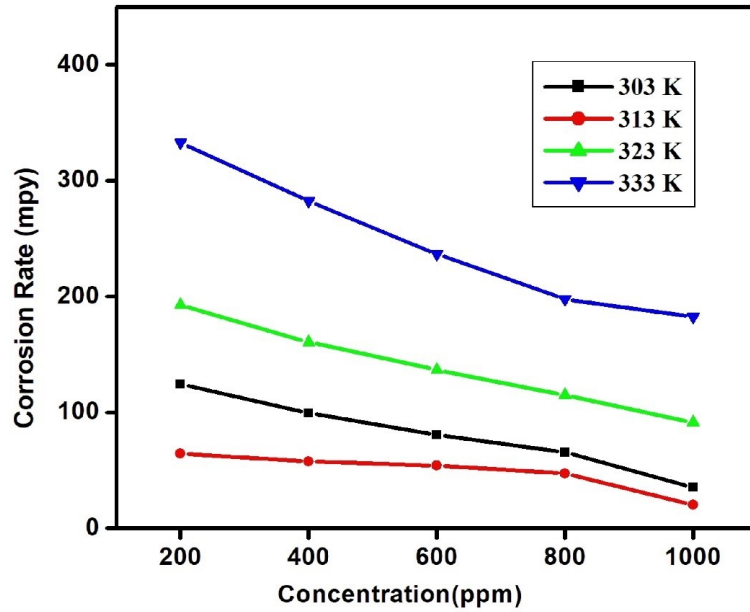


Figure 2.3: Rate of Corrosion of MS in 0.5M H₂SO₄ with 200-1000 ppm of EBT at 303-333 K

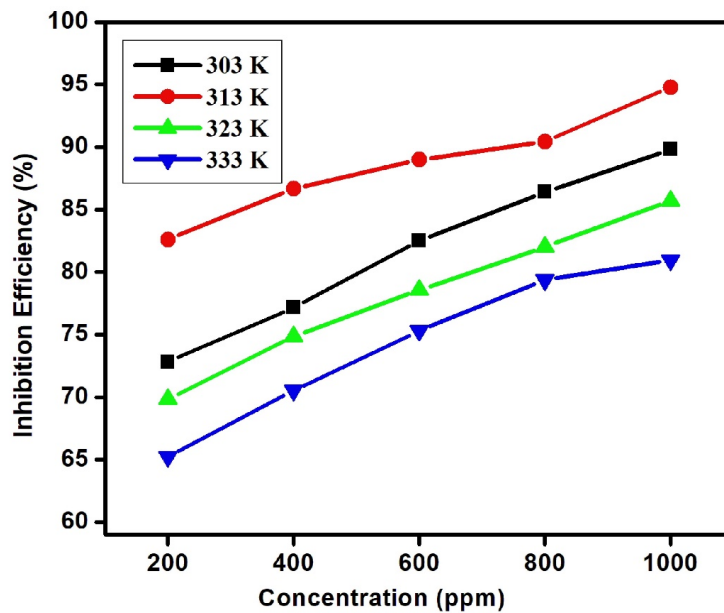


Figure 2.4: IE of EBT against MS in 0.5M H₂SO₄ at 303-333K with 200-1000 ppm of EBT

The desorption process from the metal surface is triggered by a reduction in surface area as the temperature rises. This resulted in the inference that higher temperatures result in a lessening in strength of the adsorption process, signifying the inhibitor's physisorption onto the metal surface.

Table 2.1: IE, C_r , and θ of EBT with mild steel at 303K and 313K temperature with different concentration range

Temp. (K)	303			313		
Conc. (ppm)	C_r (mpy)	θ	I.E. (%)	C_r (mpy)	θ	I.E. (%)
BLANK	348.14	-	-	583.05	-	-
200	124.64	0.65	72.82	64.41	0.83	82.61
400	99.43	0.72	77.18	57.74	0.87	82.61
600	80.84	0.78	82.52	54.22	0.89	88.99
800	65.77	0.79	86.41	47.32	0.90	90.43
1000	35.49	0.83	89.81	23.42	0.93	92.78

Table 2.2: IE, C_r , and θ of EBT with mild steel at 323K and 333K temperature with different concentration range

Temp. (K)	323			333		
Conc. (ppm)	C_r (mpy)	θ	I.E. (%)	C_r (mpy)	θ	I.E. (%)
BLANK	638.82	-	-	958.23	-	-
200	192.66	0.75	69.84	332.93	0.69	65.26
400	160.55	0.80	74.87	282.23	0.71	70.55
600	136.89	0.82	78.57	236.6	0.75	75.31
800	114.92	0.85	82.01	197.73	0.79	79.37
1000	91.26	0.88	85.71	165.62	0.83	80.95

b) Kinetic and Thermodynamic Parameters

The study primarily focused over justifying the deterioration properties of mild steel while concurrently investigating impact from temperature variations, with the goal of discriminating trends in inhibition efficiency and corrosion patterns across a temperature range spanning from 30°C to 60°C. This analysis was conducted in an acidic environment involving 0.5 M sulphuric acid (H_2SO_4), with the addition of corrosion inhibitors. The fluctuations in temperature induce various changes on the metal substrate, encompassing processes such as the adsorption, desorption, rearrangement, along with dissociation of inhibitors. Temperature's influence plays a significant role in corrosion phenomena and can be leveraged to get familiar with the underlying mechanisms of drug inhibition. By drawing the plot of $\log C_r$ versus $1/T$ (Figure 2.5), values of activation energy (E_a) and Arrhenius factor (A) can be calculated (Table 2.3) from the intercept and slope of a straight line respectively employing the following Arrhenius equation:

$$\log C_r = \frac{-E_a}{2.303RT} + \log A$$

Where, E_a : Apparent effective activation energy,

R: Molar gas constant

A: Arrhenius pre-exponential factor.

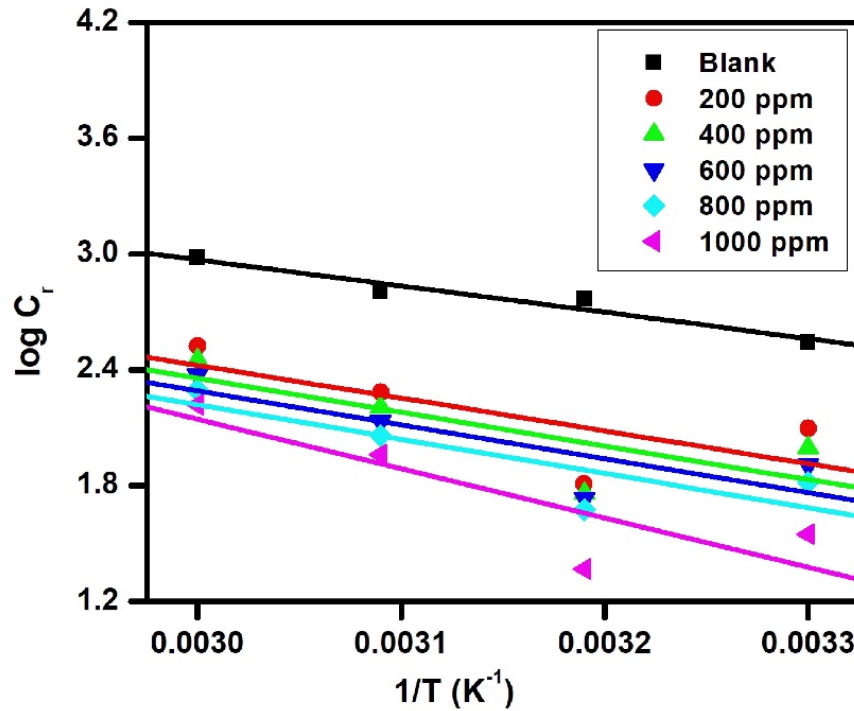


Figure 2.5: Arrhenius plot: $\log C_r$ vs $\frac{1}{T}$ at varying EBT concentrations.

reflected that the values of ' E_a ' and ' A ', showed an increment with increasing EBT concentration. The table revealed that the E_a values rise when EBT is incorporated as compared to the blank solution.

Table 2.3: Kinetic and Thermodynamic parameters of EBT with MS at different temperatures and inhibitor concentration range

Conc. (ppm)	E_a (kJ/mol)	A (10^5)	ΔH (kJ/mol)	$-\Delta S$ (kJ/mol/K)	ΔG (kJ/mol)			
					303 (K)	313 (K)	323 (K)	333 (K)
Blank	26.28	1.24	23.64	0.014	27.882	28.022	28.162	28.302
200	33.24	4.43	30.61	0.051	46.063	46.573	47.083	47.593
400	34.21	5.39	31.57	0.062	50.356	50.976	51.596	52.216
600	34.28	5.71	32.62	0.074	55.042	55.782	56.522	57.262
800	35.64	5.99	34.01	0.077	57.341	58.111	58.881	59.651
1000	49.59	23.14	46.95	0.079	70.887	71.677	72.467	73.257

As the temperature rises, an increment in activation energy tends to decrease the adsorption of the inhibitor. Due to the increased surface area exposure to the HCl solution, the

noticeable drop in adsorption rate promotes the extent of corrosion. The value of pre-exponential factor (A) is also high in inhibited solution in comparison with uninhibited medium. Physisorption is suggested by a rise in pre-exponential factor and activation energy values together with a positive shift in EBT concentration. This results in a reduction in interaction and an increase in the degree of corrosion. From the plot of $\log(C_r/T)$ versus $1/T$ (Figure 2.6), apparent entropy of activation ΔS and enthalpy of activation ΔH may be derived by applying the transition state equation based on the slope as well as the intercept of the lines, respectively.:

$$C_r = \frac{RT}{N_h} \exp\left(\frac{\Delta S}{R}\right) \exp\left(\frac{-\Delta H}{RT}\right)$$

(h: Planck's constant; N: Avogadro's number)

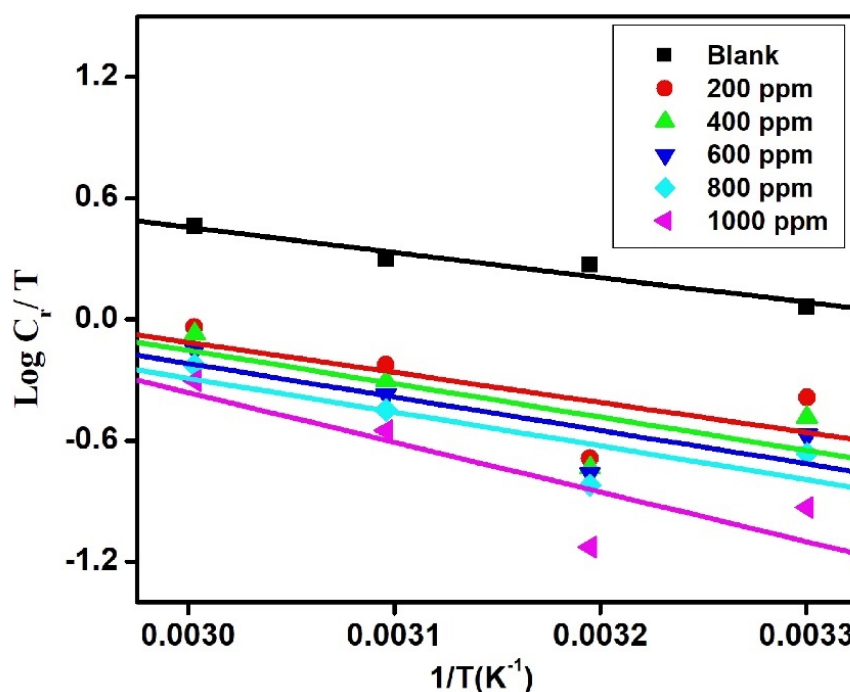


Figure 2.6: Plot of $\log C_r/T$ vs $1/T$ at different concentrations of EBT

The higher value of ΔH for the solution with EBT compared to the blank solution indicated a harder time for the degradation process to happen, which ultimately suggests greater shielding when an inhibitor is included. Interaction of inhibitor with MS surface increases the value of ΔH and resulting in drop in C_r value. E_a showed the trend in matching with ΔH for each concentration at every temperature (Figure 2.7). Also, the values of ΔS for EBT are extremely high in the uninhibited system when compared to the inhibited system, demonstrating that a decreasing pattern in disorder occurs while progressing from the reagent to the activated complex, illustrating that the activated complex is an attachment rather than a division in the rate-determining phase.

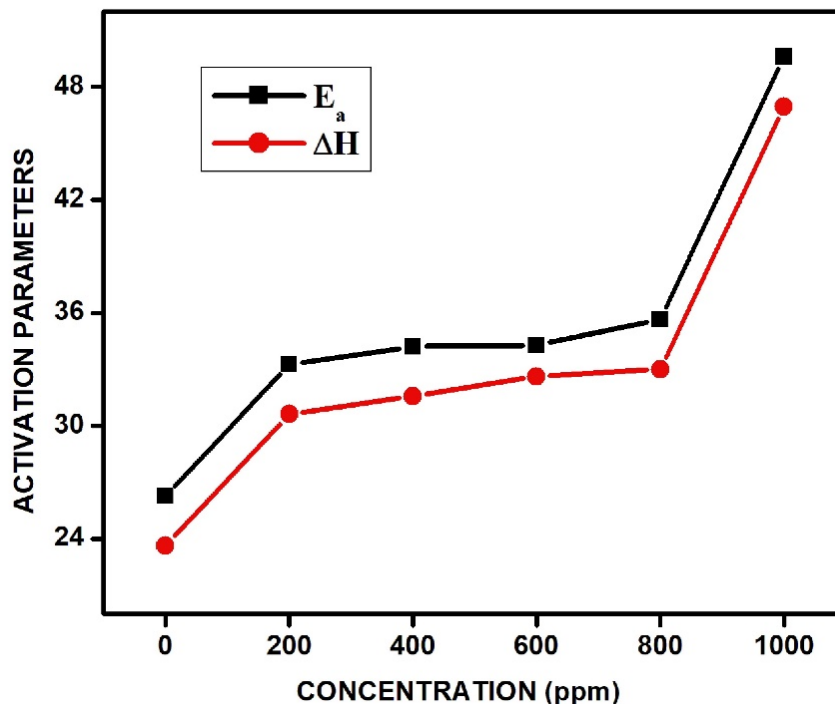


Figure 2.7: Plot of activation parameters, E_a and ΔH vs. concentration of EBT

Activation free energy, ΔG at each temperature of corrosion process was calculated using the formula:

$$\Delta G = \Delta H - T\Delta S$$

Positive values of ΔG showed the negligible variation with temperature, suggested that the conception and stability of activated complex reduced fairly with upsurge in temperature. However, ΔG values shown that the corrosion-activated complex became less durable with the inclusion of the drug.

c) Adsorption Isotherms

The adsorption isotherm is crucial to understanding the process of deterioration because it provide light on the characteristics of the connection among the drug and the MS. the adsorption isotherm is important in explaining the mechanism of corrosion. The adsorption isotherms proposed by Temkin, Freundlich, Langmuir, Parsons, Floary-Huggins, Frumkin, and Bockris-Swinkels are the most widely used isotherms. The isotherms were then fitted with the data computed from the various inhibitor concentrations. The Langmuir isotherm's fit to the experimental data was examined using the following calculation:

$$\frac{C}{\theta} = \frac{1}{K_{ads}} + C$$

'C' symbolizes inhibitor concentration.

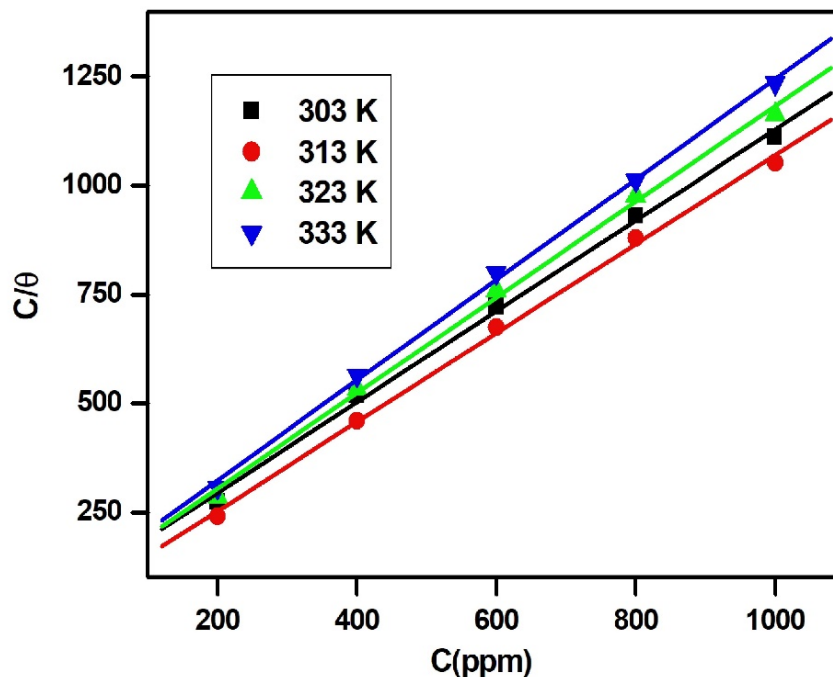


Figure 2.8: Langmuir adsorption isotherm for EBT.

Plot of C/θ against C as straight lines (Figure 2.8) on graph and the values of the regressive coefficient approaching almost close to unity confirmed Langmuir adsorption isotherm fitment with experimental data at all temperature range.

$$K_{ads} = \frac{1}{1 \times 10^6} \exp\left(-\frac{\Delta G_{ads}}{RT}\right)$$

This equation can also be expressed as:

$$\Delta G_{ads} = 2.303RT \log(1 \times 10^6 K_{ads})$$

K_{ads} value was calculated from the intercept of adsorption isotherm (Figure 2.8). R^2 and ΔG_{ads} of EBT at different temperatures were computed using adsorption isotherm and tabulated (Table 2.4).

Table 2.4: EBT Langmuir adsorption isotherm parameters at 303-333 K.

Temp. (K)	Slope	R^2	$K_{ads} \times 10^3$	ΔG_{ads} (kJ/mol)
303	1.042	0.998	14.08	-24.07
313	1.021	0.999	22.2	-26.05
323	1.098	0.998	11.84	-25.19
333	1.151	0.999	11.19	-25.82

ΔG_{ads} the adsorption free energy and K_{ads} adsorption-desorption equilibrium constant have the following relation: Higher values of K_{ads} indicate inhibitor-metal surface strong interactions and hence result in superior inhibition efficiency. A negative value

for ΔG_{ads} indicates spontaneous adsorption, which also indicated the persistence of the adsorbed inhibitor on the MS surface. ΔG_{ads} values equal or lower than -20 kJ mol^{-1} are in good agreement with physisorption while the values larger than -40 kJ/mole indicate chemisorption. For the EBT, the values of ΔG_{ads} lie between -20 to -40 kJ/mol , indicating physical as well as chemical adsorption of drug on MS surface.

2.3.3 Electrochemical Study

a) Linear Polarization Resistance

For MS surface in $0.5\text{M H}_2\text{SO}_4$ in an uncontrolled and inhibited solution comprising varied concentrations, the values of polarization resistance (R_p) were calculated and are shown in Table 2.5 where in a sudden increase in value from 26.95 to 70.91 is seen on introduction of inhibitor and reaches to a maximum of 131.2 for 1000 ppm. IE% also confirms the direct relation with concentration.

Table 2.5: Linear polarization resistance variables of MS with EBT in $0.5\text{M H}_2\text{SO}_4$

Conc. (ppm)	E_{corr} (mV (Ag/AgCl))	I_{corr} ($\mu\text{A}/\text{cm}^2$)	IE (%)	R_p (Ωcm^2)	IE (%)
Blank	-443.5	966.67	-	26.95	-
200	-429.7	374.9	61.22	70.91	61.99
400	-429	305.4	68.41	82.59	67.37
600	-434.9	226.5	76.57	115	76.57
800	-426.9	212	78.07	122.9	78.07
1000	-428.9	198.5	79.47	131.2	79.46

b) Potentiodynamic Polarization:

PDP curves (Fig 2.9) (Tafel plots) are obtained for MS incorporating different EBT concentrations (200-1000 ppm) into $0.5\text{M H}_2\text{SO}_4$ solution, and important electrochemical parameters were computed in Table 2.6, including E_{corr} (Corrosion Potential), I_{corr} (current density), and β_a and β_b (Tafel constants). I_{corr} is found to fall from $813 \mu\text{A}/\text{cm}^2$ to $234 \mu\text{A}/\text{cm}^2$ with the introduction of the inhibitor and achieve a value of $99.6 \mu\text{A}/\text{cm}^2$ at 1000 ppm of the inhibitor. Values of E_{corr} suggest that the inhibitory action is most likely caused by a mixed-type inhibitor.

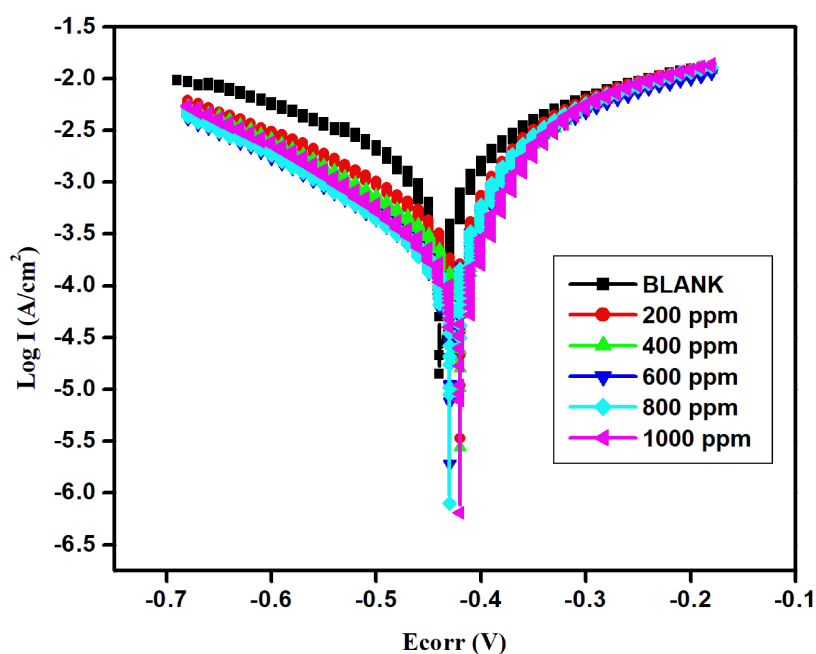


Figure 2.9: Curves of Potentiodynamic polarization for MS in 0.5M H₂SO₄ solution with 200-1000 ppm of EBT

Table 2.6: Tafel polarization variables of MS with EBT in 0.5M H₂SO₄.

Conc. (ppm)	β_a (mV/dec)	β_c (mV/dec)	E_{corr} (mV (Ag/AgCl))	I_{corr} ($\mu\text{A}/\text{cm}^2$)	IE (%)
Blank	95.3	-113.6	-436	813	-
200	45.3	-86.7	-423	234	71.22
400	51	-119.9	-423	205	74.78
600	50.9	-140.5	-428	151	81.43
800	44.3	-131.3	-427	137	83.15
1000	46	-76.7	-420	99.6	87.75

c) Electrochemical Impedance Spectroscopy

Electrochemical impedance spectroscopy is performed to simulate how surface interacts with the solution, with or without the studied drugs, for mild steel under 0.5M H₂SO₄, and the obtained Nyquist plot is shown in Figure 2.10. The imperfection of the semicircles in the Nyquist plots may be caused by dislocation, surface roughness, or inhibitor molecule adsorption. Nyquist plots (Figure 2.10) were validated with data fitment to basic electrical equivalent circuit (Figure 2.11) comprising solution resistance (R_s), charge transfer resistance (R_{ct}) and constant phase element (CPE).

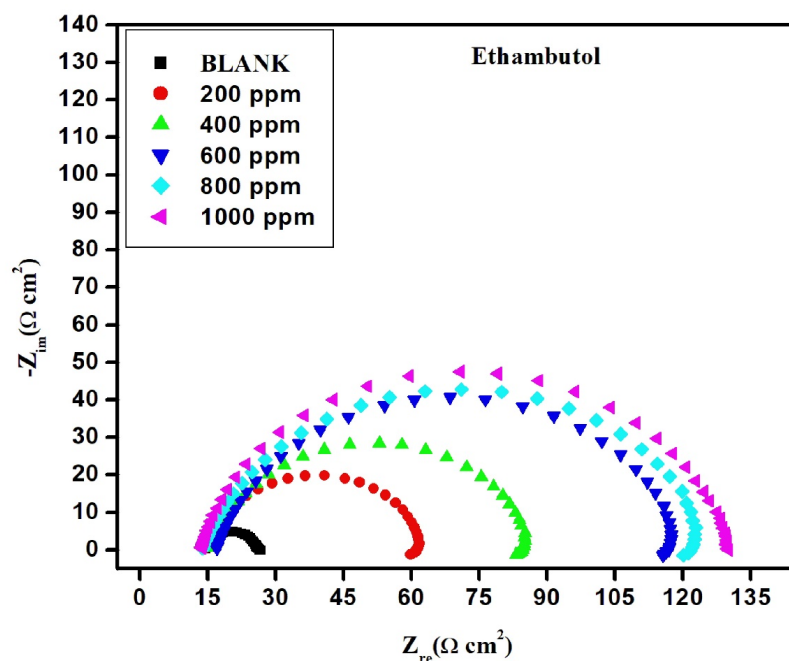


Figure 2.10: Nyquist plots for MS in 0.5M H₂SO₄ solution containing 200-1000 ppm of EBT

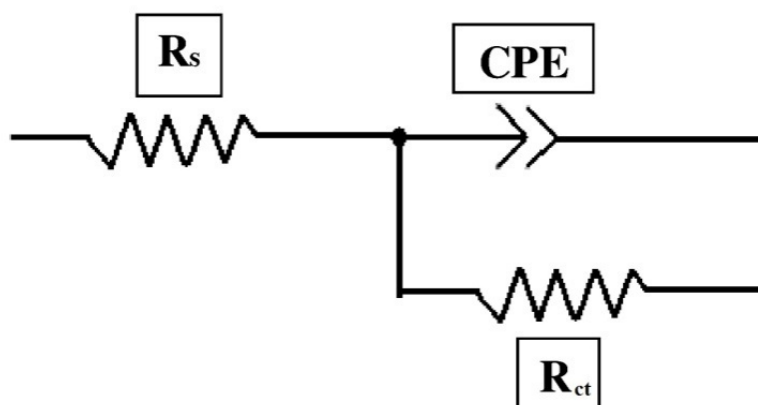


Figure 2.11: Equivalent Circuit Scheme

Impedance of constant phase element, Z_{CPE} may be calculated as follows:

$$Z_{CPE} = Y_0^{-1}(i\omega)^{-n}$$

Where; Y_0 - CPE constant; ω - angular frequency (rad s^{-1})

$i = (-1)^{1/2}$ and n - exponent to CPE[117] . Value of n defines the nature and units of CPE.

The following formula was used to compute the double layer capacitance, C_{dl} at varied concentrations.

$$C_{dl} = (Y_0 R_{ct}^{1-n})^{1/n}$$

A decrease in double layer capacitance, C_{dl} value, at the acid-metal interface with a gradual rise in drug doses may be used to examine how introducing an inhibitor altered the surface electrode property.

It is apparent from various parameters computed via EIS (Table 2.6) revealed as the EBT concentration rise, the R_{ct} values increased. As an accurate representation of electron transport across the surface, the R_{ct} value provides an inverse image of the rate of corrosion. A lower C_{dl} value implies the thickening of the adsorbed layer of inhibitor or protective layer. The fall of C_{dl} value with the increasing surface modulus shows that EBT inhibitor adsorption over the metallic surface reduces the roughness of the metal surface.

Table 2.7: EIS Parameters for Mild Steel with EBT in 0.5M H₂SO₄

Conc. (ppm)	R_s ($\Omega \text{ cm}^2$)	R_{ct} ($\Omega \text{ cm}^2$)	Y_0 ($10^{-6} \Omega^{-1} \text{ cm}^2$)	n	C_{dl} ($\mu\text{F cm}^{-2}$)	I.E. (%)
Blank	15.54	12.15	241.8	0.916	502.9	-
200	12.24	45.36	176.9	0.924	370.56	73.21
400	12.47	68.18	158	0.918	362.11	82.18
600	12.91	98.66	112.7	0.953	178.42	87.68
800	13.03	106.33	85.8	0.955	131.85	88.57
1000	13.95	120.43	74.6	0.979	90.68	89.91

2.3.4 Quantum Chemical Study

E_{HOMO} measures the compound's propensity to donate electrons, E_{LUMO} measures its propensity to gain electrons. For a molecule to act as an efficient inhibitor, it should have elevated E_{HOMO} and lower E_{LUMO} values, resulting in a small energy gap. The experimental compound has a higher E_{HOMO} and lower E_{LUMO} ($\Delta E = 8.84$), making it an efficient inhibitor.

The dipole moment gives the polarity, and a molecule with higher polarity tends to have dipole-dipole attractions. The dipole moment is related to inhibition efficiency. The number of electrons transferred (ΔN) provides information about the electron acceptance or donation property. A positive and higher value of ΔN indicates electron donation, while a negative and lower value indicates electron acceptance. For a molecule with a fraction of transferred electrons (ΔN) less than 3.6, there is an increased efficacy with a rise in electron-giving capability. A larger fraction of transferred electrons is associated with increased inhibition efficiency, while the least value of the fraction of

transferred electrons is associated with lower inhibition efficacy. For the present inhibitor, the ΔN value is less than 3.6, indicating its high electron donation capacity, making it an efficient corrosion inhibitor[118]. Chemical hardness is an imperative factor to indicate the propensity of the molecule for electrons acceptance. Positive value of chemical hardness of EBT indicates its electron donation characteristic resulting in lesser dissolution of the metal. The chemical hardness value for the compound is in agreement with experimental results. The various quantum chemical parameters of EBT have been mentioned in table 2.8 and the optimized structure and corresponding HOMO and LUMO for EBT are shown in Fig 2.12.

Table 2.8: Quantum Chemical parameters for EBT

E_{HOMO} (eV)	E_{LUMO} (eV)	I (eV)	A (eV)	χ (eV)	η (eV)	ΔE (eV)	μ (D)	ΔN
-7.94	4.31	7.94	-4.31	1.815	6.125	12.25	3.45	0.423

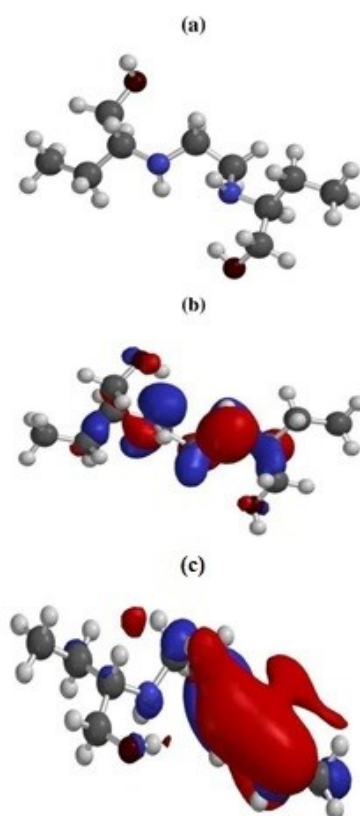


Figure 2.12: Optimized Structure(a) and the corresponding HOMO (b) and LUMO (c) for EBT

2.3.5 Surface Study: Atomic Force Microscopy (AFM)

The surface study of MS specimen was carried out in 0.5M H_2SO_4 , with or without EBT at the dosage of 1000 ppm with an immersion period of 4 hours by atomic force microscopic technique. The surface analysis quantified the surface roughness on a $10\ \mu m \times 10\ \mu m$ areal scale. The average surface roughness values of MS without the use of EBT were calculated to be 226.6 nm, and with the inhibitor, they were 89.3 nm (Figure 2.13). It clearly shows that the mild steel surface appeared to be fractured in the absence of the inhibitor with a corrosive medium, whereas with the inhibitor, the surface was less disintegrated due to protective film formation.

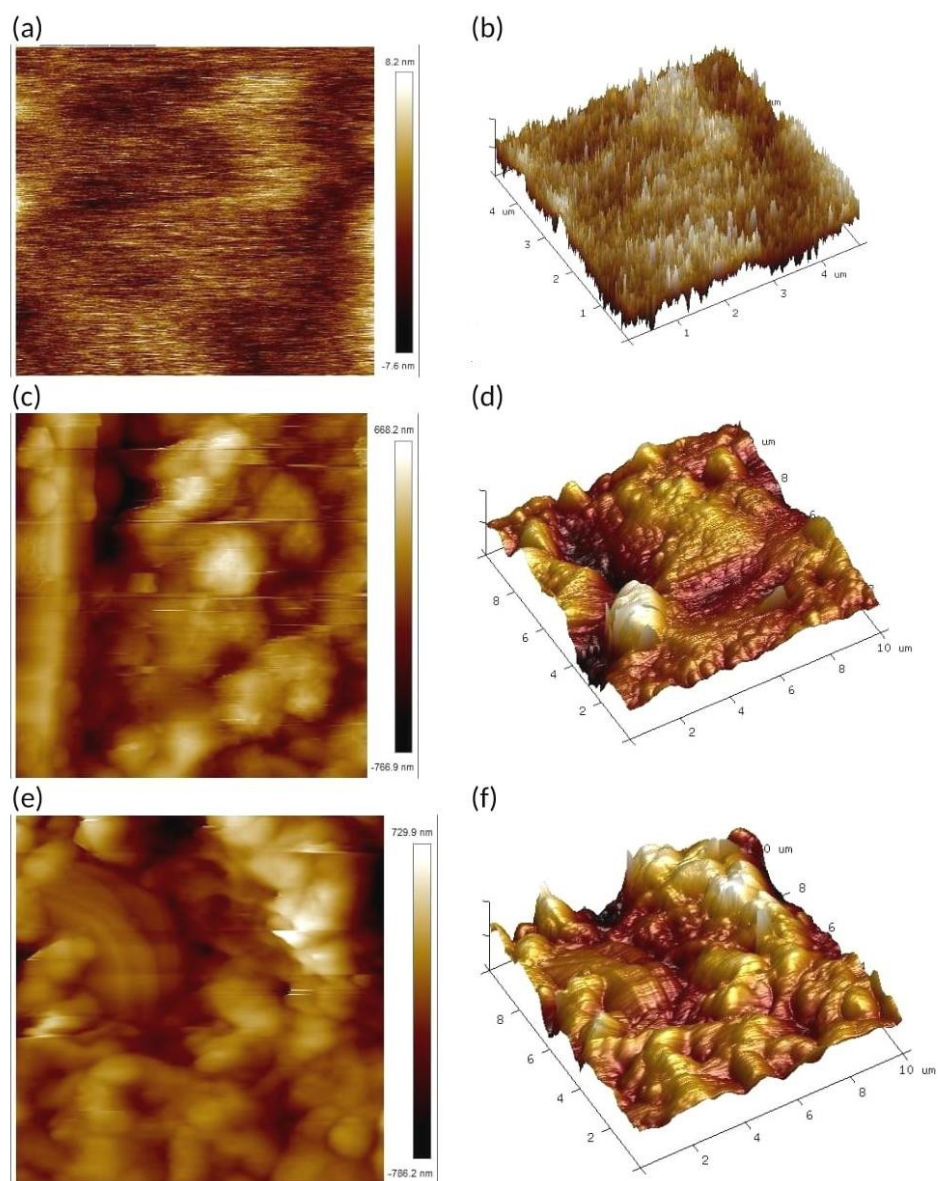
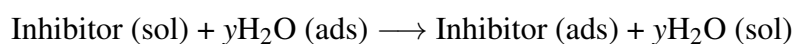


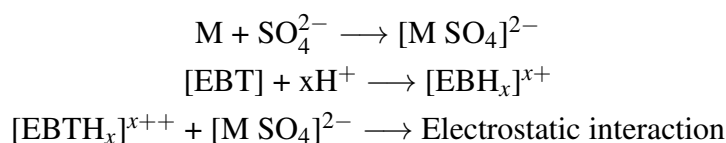
Figure 2.13: (a) & (b) are 2D, 3D images of polished metal (reference); (c) & (d) are 2D, 3D images of MS surface immersed in 0.5M H_2SO_4 (blank); (e) & (f) are 2D, 3D images of MS immersed in 0.5M H_2SO_4 with EBT

2.4 MECHANISM OF INHIBITION

Electrochemical and weight loss studies over on mild steel have been done for the in-depth analysis of the inhibitory behaviour of EBT in H₂SO₄ acid. Electrochemical studies illustrate the mixed type via preventing both anodic and cathodic reactions behavior of inhibitor in H₂SO₄. Thermodynamic and kinetic parameters derived from weight loss measurement justify the physisorption of EBT on MS surface in sulphuric acid solution. Electrochemical interactions between adsorbent and adsorbate are the driving force for physisorption. Metal surface in H₂SO₄ solution remain negatively charged due to adsorbed sulphate ions on it. Water molecules are adsorbed on metal substrate which are displaced from EBT molecules from the metal by displacement reaction as the dipole moment of inhibitor is greater than water.



The inhibitor EBT having electron rich heteroatoms (O and N), which are the sites for active adsorption; in sulphuric acid get easily protonated and prevail as neutral species as well as in protonated form existing in equilibrium with each other.



The interaction amongst protonated EBT molecules and oppositely charged MS results in physisorption and thus inhibition occurs at anodic site. The pronated inhibitor molecule may also compete with H⁺ ions of acid and get adsorbed directly on cathodic sites and hence inhibit corrosion at cathodic site by reduction of evolution of hydrogen gas[119]. Chemical quantum chemical study reveals strong interaction between metal and inhibitor through donation of electron from inhibitor to metal.

2.5 CONCLUSION

The suppression of mild steel corrosion by EBT in 0.5M H₂SO₄ was studied at a concentration range of 200-1000 ppm at 303-333 K temperature range, and the following conclusions were drawn

1. EBT inhibited corrosion of mild steel in 0.5M H₂SO₄ quite effectively, and as concentration rises, so does the EBT's effectiveness and the pace at which corrosion occurs.
2. EBT effectiveness drops with rise of temperature and it was found to be of maximum value of 92.78% at 313K.

3. Thermodynamic parameters of inhibitor's adsorption revealed spontaneous, exothermic and physisorption of EBT on metal.
4. Langmuir adsorption isotherm is followed at all temperature ranges by EBT inhibitor.
5. Potentiodynamic polarization experiments demonstrated the existence of mixed-type inhibition mechanisms for EBT and the co-existence of anodic and cathodic types of responses.

CHAPTER 3

ANTIDEPRESSANT DRUG SERTRALINE AS AN EFFICIENT CORROSION INHIBITOR FOR MILD STEEL

3.1 INTRODUCTION

Mild steel (MS) is a crucial component of engineering materials used in oil and gas refinement and extraction, boilers, process industries, water pipelines and petrochemical industries. Among various acids and a mixture of acids, hydrochloric acid is most commonly used at various concentrations to clean and remove rust or other corrosion-resulting products in many industries. Materials undergo severe regression due to corrosion in acidic media by adsorption of compounds physically or chemically[120]. There is an immediate need to resolve this problematic situation because it results in material, time, and financial losses. Towards this end, a variety of corrosion inhibitors have been investigated for corrosion prevention[121]. Presently, corrosion inhibitors have emerged as an environmentally sustainable approach to control corrosion, primarily due to their minimal usage requirements, ready availability and exceptional performance efficiency. These inhibitors demonstrate the ability to achieve substantial adsorption on the metal surface through physical or chemical interactions, thereby enhancing their corrosion control capabilities[122]. Formerly unused medications are currently being used to deal with the problem of solid waste storage concerns and additionally to offer an alternative harmless inhibitor for preventing energy. The entire expense of making or transporting chemical inhibitors that prevent corrosion leads to approximately 7% of the entire income allocated to the prevention of corrosion of metals and alloys usage in industry[123]. In general, pharmaceuticals belong to a number of prominent and widely adopted chemicals, since they are consumed on a regular and constant basis in our residences. Expired pharmaceuticals are wiped out in certain nations by placing them in pits beyond towns in arid regions, contaminating substances that are outdated medical pharmaceutical components in groundwater supplies. It contaminates the groundwater via these pharmaceuticals. All of these issues prompted interest and awareness in looking for innovative uses for outdated pharmaceuticals and drugs. An extensive study on the application of expired medicinal products as corrosion preventatives for certain

metals and alloys is now underway. Considerable endeavors have been dedicated to exploring the potential of expired pharmaceuticals for mitigating corrosion on metal surfaces, resulting in the development of a potent new class of corrosion inhibitors. These innovative inhibitors not only exhibit remarkable cost-effectiveness but also offer significant environmental advantages.

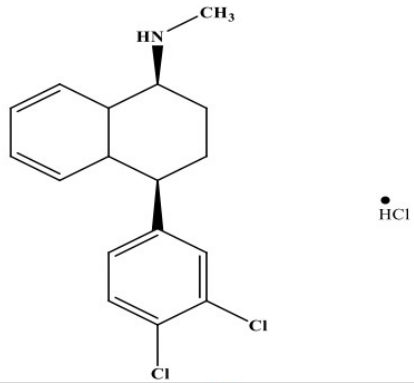
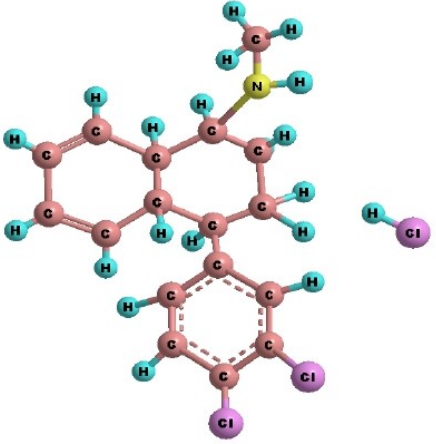
Drug Name	Sertraline (SRT)
IUPAC Name	(1S,4R)-4-(3,4-dichlorophenyl)-N-methyl-1,2,3,4,4a,8a-hexahydronaphthalen-1-amine hydrochloride
Molecular Formula	$C_{17}H_{20}Cl_3N$
Chemical Structure Formula	
3D Structure Formula	

Figure 3.1: Structural information of Sertraline

Sertraline [(1S,4R)-4-(3,4-dichlorophenyl)-N-methyl-1,2,3,4,4a,8a-hexahydronaphthalen-1-aminehydrochloride] (SRT) in stereoisomeric cis form is a widely prescribed medication belonging to the class of selective serotonin reuptake inhibitors (SSRIs). It is primarily used as an antidepressant to treat various mood disorders, including major depressive disorder, obsessive-compulsive disorder (OCD), panic disorder, and social anxiety disorder. Sertraline works by increasing the levels of serotonin, a neurotransmit-

ter in the brain, which can help improve mood, reduce anxiety, and alleviate symptoms of depression. It is typically administered orally in the form of tablets or liquid and is considered safe and effective when prescribed and monitored by healthcare professionals. Sertraline's broad spectrum of applications and relatively favorable side effect profile have made it one of the most commonly prescribed antidepressant medications globally, providing relief and improved quality of life for millions of individuals struggling with mental health conditions. The present study aims to present the efficient anti-corrosive properties of the SRT containing active centers along with lone pair of electrons and delocalized aromatic π -electrons by virtue of which the compound shows the potential of being used as corrosion inhibitor over mild steel in 1M HCl media. The anti-corrosive property of SRT for the corrosion of mild steel in acidic media was evaluated using gravimetric analysis at various temperatures, electrochemical studies (Tafel and EIS) and surface topography (AFM). Also, utilizing Density Functional Theory (DFT), quantum chemical calculations were undertaken to examine the interactions and energy levels between the corrosion inhibitor and mild steel surface.

3.2 EXPERIMENTAL AND METHODS

3.2.1 Preparation of metal sample and test solution

Mild steel coupons, measuring 10 cm^2 and 0.1 mm thick, were employed for the mass reduction trials. The chemical composition of the mild steel was nickel (0.10%), carbon (0.14%), copper (0.14%), manganese (0.15%), silicon (0.20%), and the rest iron (wt.%). The coupons were consecutively polished with 200-1200 grit sizes emery paper to achieve a smooth specimen surface. Subsequently, they underwent a series of treatments, including washing with double-distilled water, sonicating, degreasing with acetone, followed by desiccation in air, and final drying in an oven in all experimental studies. Sertraline (SRT), an anti-depressant drug, was used in tablet form as Sertraline hydrochloride (brand name- Zoloft) purchased from the local market. It was extracted and utilized as a corrosion inhibitor. Dilution of HCl (1M) with double-distilled water was done to prepare the test solutions with different inhibitor concentrations of the SRT. The SRT tablet was characterized through Fourier Transform Infrared (FT-IR) spectroscopy using a Perkin Elmer FT-IR Spectrophotometer (model: Spectrum 2) in the wavenumber range of $4500 - 500\text{ cm}^{-1}$.

3.2.2 Weight Loss Study

Gravimetric approach was used in this study because it is the most efficient and feasible method for estimating inhibition efficiency and corrosion rate. The chosen material for this investigation was mild steel, characterized by a density of 7.86 g/cm^3 and an area of 10 cm^2 . Gravimetric investigations were carried out with varying inhibitor

concentrations along with a blank solution. The mild steel coupons were immersed at 308-338 K temperatures and carried out for 3 hours of immersion time. All the experiments have been done in triplicate, and average outcomes have been taken. The IE%, θ , and C_r have been used to quantify the inhibitory performance utilizing the calculation:

$$IE\% = \frac{W_o - W_i}{W_o} \times 100$$

$$\theta = \frac{W_o - W_i}{W_o}$$

Where; IE (%): Inhibition efficiency; θ : Surface coverage; W_o : Weight loss of metal specimen uninhibited solution ; W_i : Weight loss of metal specimen inhibited solution;

$$C_r = \frac{534 \times W}{A \times t \times d}$$

Where W - weight loss (mg); t - time of immersion (hours); Cr - Corrosion rate; A - Surface area of the coupon cm²; d – density of metal g/cm³.

3.2.3 Electrochemical Study

For electrochemical studies, a Gamry Interface Potentiostat (IFC1010-28152) was used. These measurements were conducted using a three-electrode cell assembly on a mild steel (MS) surface with a contact region of 1 cm² at room temperature. Platinum wire, Ag/AgCl, and the mild steel (MS) coupon were used as the counter electrode, reference electrode, and working electrode, respectively. To improve an unstable or marginally stable cell system and avoid noise during the electrochemical process, keep the cell with the tested solution steady according to their positions. Afterward, the open circuit potential (E_{OCP}) vs. time (0-600s) was measured to determine the exact stability of the inhibitors, which aids in noise reduction and output stabilization. It also helps to determine the charge process transitions from unstable to stable behavior as well as demonstrate the inhibitors' adsorptive nature in comparison to an uninhibited solution. The drug molecule compares the uninhibited solution to the positive and negative OCPs, adsorbing and shifting them. After the E_{OCP} measurements, electrochemical and potentiodynamic polarization were performed using linear polarization resistance and the Tafel plots, which were extrapolated anodically or cathodically to obtain corrosion current and potential, I_{corr} and E_{corr} respectively. These measurements were done by simply scanning the electrode potential from -0.02 V to $+0.02$ V and from $+250$ mV to -250 mV correspondingly, with a rate of scan of 1 mV/s with regard to the corrosion potential[124]. The relationship between linear polarization resistance and inhibition efficiency is shown as :

$$IE\% = \frac{(R_p' - R_p^{\circ})}{R_p^{\circ}} \times 100$$

Where R_p° : polarization resistance in blank solution, R_p' : polarization resistance with inhibitor To get Nyquist plots, the EIS was performed using AC signals by the use of 10^5 Hz to 0.2 Hz of frequency range with amplitude of 10 mV. Using provided formula, the inhibition efficiency of inhibitor was determined by using charge transfer resistance (R_{ct}) values.

$$IE\% = \frac{(R_{ct}' - R_{ct}^{\circ})}{R_{ct}'} \times 100$$

Where, R_{ct}' : charge transfer resistance with inhibitor and R_{ct}° : charge transfer resistance in blank solution. Calculating the values of I_{corr} from the extrapolation of the anodic and cathodic Tafel plot curves. This method gave significant understanding into the corrosion characteristics of the substance under investigation through accurately estimating the corrosion current densities. The inhibitory performance (IE%) of the inhibitor was calculated using current densities (I_{corr}) by the formula:

$$IE\% = \frac{I_{corr}^{\circ} - I_{corr}'}{I_{corr}^{\circ}} \times 100$$

Where I_{corr}° is the corrosion current density in 1 M HCl, and I_{corr}' is the corrosion current density at various concentrations of the inhibitor.

3.2.4 Quantum Chemical Study

Using Gaussian 16 software, theoretical analyses were employed to assess the DFT variables. The optimized structure of Sertraline and its associated HOMO and LUMO were obtained using DFT calculations with the B3LYP method and the 6-31 G* basis set. This study determined various parameters like highest occupied orbital energy (E_{HOMO}), lowest unoccupied orbital energy (E_{LUMO}), the dipole moment (μ), and energy barrier (ΔE) evaluated. Also, other parameters like Ionization Potential (I), Electron Affinity (A), number of transferred electrons (ΔN), Electronegativity (χ), Global hardness (η) using the following equations[125]: Ionization potential (I) measures the tendency of a chemical species to lose electrons and is related to the (E_{HOMO}) by the expression:

$$I = -E_{HOMO}$$

Electronegativity is the atom's propensity for grabbing electrons and can be calculated using the following equation:

$$\chi = (I + E)/2$$

Electron affinity (A) is the tendency of a chemical species to gain electrons and is associated with E_{LUMO} by the expression:

$$A = -E_{\text{LUMO}}$$

The formula for calculating chemical hardness (η), which expresses an atom's ability to resist a charge exchange, is as follows:

$$\eta = (I - A)/2$$

The portion of electrons that are transferred during a chemical process is given by the equation:

$$\Delta N = \frac{\chi_{\text{Fe}} - \chi_{\text{inh}}}{2(\gamma_{\text{Fe}} + \gamma_{\text{inh}})}$$

Where γ_{Fe} – electronegativity of iron (7 eV/mol), η_{Fe} – global hardness of iron (0). The values have been reported in the literature.

3.2.5 Surface Study

The surface study was carried out using Atomic Force Microscope (AFM) with Peak Force Tapping technology and a sharp tip 5 m tall and less than 10 nm in diameter at the apex. The specimen was submerged in 1 M corrosive media and with inhibitor solution in corrosive media (50 ppm) for 4 hours prior to surface characterization.

3.3 RESULTS AND DISCUSSION

3.3.1 Characterization

The Infrared spectra of the compound was studied between 4000-500 cm^{-1} and after close scrutiny of the spectrum (Figure 3.2). The peaks at 2916 cm^{-1} (aliphatic C-H stretching), 2682 and 2461 cm^{-1} (N-H stretching), 2244 cm^{-1} (C-N stretching), 1584 cm^{-1} (C=C stretching), 1454 cm^{-1} (aliphatic C-H deformation), 1042 cm^{-1} (C-H stretching), 781 cm^{-1} (aromatic C-H stretching), which are the characteristics of Sertraline. These results are in good agreement with earlier studies[124].

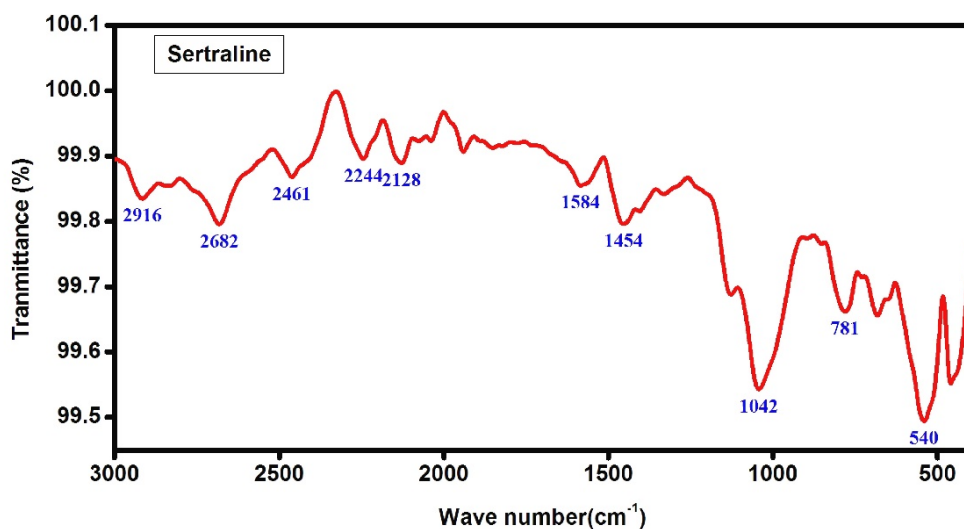


Figure 3.2: FT-IR Spectrum of SRT

3.3.2 Weight Loss Study

a) Effect of temperature and concentrations:

The efficacy of SRT over MS in hydrochloric acid with and without concentrations ranging (10-50 ppm) of inhibitor was evaluated at various temperatures (303-333K) using the gravimetric study.

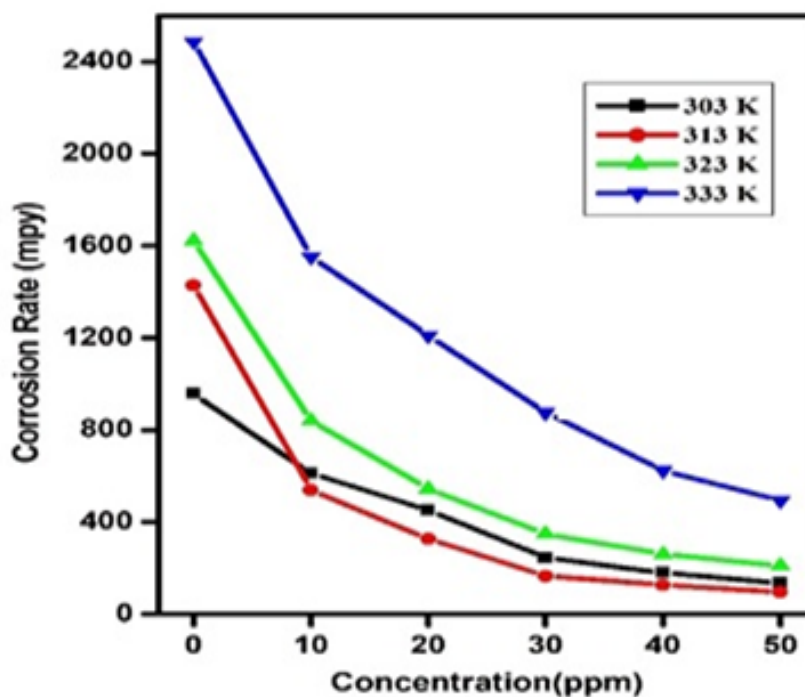


Figure 3.3: Corrosion Rate (mpy) of mild steel surface in 1 M HCl at 10-50ppm concentration of SRT and 303-333K temperature

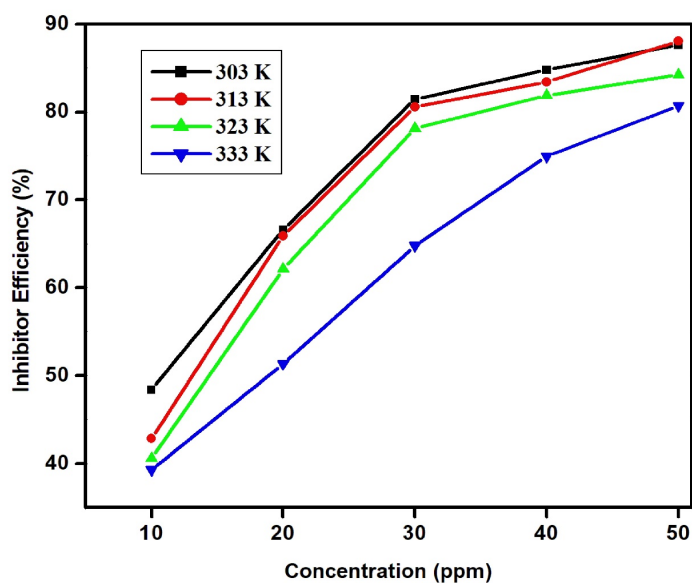


Figure 3.4: Inhibition efficiency (%) of mild steel surface in 1 M HCl at 10-50ppm concentration and 303-333K temperature

It is revealed from Table 3.1, 3.2 that with the rise in SRT dosage from 10-50 ppm concentration range, inhibition efficiency (%) increases (Figure 3.4), and corrosion rate decreases (Figure 3.3). On the other hand, as the temperature rises, the extent of corrosion also increases, and inhibition potential declines. Furthermore, it is clear that although surface coverage (θ) of SRT diminishes with higher temperatures, it expands with concentration (10–50 ppm). At 50 ppm at 313 K, the highest possible inhibitory effectiveness is determined to be 93.37%. This finding suggests that chemisorption on MS substrate is reinforced by an intense chemical interaction that takes place through the exchange of electrons or transmission of charge from SRT to the vacant d-orbital of MS.

Table 3.1: IE, C_r , and θ of Sertraline with mild steel at 303K and 313K temperature with different concentration range

Temp.	303 K			313 K			
	Conc. (ppm)	C_r (mpy)	θ	IE. (%)	C_r (mpy)	θ	IE. (%)
Blank		956.54	-	-	1428.05	-	-
10		611.78	0.48	48.23	539.11	0.62	62.25
20		451.23	0.66	66.46	326.17	0.77	77.16
30		245.05	0.78	78.54	165.62	0.88	88.4
40		179.14	0.83	83.96	126.75	0.91	91.12
50		135.2	0.87	87.08	94.64	0.93	93.37

Table 3.2: IE, C_r , and θ of Sertraline with mild steel at 323K and 333K temperature with different concentration range

Temp.	323 K			333 K			
	Conc. (ppm)	C_r (mpy)	θ	I.E. (%)	C_r (mpy)	θ	I.E. (%)
Blank		1622.4	-	-	2485.99	-	-
10		839.93	0.46	46.04	1553.11		37.53
20		544.18	0.58	58.83	1210.04	0.51	51.33
30		348.14	0.74	74.38	875.42	0.65	64.79
40		260.26	0.81	81.27	623.61	0.75	74.92
50		209.56	0.86	85.87	493.48	0.8	80.15

b) Activation and Adsorption Parameters

Temperature influences corrosion substantially, and this effect could potentially utilized to clarify the process of deterioration prevention. Correlation between temperature and corrosion rate is given by Arrhenius equation[126].

$$\log C_r = \frac{-E_a}{2.303RT} + \log A$$

Where E_a : apparent energy of activation, A: Arrhenius pre-exponential factor and R: molar gas constant

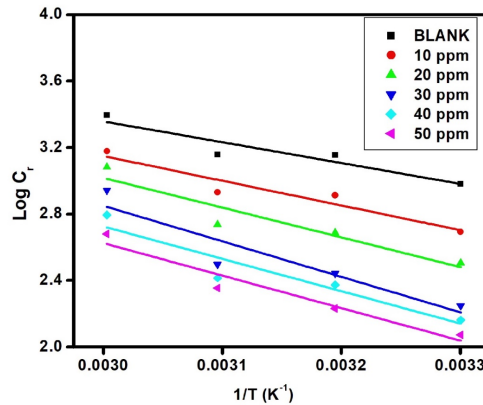


Figure 3.5: Arrhenius Plot in blank and with different concentrations of SRT in 1 M HCl for mild steel corrosion.

The intercept of graph of the log of corrosion rate against inverse of temperature (Figure 3.5) provided a pre-exponential component (A), while the slope of curve provided apparent activation energy (E_a). According to Table 3.3, the inclusion of SRT into the corrosive medium resulted in increased A (pre-exponential factor) and E_a (activation energy) values and when compared to the alone corrosive solution. These findings indicate that the presence of SRT influenced the corrosion process, leading to higher activation energies and pre-exponential factors, which may imply enhanced corrosion inhibition properties. In addition, it also shows binding of the SRT on MS substrate and this attainability of adsorption rate makes the weight loss method efficient.

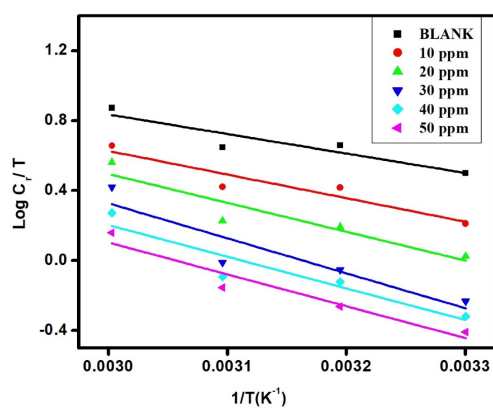


Figure 3.6: Transition state plot in blank and with different concentrations of Sertraline in 1 M HCl for mild steel corrosion.

Table 3.3: Activation and thermodynamic parameters of corrosion in different sertraline concentrations in 1 M HCl

Conc. (ppm)	Activation energy, E_a (kJ/mol)	Pre-exponential factor, A ($\times 10^3$)	Enthalpy of Activation, ΔH (kJ/mol)	Entropy of Activation, $-\Delta S$ (kJ/mol/K)
Blank	25.07	20.43	22.43	0.115
10	26.75	20.37	24.11	0.115
20	28.5	27.22	25.86	0.112
30	37.54	50.71	33.9	0.092
40	38.04	273.79	35.01	0.083
50	38.57	422.81	35.93	0.095

Table 3.4: Free energy of activation of Sertraline with MS at different temperatures and inhibitor concentration range

Conc. (ppm)	Free Energy of Activation, ΔG (kJ/mol)			
	303 (K)	313 (K)	323 (K)	333 (K)
Blank	57.28	58.43	59.58	60.73
10	58.96	60.11	61.26	62.41
20	59.8	60.92	62.04	63.16
30	61.78	62.7	63.62	64.54
40	60.16	60.99	61.82	62.65
50	64.72	65.67	66.62	67.57

The transition state equation calculates the ΔH and ΔS [127].

$$C_r = \frac{RT}{N_h} \exp\left(\frac{\Delta S}{R}\right) \exp\left(-\frac{\Delta H}{RT}\right)$$

Where ΔH : Apparent enthalpy of activation , N_h : product of Avogadro's number and Plank's constant, ΔS : Apparent entropy of activation.

Log C_r/T against $1/T$ was plotted, and it was observed to be a straight line (Figure 3.6). The ΔH values (enthalpy change) and ΔS values (entropy change) were determined by evaluating the slope and the intercept of the curve, and these values were subsequently recorded in table 3.3. This methodology allowed for the quantitative characterization of the thermodynamic parameters associated with the studied process. It is evident that the suppressed system has a higher enthalpy of activation values than the free acid solution with SRT, indicating a higher protection efficiency. The value of enthalpy of activation (ΔH) are positive, which leads to an endothermic process, which signifies attributing nature to chemisorption. In contrast, the negative value leads to an exothermic process, indicating either physisorption or chemisorption. These results suggest that the adsorption rate is high on the metal substrate, elevating the heat transfer and reaction rate and increasing their efficiency. The lower value of entropy of activation for SRT at all concentration than the uninhibited solution, suggesting the formed activated complex is an association instead of a dissociation in the rate-determining step. By using following formula, the change in free energy of activation at all temperature ranges for corrosion process can be determined.

$$\Delta G = \Delta H - T\Delta S$$

The adsorption by SRT was purely chemisorption as ΔG values are higher than -40kJ/mol across the series (Table 3.4). These results indicate the instability of activated complex and with increase of concentration of inhibitor, values increased indicating non probability of formation of activated complex.

The interaction of metal with inhibitors examined with the aid of adsorption isotherm. Various experimental adsorption data were applied to different isotherm adsorption models such as Freundlich, Temkin, Langmuir, El-Awady isotherms of adsorption process. SRT inhibitor follows with Langmuir adsorption isotherm (Figure 3.5) indicating monolayer adsorption. The surface coverage (θ) is directly linked to the adsorption isotherms, depicting the relationship between surface coverage, inhibitor concentration (C) and equilibrium constant (K_{ads}) as follows:

$$\frac{C}{\theta} = \frac{1}{K_{ads}} + C$$

The plot of $\frac{C}{\theta}$ vs. C yields straight lines at all studied temperatures, specifying that the experimental results fit the isotherm with an estimated regression coefficient (R^2) value around 1 (Figure 3.7). The equilibrium constant values were calculated by the inverse of the intercept of the fitted lines, and with an increase in temperature, the equilibrium

constant value decreases. The extent of interaction between SRT and MS is represented by K_{ads} , implying that larger values of K_{ads} shift the adsorption in a positive direction, showing that the fitted isotherm was unfavorable at higher temperatures. Values of ΔG_{ads} evaluated by the given expression are reported in Table 3.4.

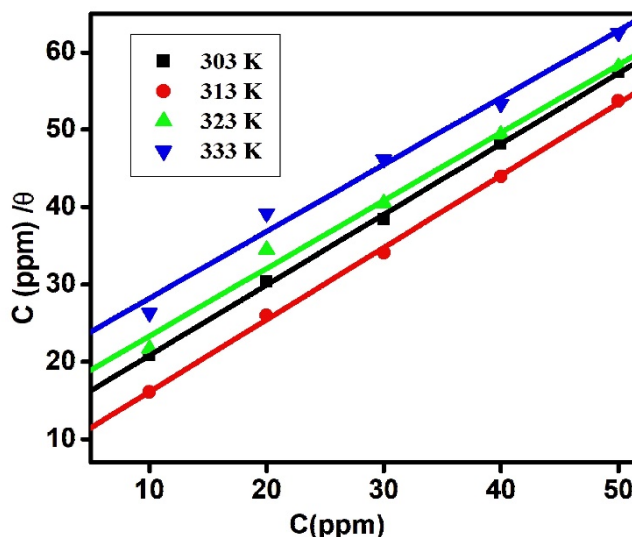


Figure 3.7: SRT adsorption on mild steel surface using the Langmuir isotherm in 1 M HCl

$$\Delta G_{ads} = -2.303RT \log(1 \times 10^6 K_{ads})$$

where, ΔG_{ads} , R , T are Gibbs free energy of adsorption, gas constant, and temperature (Kelvin), and 10^6 shows the concentration of water in ppm. The values of Gibbs free energy are negative, indicating the stability and spontaneity of the chemical reaction occurring at the interface of the MS substrate. Values close to -20 kJ/mol or below are often indicative of physical adsorption with electrostatic interactions, whereas values over -40 kJ/mol are representative of chemisorption with chemical bonding. The studied inhibitor SRT is favorable to physisorption, as well as chemisorption.

Table 3.5: Parameters of adsorption computed from Langmuir isotherm of adsorption

Temp. (K)	Slope	R^2	$K_{ads} \times 10^3$	ΔG_{ads} (kJ/mol)
303	0.9117	0.999	85.48	-28.61
313	0.9326	0.995	147.06	-30.97
323	0.877	0.994	68.77	-29.92
333	0.865	0.993	51.15	-30.02

3.3.3 Electrochemical Study

a) Linear Polarisation Resistance

The inhibition efficiency and polarization resistance (R_p) in presence and absence of varied Sertraline dosage in acidic solution for MS substrate were measured and enumerated in Table 3.6. The R_p at 50 ppm inhibitor concentration was maximum and increased from 50.35 of the uninhibited to 71.80, 84.54, 89.32 and 91.92 suggesting that as concentration of SRT increases, so does its ability to stop corrosion.

Table 3.6: Linear polarization resistance variables of mild steel in blank and in the presence of Sertraline inhibitor at various concentrations in 1 M HCl.

Conc. (ppm)	E_{corr} (mV (Ag/AgCl))	I_{corr} ($\mu A/cm^2$)	I.E. (%)	R_p (Ωcm^2)	I.E. (%)
Blank	-754.1	1157	-	22.51	-
10	-443.1	574.6	50.34	45.34	50.35
20	-430.3	326.4	71.79	79.82	71.8
30	-438	178.9	84.54	145.6	84.54
40	-436.9	123.6	89.32	210.8	89.32
50	-443.7	93.56	91.91	278.5	91.92

b) Potentiodynamic Polarization (Tafel)

PDP analysis was performed to study the passivity and passive stability of the MS, compactness of the passive film, corrosion potential, and corrosion resistance ability of the material. In this investigation, polarization curves were generated when exposed to 1M HCl, both in the uninhibited and inhibited of diverse amount (ranging from 10 to 50 ppm) of SRT (Figure 3.8). The electrochemical variables, like Tafel constants (β_a and β_c), E_{corr} , I_{corr} , values were then estimated using the graph. Furthermore, the inhibition efficiency of SRT was evaluated and compiled in Table 3.7. This comprehensive analysis allowed for a detailed assessment of the inhibitive properties of SRT in mitigating the degradation of MS in the aggressive environment.

This analysis revealed that SRT behaved as mixed-type inhibitors when bonded on the MS substrate, suppressing both the reduction and oxidation process due to their minimal changes on such reactions, with the E_{corr} remaining relatively close to that of the uninhibited sample. It is observed that the SRT adsorbed on MS at geometrical sites and formed a protective layer, causing a remarkable shift in the E_{corr} to a more negative side and lowers current densities by altering the anodic and cathodic Tafel curves. This curve starts with an anodic reaction having an active region, and on rising the concentration of SRT, the I_{corr} values increase, and an oxidation reaction takes place. At the mid-point, this current density starts to decline, and the corrosion potential rises to have the material's passive region[128]. It is seen from the result that the inhibited solution caused a significant reduction in I_{corr} value compared to that of the uninhibited solution.

By rising doses of the SRT from 10-50 ppm, the I_{corr} value further reduced, and thus, I.E. (%) increased. At 50 ppm, the efficacy of SRT reaches to 88.36%. From this study, it is concluded that the SRT gives better handling to MS surface and highest inhibition efficiency.

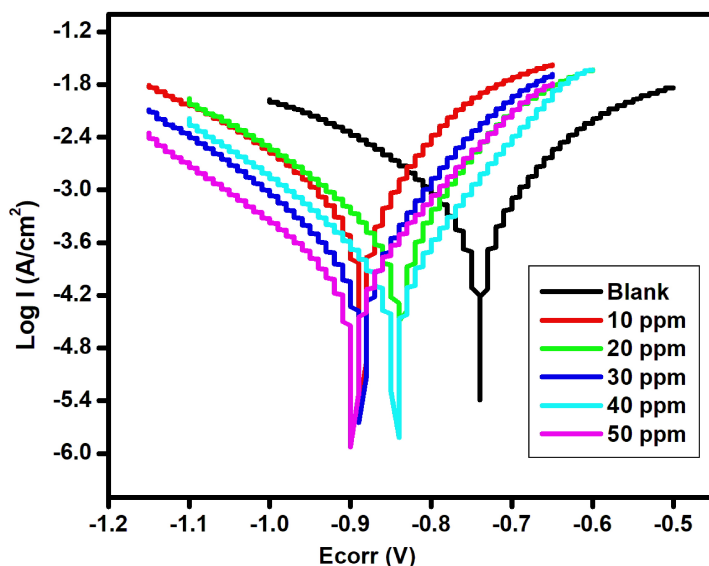


Figure 3.8: Tafel plot for mild steel in 1N HCl solution containing various Concentrations of SRT

Table 3.7: Tafel polarization parameters of mild steel in the presence of Sertraline in 1M HCl

Conc. (ppm)	β_a (mV/dec)	β_c (mV/dec)	E_{corr} (mV (Ag/AgCl))	I_{corr} ($\mu\text{A}/\text{cm}^2$)	IE (%)
Blank	93	117.4	-432	635	-
10	69.3	95.1	-428	204	67.87
20	77.7	108.2	-418	182	71.34
30	82.7	113.3	-427	105	83.46
40	89.5	125.9	-428	89.3	85.94
50	92	112.9	-439	73.9	88.36

c) Electrochemical Impedance Spectroscopy

EIS was utilized to examine the working process of SRT and the surface characteristics. The mild steel Nyquist graph in acidic medium uninhibited and inhibited different SRT doses (Figure3.7) and these spectra were recorded throughout a range of frequency from 1,00,000Hz to 0.2Hz at open network voltage.

Figure 3.9 displays the Nyquist plots of mild steel immersed in tested corrosive media with exclusion and inclusion of various concentrations of SRT. The perfection of semi-circles showing the optimal position, surface uniformity, specimen surface consistency and penetration of inhibitor[129]. The concentration of SRT enhanced the dimensions of the impedance plots, indicating that the prohibitive components of the SRT produced a layer of coating on the MS substrate in corrosive media. These studies focused on whether the investigated inhibitor formed a preventing layer over mild steel surface. The rising value of R_{ct} (Charge Transfer Resistance) and falling values of C_{dl} (Double Layer Capacitance) signified the presence of coating formed on the substrate by the SRT. If both C_{dl} and R_{ct} values rise at any point when moving from low to high concentration of inhibitor, represent a decreasing trend for the formation of an oxide layer on the substrate and an increment trend for the effectiveness of the developed coating as a protective layer respectively[130].

Uncoated sample with the tested solution gave R_{ct} value of $18.32 \Omega\text{cm}^2$ in HCl and C_{dl} value of $438.91 \mu\text{Fcm}^{-2}$ in HCl and R_s value of $4.32 \Omega\text{cm}^2$ which shows ion migration-induced resistance value to current flow through the solution. The introduction of SRT into the tested solution gave significant results at 50 ppm with respect to double-layer capacitance having $74.03 \mu\text{Fcm}^{-2}$ and charge transfer resistance $273.34 \Omega\text{cm}^2$ at 50 ppm. The SRT showcases better efficiency of the developed coating on the substrate in 1M HCl due to it achieving the lowest C_{dl} value to $74.03 \mu\text{Fcm}^{-2}$ and the highest R_{ct} value to $273.34 \Omega\text{cm}^2$.

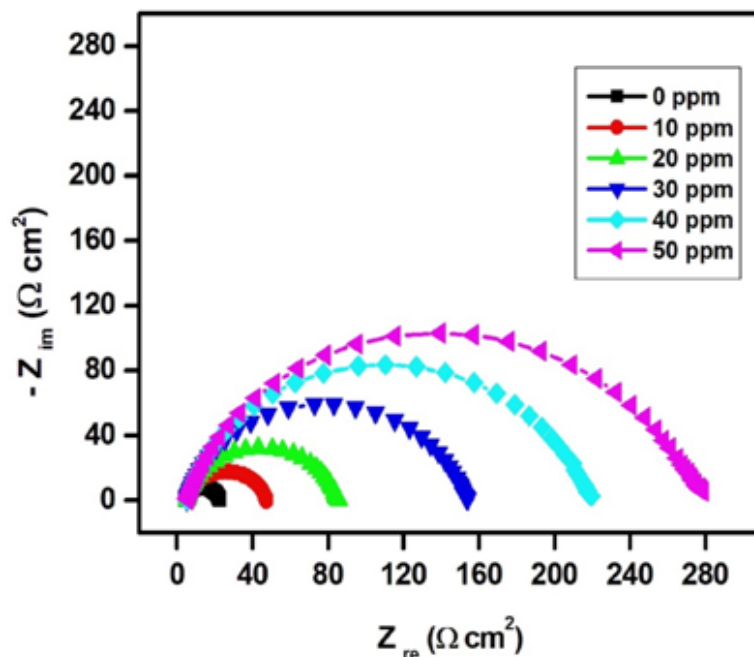


Figure 3.9: Nyquist plot of the EIS for mild steel in 1M HCl solution containing various concentrations of SRT

To simulate how mild steel interacts with the solution, with or without the studied inhibitor, the obtained electrochemical impedance spectroscopy (EIS) data was meticulously associated with a suitable electrical equivalent circuit (illustrated in Figure 3.10). Instead of using a constant phase element, the capacitance found at the interface between the metal sample and the SRT was employed for a more accurate adapting EIS data.

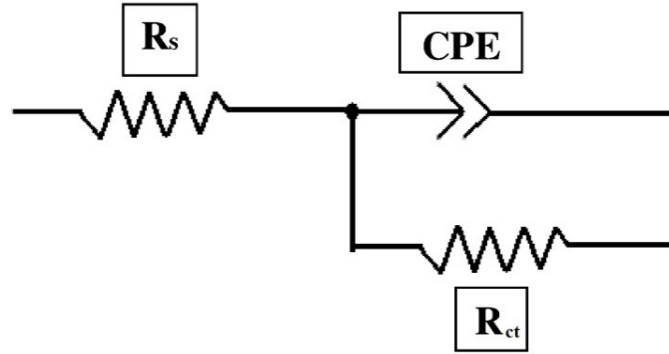


Figure 3.10: Equivalent Circuit model of the EIS for mild steel in 1M HCl solution containing various concentrations of SRT

Within the impedance formulation, CPE (Constant Phase Element) is utilized to represent a phase displacement that remains constant across different frequencies, accurately expressing the relationship between the transmitted AC voltage and its corresponding current, as seen in expression below:

$$Z_{CPE} = \frac{1}{Y_o(j\omega)^n}$$

Where, the symbol Y_o signifies the value of the Constant Phase Element (CPE), while the symbol ω represents the angular frequency. The symbol j denotes the imaginary unit, and the parameter n corresponds to the deviation index value. These symbols and parameters play crucial roles in the scientific analysis and characterization of complex impedance and electrical behavior in the system under investigation. The equation utilized to determine the value of C_{dl} is described below.

$$C_{dl} = \left(Y_o R_{ct}^{(1-n)} \right)^{\frac{1}{n}}$$

The unique value assigned to the parameter "n" imparts varying interpretations to the Constant Phase Element (CPE) in accordance with the fitted data. Specifically, when n assumes a value of 0 or 1, the CPE represents pure resistance and pure capacitance, respectively. Conversely, for n values of -1 and 0.5, the CPE signifies inductance and Warburg impedance, respectively. These distinct interpretations of the CPE based on the

value of "n" are essential in the analysis and understanding of the complex impedance behavior exhibited by the studied system.

Table 3.8: Electrochemical Impedance Variables of Mild Steel in blank and in presence of variable concentrations of Sertraline in 1M HCl

Conc. (ppm)	R_{sc} ($\Omega \text{ cm}^2$)	R_{ct} ($\Omega \text{ cm}^2$)	Y_0 ($10^{-6} \Omega^{-1} \text{ cm}^{-2}$)	n	C_{dl} ($\mu\text{F cm}^{-2}$)	I.E. (%)
Blank	4.32	18.32	186.8	0.905	438.91	-
10	5.11	42.21	111.2	0.878	359.97	56.6
20	5.2	80.62	89.4	0.887	277.2	77.28
30	5.26	148.74	65.7	0.894	195.27	87.68
40	5.2	214.2	54.9	0.927	114.84	91.45
50	5.36	273.34	41.8	0.942	74.03	93.3

The estimated results obtained from EIS plots are summarized in table and this table elaborates that elevating the concentration of SRT enhanced the impedance of the suppressed system despite lowering the values of in tested acid media. The above decrease in the value of Double capacitance layer, is due to significant diminution in the value of local dielectric constant (ϵ) or an enhancement in the thickness value of the dual layer, implying that the molecules of inhibitor prevent the degradation of metal through the adsorption process at the metal/solution contact. A uniform and efficient protective layer emerges on the mild steel/solution contact as the SRT replaces the water molecules present on the surface of low-carbon steel. As a result, the portion of low-carbon steel electrode constantly prone to acid solutions is diminished. In accordance with the results of the preceding interpretation, more the water molecules eliminated by SRT at the mild steel/solution interface, greater the inhibition efficiency and therefore the more apparent decrease in the value of double layer capacitance.

3.3.4 Quantum Chemical Study

DFT analysis can be used to evaluate the adsorptive action of materials. The designations HOMO and LUMO indicate various regions with different tendencies for giving electrons to electron-donating species and accepting electrons from protonated species, respectively. The optimized structures, HOMO and LUMO of SRT used in the calculations are displayed in Figure 3.11. The E_{HOMO} and E_{LUMO} are critical parameters used to determine each structure's ability to be used for anti-corrosive properties. The highest occupied molecular orbital (HOMO) exhibits exclusive localization on the anion moiety, indicating that upon interaction with the metal surface, the inhibitor engages in bonding with the metal through electron donation from the anionic unit. Across all studied dyes, the lowest unoccupied molecular orbital (LUMO) consistently demon-

strates a pronounced π^* (antibonding) nature. Nevertheless, electron acceptance within this orbital is hindered due to the aromatic constraints imposed by the ring structure.

Table 3.9: Quantum Chemical parameters for Sertraline

E_{HOMO} (eV)	E_{LUMO} (eV)	ΔE (eV)	I (eV)	A (eV)	χ (eV)	η (eV)	ΔN
-4.84	-0.83	4.01	4.84	0.83	2.84	2.01	1.98

The E is a measure of the affinity of the molecule to interact with the mild steel (MS) substrate, and the lower energy barrier in sertraline (SRT) (4.01 eV), given in Table 3.9 facilitates its higher adsorption tendency on the metal surface. A lower value of electronegativity also confirms high inhibition efficiency.

For a molecule to be an efficient inhibitor, it must donate electrons to the unoccupied orbitals of MS and accept electrons from MS. Consequently, during the process of adsorption, it is probable for the adsorbate to interact preferentially with the region of the molecule where softness attains its maximum value. The electron-donating characteristic of the molecule is directly proportional to the number of electrons donated. A positive value of ΔN and the chemical hardness of SRT indicate its electron-donation characteristic, resulting in lesser dissolution of the metal.

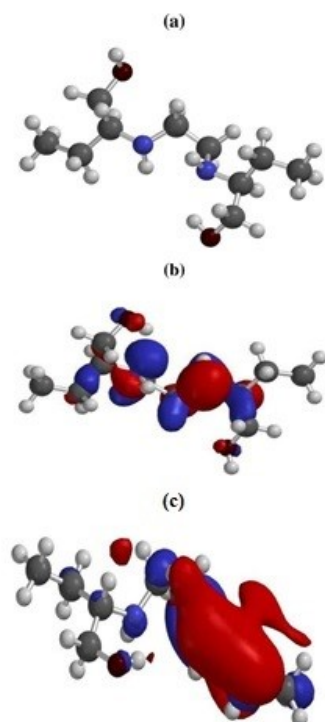


Figure 3.11: Optimized Structure(a) and the corresponding HOMO(b) and LUMO(c) for SRT

3.3.5 Surface Study: Atomic Force Microscopy (AFM)

AFM scan is conducted to do surface characterization on an MS specimen in 1 M corrosive solution and in 50 ppm solution Sertraline in corrosive medium over a 4-hour immersion time. On an area of $10 \mu\text{m} \times 10 \mu\text{m}$, the surface analysis (Figure 3.12) assessed the surface roughness. Without using an inhibitor, the average roughness of surface of mild steel were calculated to be 221 nm in blank solution while using an inhibitor, it was found to be 50 nm. It is evident that mild steel surfaces with corrosive medium scrutinized to be splintered in the uninhibited but in inhibited solution, the substrate surface were less disintegrated because the inhibitor protected the surfaces from corrosion.

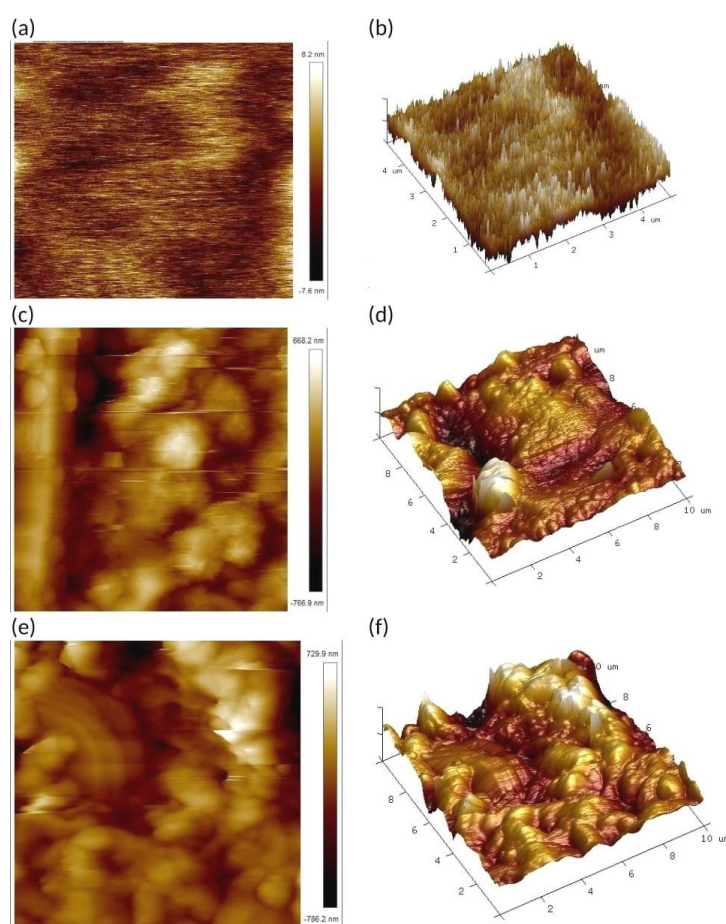
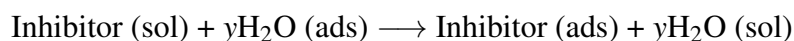


Figure 3.12: (a) & (b) - 2D and 3D scan of reference material (polished metal), (c) & (d) - 2D and 3D scan of 1M HCl immersed metal surface (blank), (e) & (f) - 2D and 3D scan of 50 ppm SRT in 1 M HCl immersed metal surface.

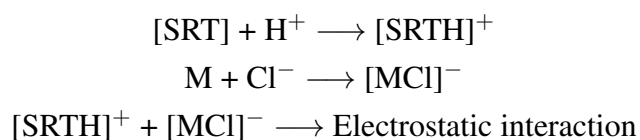
3.4 MECHANISM OF INHIBITION

Electrochemical and mass loss investigations were conducted on MS to undertake a comprehensive analysis of the process of inhibition of SRT, MS was immersed in acidic

environment. These studies allowed for a thorough examination of the effectiveness of SRT as an anti-corrosion agent, providing valuable insights into its protective capabilities and its potential application in mitigating corrosion-related issues in acidic conditions. Water molecules are adsorbed on MS substrate which are displaced by SBT molecules from the metal by displacement reaction.



Based upon the atoms with non-bonding electron and delocalized ring electrons, the following mechanism has been proposed. Gravimetric measurements proclaimed physical adsorption mechanism. The drug molecule may get protonated at active centre having lone pair of electrons to generate charge in acidic media and there exist dynamic equilibria in protonated and neutral species. Chloride ions of hydrochloric acid gets adsorbed on charged metal surface to give rise to negative charge and negatively charged metal and protonated inhibitor undergo electrostatic interaction giving rise to physical adsorption.



The Langmuir adsorption isotherm indicates that the drug develops a monolayer on the MS substrate. The electrochemical measurements show that the SRT exhibits suppression of both anodic and cathodic processes when interacting with MS in hydrochloric acid solution. Inhibitor prevents corrosion at anodic site by reducing evolution of hydrogen as well as at cathodic site by adsorbing directly on metal surface. Theoretical quantum chemical investigations have elucidated that inhibitors exhibiting lower band gap energy, hardness, and electronegativity tend to be more efficient. This propensity arises from their reduced tendency to facilitate electron transfer from metal ions to inhibitor species, leading to the production of stronger interactions between the MS substrate and SRT molecules. These findings shed light on the underlying mechanisms governing the corrosion inhibition process and provide valuable guidelines for designing and selecting effective inhibitors for metal protection in various environments.

3.5 CONCLUSION

The anti-corrosive effectiveness of MS substrate using Sertraline (SRT) in 1N HCl was examined in the concentration range of 10-50 ppm at 303-333K temperature range using weight loss, electrochemical study, quantum chemical studies and surface analysis .

1. Sertraline successfully prevented degradation of MS in 1 M HCl and with the increase in the concentration of inhibitor, the inhibitory performance improves

and its corrosion rate declines. Inhibition efficiency declined from 93% at 303 K as temperature increased.

2. The value of activation energies rises along with the rise in SBT drug concentration. Rise in value of activation enthalpy with temperature demonstrated the endothermic nature of the phenomenon of degradation. Thermodynamic measurements of the inhibitor's adsorption on mild steel revealed spontaneous, endothermic, and physisorption of the drug.
3. The SRT develops monolayer as followed Langmuir adsorption isotherm.
4. SRT behaved as a mixed-type indicator according to electrochemical measurements.
5. The quantum chemical analysis is consistent with the experimental and electrochemical results due to SRT having higher E_{HOMO} , lower E_{LUMO} , and lower band gap energy values that are showing a lesser number of electrons transferred from the metal surface to SRT, and hence the corrosion process slows down. However, SRT could develop a rather persistent molecule single layer at the mild steel/solution interface in 1 M HCl, thereby preventing mild steel degradation in a specific range of temperature.

CHAPTER 4

ANTI-DEPRESSANT DRUG PAROXETINE AS EFFICIENT CORROSION INHIBITOR FOR MILD STEEL

4.1 INTRODUCTION

Mild steel, also known as low carbon steel, is a widely used form of carbon steel characterized by its relatively low carbon content, typically ranging from 0.05% to 0.25%. Its popularity can be attributed to its versatility, cost-effectiveness, and ease of fabrication. Mild steel finds extensive applications in various industries, notably in construction and manufacturing. In construction, it serves as a primary material for structural components, such as beams, columns, and reinforcing bars, due to its excellent strength and ductility. In the manufacturing sector, mild steel is employed for the production of automotive parts, machinery, pipes, and sheet metal components. Its ability to be easily welded and formed makes it a preferred choice in these applications. Additionally, mild steel is utilized in the fabrication of household appliances, furniture, and even in the production of cookware. Overall, mild steel's widespread usage is a testament to its indispensable role in modern engineering and construction. It is susceptible to corrosion due to its iron content and relatively low carbon content, which makes it prone to oxidation when exposed to moisture and oxygen. Corrosion of mild steel can occur in various environments, including outdoor exposure to moisture and air, as well as in industrial settings where chemicals and acids are present[131]. To lessen corrosion, several methods are employed, such as coating the steel with protective layers (e.g., paint or zinc coatings), using corrosion-resistant alloys, and employing cathodic protection systems. Different methods have been recommended in restraining corrosion, among which the usage of inhibitors is cost effective and practical means.

Drugs as corrosion inhibitors represent a fascinating intersection between pharmaceutical science and materials engineering. Certain pharmaceutical compounds have shown the ability to function as effective corrosion inhibitors in various industrial applications. These drugs possess chemical properties that enable them to interact with metallic surfaces and form protective layers, mitigating the corrosive effects of environmental factors. Their use as corrosion inhibitors has been explored in industries such as oil and

gas, where pipelines and equipment are exposed to harsh conditions, as well as in the field of medical implants to enhance their corrosion resistance within the human body. Also, due to their availability and less toxic effect, can be the substitute for toxic old anticorrosive inhibitors[132]. Drugs typically have heteroatoms such as nitrogen, oxygen, phosphorous, and sulphur, aromatic ring which attracted researchers to use drugs as corrosion inhibitors[133]. Recently drugs of various categories have also been used as corrosion inhibitor due to their favorable structure and environmentally benign nature. Many antibiotics, analgesics, antihistamines, antipyretics and antidepressant drugs were found to be suitable for prevention of corrosion[134].

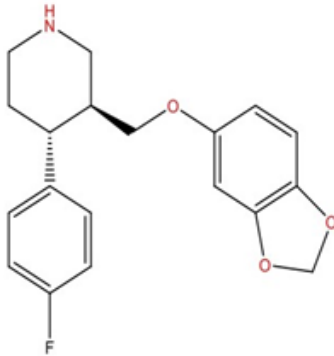
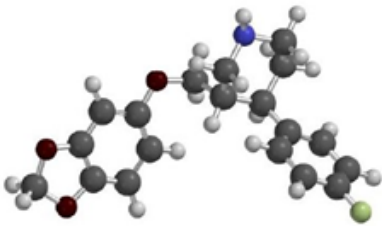
Drug name	Paroxetine
Drug category	Psychotherapeutic drug
Chemical Formula	$C_{19}H_{20}FNO_3$
IUPAC name	(3 <i>S</i> ,4 <i>R</i>)-3-(1,3-benzodioxol-5-ylomethyl)-4-(4-fluorophenyl)piperidine
Structural formula	
3 D structure	

Figure 4.1: Structural information of Paroxetine

Paroxetine is a widely prescribed medication classified as a selective serotonin reuptake inhibitor (SSRI) (Figure 4.1). It is commonly used to treat various mental health conditions, notably depression, generalized anxiety disorder, social anxiety disorder, and obsessive-compulsive disorder. Paroxetine works by increasing the levels of serotonin, a neurotransmitter in the brain that plays a crucial role in regulating mood and emotions. By doing so, it helps alleviate the symptoms associated with these disorders,

such as persistent sadness, anxiety, and intrusive thoughts. Paroxetine is available in different forms, including tablets, extended-release tablets, and oral suspension, allowing for tailored treatment plans to meet individual patient needs. While it can be highly effective in managing mental health conditions, it should be used under the guidance of a healthcare professional, as it may have side effects and potential interactions with other medications. Regular monitoring and dose adjustments are essential to ensure its safe and optimal use. In this context, the current investigation focuses on the examination of paroxetine as a anti-corrosion agent utilizing mass loss analysis, electrochemical assessments, quantum chemical approaches, and atomic force microscopy. Paroxetine drug available in the form of tablets. Paroxetine is the derivative of phenylpiperidine and belongs to selective serotonin reuptake inhibitor (SSRI). Paroxetine is an antidepressant drug used in treatment of panic disorders, depression, post-traumatic stress disorders and chronic headache[?]. Because of its structural characteristics, such as active sites, a lone electron pair, and electrons distributed throughout its aromatic ring, the drug has the properties which can be utilized to act as effective inhibitor.

4.2 EXPERIMENTAL AND METHODS

4.2.1 Preparation of metal sample and test solutions

The MS sample of the same size (2 cm × 5 cm) has been utilized for the present experimental study. MS coupons were abraded mechanistically with emery papers of various kinds to get the smooth shiny surface and cleaned with double-distilled H₂O, decontaminated with (CH₃)₂CO, and dried in air. The gravimetric composition of the metal coupon was C (0.17%), Fe (98.7), Mn (0.54), Si (0.20%), P (0.16%). The corrosive medium of 1M HCl was prepared by adding double-distilled water to analytical grade 37% HCl. The 10 mg tablet of paroxetine drug (Brand-Part-10; Ipca Laboratories) was purchased from a local pharmacy and contained paroxetine hydrochloride hemihydrate (10 mg) and titanium dioxide. The paroxetine was in pure form, extracted, and the inhibitor solutions of different concentrations (5-20 ppm) were made by dissolving the drug in aggressive media[135].

4.2.2 Weight Loss Study

To examine how temperature influences the ability of paroxetine in 1 M HCl to protect MS, both uninhibited and inhibited with varying drug amounts (ranging from 5 to 20 ppm) at temperatures between 303 K and 333 K, mass loss analysis is widely regarded as the primary means of assessing the effectiveness of inhibition. Metal coupons were weighed both before and after being immersed for 4 hours in the corrosive environment and in inhibitor solutions with different concentrations[136]. IE%, θ , and C_r were measured utilizing the expression:

$$IE\% = \frac{W_0 - W_i}{W_0} \times 100$$

$$\theta = \frac{W_0 - W_i}{W_0}$$

$$C_r(\text{mpy}) = \frac{534 \times W}{A \times t \times D}$$

Where; A - sample surface area (cm²); IE - Inhibition efficiency; C_r - Corrosion rate; W₀ – Weight loss of metal coupon in blank solution; W_i - weight loss of inhibited metals, W - Weight loss (mg); θ - surface coverage; t - immersion time (hours), D - sample density (g/cm³).

4.2.3 Electrochemical Study

3-electrode system used for the electrochemical measurements on an electrochemical workstation (Gamry Potentiostat - IFC-1010E). Data fitting was done with the help of Echem Analyst 5 software. The installation of the three-electrode system was done carefully in the system, and 300 ml solutions were used for electrochemical testing. Mild steel coupon was used as the working electrode, which was polished using emery papers of different kinds, cleaned, and decontaminated with (CH₃)₂CO prior to use[137]. Platinum wire was used as a counter electrode while Ag/AgCl was used as reference electrode. Before electrochemical testing, solutions were stabilized for an hour. Electrochemical tests were performed on stabilized OCP with high frequency of 100 KHz and low frequency of 0.1 Hz with 5mV drive signal. The linear polarization resistance was studied with the potential setting between -0.02 and +0.02V with a 1mV/s scanning rate. The equation below shows the relationship between linear polarisation resistance and inhibitory effectiveness.

$$IE\% = \frac{(R_p' - R_p^\circ)}{R_p^\circ} \times 100$$

Where R_p[°] is polarization resistance in the blank solution, R_p['] is polarization resistance with inhibitor.

To get Nyquist plots, the EIS was performed using AC signals with a frequency range of 0.2 Hz to 105 Hz and an amplitude of 10 mV. Using the provided formula, the drug's effectiveness was determined from the charge transfer resistance (R_{ct}) values[138].

$$IE\% = \frac{R_{ct}' - R_{ct}^\circ}{R_{ct}^\circ} \times 100$$

Where, R_{ct}[°] is the charge transfer resistance in the blank solution, and R_{ct}['] is the charge transfer resistance with the inhibitor.

With a potential range of -250 to +250 mV and a rate of scan of 1 mV/s, a plot was produced to assess the effects of corrosion on metal. To determine corrosion current

densities, the linear Tafel plot's cathodic and anodic curves were extrapolated to obtain the corrosion potential. Using current densities, the inhibitor's inhibitory performance (IE%) was estimated using the following formula[139].

$$IE\% = \frac{I_{\text{corr}}^{\circ} - I'_{\text{corr}}}{I_{\text{corr}}^{\circ}} \times 100$$

where I_{corr}° is the corrosion current density in 1 M HCl, I'_{corr} is the corrosion current density at various concentrations of the inhibitor. All electrochemical experiments were repeated three times to acquire reproducibility.

4.2.4 Quantum Chemical Study

DFT was used to describe various quantum molecular features and to determine the connection between inhibition potential and drug molecular characteristics, as well as the inhibition mechanism. The optimized structure and DFT variables of paroxetine in both gas and aqueous phases were obtained using DFT calculations on the basic set 6-31 G* with the B97X-D method in Spartan 20 software. DFT has been documented to offer dependable outcomes in characterizing diverse molecular attributes, including calculations of the Lowest Unoccupied Molecular Orbital (LUMO) energy, Highest Occupied Molecular Orbital (HOMO) energy, electronegativity (χ), and various other variables derived from these parameters[140].

Ionization potential (I) characterizes the disposition of a chemical entity to give up electrons, and its relation with E_{HOMO} is elucidated by the equation:

$$I = -E_{\text{HOMO}}$$

Electron affinity (A) is the tendency of a chemical species to gain electrons and correlated to E_{HOMO} as follows:

$$A = -E_{\text{LUMO}}$$

Electronegativity is the tendency of an atom to attract electrons and can be calculated using the following equation:

$$\chi = (I + A)/2$$

Chemical hardness (η) is the measures of the resistance of an atom to a charge transfer and can be calculated by using the equation:

$$\eta = (I - A)/2$$

The fraction of transferred electrons in a chemical reaction is given by the equation:

$$\Delta N = \frac{\chi_{\text{Fe}} - \chi_{\text{inh}}}{2(\chi_{\text{Fe}} + \chi_{\text{inh}})}$$

Where χ_{Fe} – electronegativity of iron (7 ev/mol), η_{Fe} – global hardness of iron (0). The values have been reported in the literature.

4.2.5 Surface Study

In order to figure out the impact of the drug on safeguarding the MS substrate, the surface was characterized by Bruker Atomic Force Microscope after submerging the MS samples in both the uninhibited (1 M HCl) and inhibited 20 ppm solution for a duration of 4 hours.

4.3 RESULT AND DISCUSSIONS

4.3.1 Characterization

a) UV-Vis Study

The UV spectra for the drug was studied and maximum absorption was observed at 293 nm which is the landmark for paroxetine[141] (Figure 4.2).

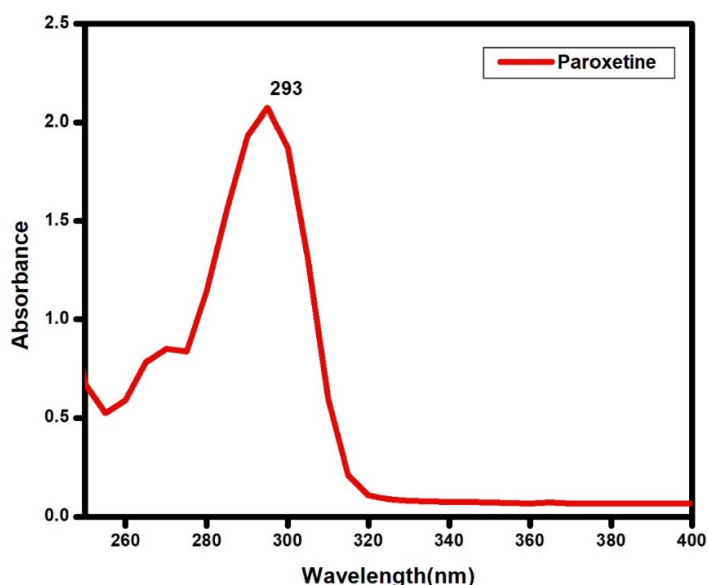


Figure 4.2: UV spectrum of Paroxetine

b) FT-IR Study

IR spectrum of the drug was studied and the peaks at 3323 cm^{-1} (O-H stretching), 2912 cm^{-1} (aliphatic C-H stretching), 2749 cm^{-1} (ammonium N-H stretching), 1645 cm^{-1} (aromatic C-C stretching), 1232 cm^{-1} (ether C-O-C asymmetric stretching), 1218 cm^{-1} (fluoro aromatic C-F stretching), 1097 cm^{-1} (ether C-O-C symmetrical stretching), 980 cm^{-1} (acetal C-O-C stretching), 836 cm^{-1} (aromatic C-H out of plane bending) were observed which are characteristics of paroxetine[142](Figure 4.3).

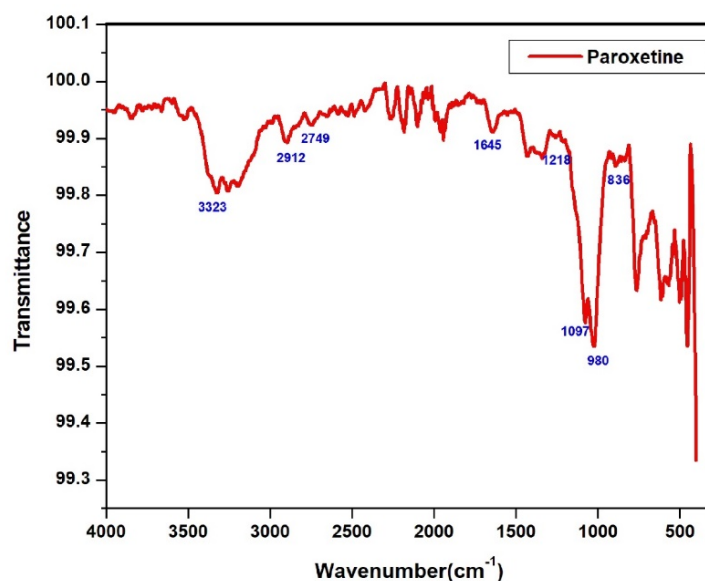


Figure 4.3: FT-IR spectrum of Paroxetine

4.3.2 Weight Loss Study

a) Effect of inhibitor concentration on Corrosion rate and Inhibition efficiency

Weight loss study was performed to calculate (% I.E), (θ) and (C_r) of MS in 1 M HCl. The MS specimen was immersed under inhibitor solutions of variable concentrations ranging from 5 to 20 ppm in an acidic environment for 4 hours in the temperature between 303 to 333 K. Weight loss experimental results such as weight loss, corrosion rate, average surface coverage, and inhibitory performance have been summarized in Table 4.1, 4.2 Corrosion rate was highest in 1 M corrosive medium, but decreased corrosion rate was observed with the enrichment of the inhibitor, indicating inhibitor particles' binding on the MS substrate. Meanwhile, a rise in the extent of corrosion was seen when the temperature increased from 303 to 333 K, indicating desorption and the occurrence of degradation reactions at a faster rate (Figure 4.4). The maximum inhibitory performance (96.47%) was observed at 303 K and 20 ppm concentration as a result of a spike in the accessible surface area for drug adsorption, but inhibition efficacy decreased with an increase in temperature (Figure 4.5) due to a lack of energy to overcome adsorption and increased desorption of the inhibitor.

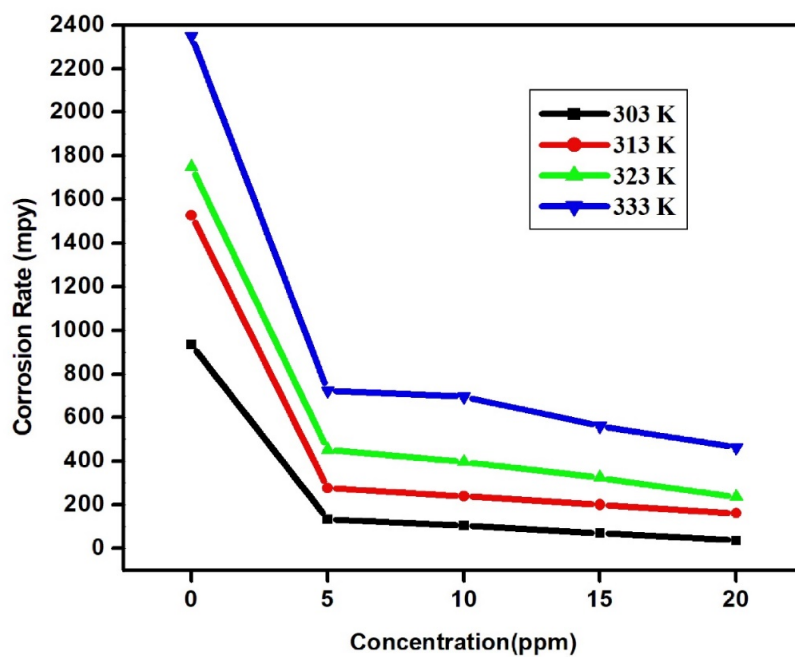


Figure 4.4: Effect of Paroxetine concentration on rate of corrosion of mild steel in 1 M HCl at various temperatures (303-333K).

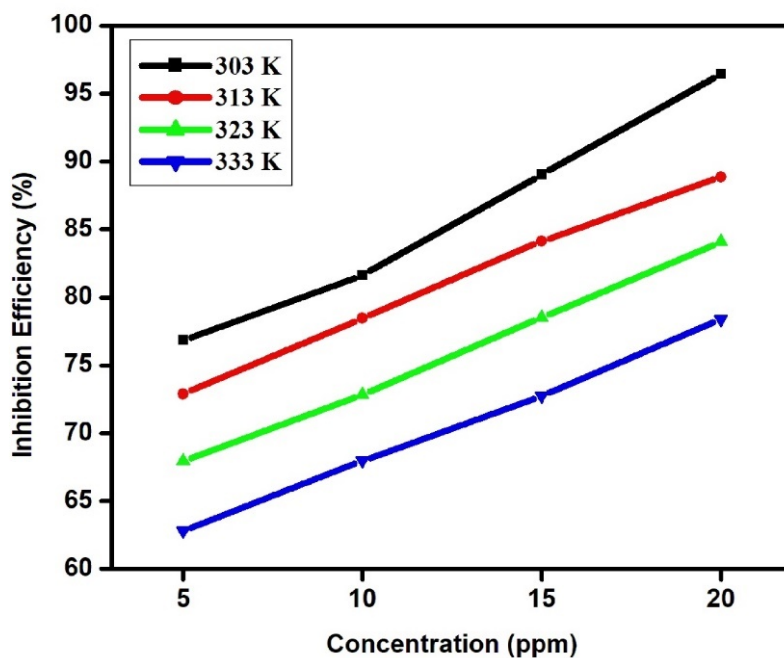


Figure 4.5: Inhibition Efficiency of Paroxetine versus concentrations (5-20 ppm) at different temperatures

Table 4.1: IE, C_r , and θ of Paroxetine with mild steel at 303K and 313K temperature with different concentration range

Temp.	303 K			313 K		
Conc. (ppm)	C_r (mpy)	θ	I.E. (%)	C_r (mpy)	θ	I.E. (%)
Blank	956.54	-	-	1428.05	-	-
5	221.39	0.77	76.86	387.01	0.73	72.90
10	175.76	0.82	81.63	307.58	0.78	78.46
15	104.78	0.89	89.05	226.46	0.84	84.14
20	33.8	0.96	96.47	158.86	0.89	88.88

Table 4.2: IE, C_r , and θ of Paroxetine with mild steel at 323K and 333K temperature with different concentration range

Temp.	323 K			333 K		
Conc. (ppm)	C_r (mpy)	θ	I.E. (%)	C_r (mpy)	θ	I.E. (%)
Blank	1487.2	-	-	2485.99	-	-
5	476.58	0.68	67.95	924.43	0.63	62.81
10	403.91	0.73	72.84	795.99	0.68	67.98
15	319.41	0.79	78.52	677.69	0.73	72.74
20	236.6	0.84	84.09	537.42	0.78	78.38

b) Kinetic and Thermodynamic Studies

By examining how temperature affects corrosion, the process of inhibition may be identified. The relationship between temperature and corrosion rate can be studied with the help of Arrhenius equation[143].The graph of Log C_r Versus $1/T$ was plotted (Fig 4.6) and pre-exponential component (A) was calculated from the intercept and apparent activation energy E_a from the slope of straight-line curve.

$$\log C_r = \frac{-E_a}{2.303RT} + \log A$$

where A is the Arrhenius pre-exponential factor, E_a is the apparent energy of activation, and R is the molar gas constant.

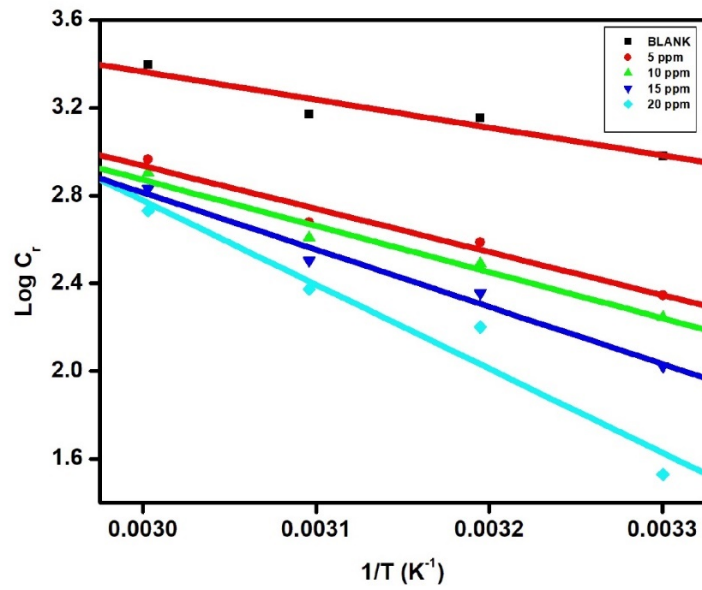


Figure 4.6: Arrhenius Plot in blank and with different concentrations of Paroxetine in 1 M HCl for mild steel corrosion.

Table 4.3: Kinetic and Thermodynamic parameters of Paroxetine with MS at different temperatures and inhibitor concentration range

Conc. (ppm)	E_a (kJ/ppm)	A(Sec ⁻¹)	ΔH (kJ/mol)	- ΔS (kJ/mol/K)	ΔG_{act} (kJ/mol)			
					303K	313K	323K	333K
Blank	24.30	1.49×10^1	21.66	0.12	57.43	58.61	59.79	60.97
5	37.63	6.84×10^3	35.00	0.09	61.00	61.85	62.71	63.57
10	40.21	1.49×10^3	37.57	0.08	61.58	62.37	63.16	63.95
15	49.84	4.23×10^4	47.20	0.05	62.67	63.18	63.69	64.20
20	73.29	1.84×10^8	70.65	0.02	64.73	64.54	64.34	64.15

Transition state equation helps in calculation of other activation parameters and this equation is also an alternative form of Arrhenius equation[141].

$$C_r = \frac{RT}{Nh} \exp\left(\frac{\Delta S}{R}\right) \exp\left(\frac{-\Delta H}{RT}\right)$$

Where Nh is the product of Avogadro's number and Planck's constant, ΔS is the apparent entropy of activation, and ΔH is the apparent enthalpy of activation.

The graph of $\log(C_r/T)$ versus $1/T$ was plotted, and a straight line was discovered from there (Fig. 4.7). From the slope and the intercept of the graph, ΔH values and ΔS values were determined respectively and mentioned in Table 4.3. It is revealed using the values that the energy of activation for corrosion of the inhibited sample was higher in contrast to the uninhibited sample, signifying the drug binding on the MS surface.

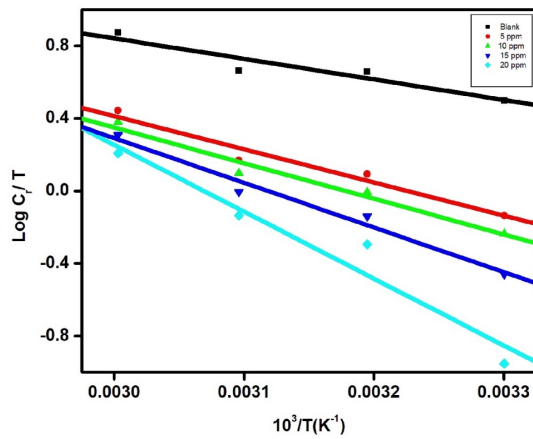


Figure 4.7: Transition state plot in blank and with different concentrations of Paroxetine in 1 M HCl for mild steel corrosion.

Because of the higher drug binding on the metal substrate, the ΔH rises as the drug concentration increases, suggesting greater metal shielding. The binding of the drug with MS raises the values of ΔH of the degradation phenomenon, which slows the rate of corrosion. The entropy of activation was very high without the drug, as the rate-determining step of the phenomenon is more ordered. However, when the inhibitor was added, the rate-determining step, which is the disposal of H^+ at the anodic part to adsorb, was reduced as the inhibitor covered the surface of the metal. The system then passed to a more random arrangement, resulting in an increase in entropy with the addition of the inhibitor. Activation energy along with enthalpy of corrosion increased with the addition of the inhibitor due to increased coverage of the surface by the enhanced binding tendency of the drug on MS (Figure 4.8).

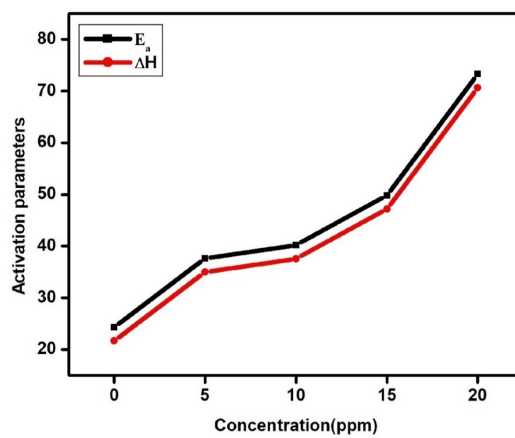


Figure 4.8: Variation of activation energy and enthalpy versus concentration of Paroxetine

Activation energy along with enthalpy of corrosion increased with the addition of the inhibitor due to increased coverage of the surface by the enhanced binding tendency of the drug on MS (Figure 4.8). The equation may be used to connect the change in free energy of activation for the phenomenon of degradation to ΔH and ΔS :

$$\Delta G = \Delta H - T \Delta S$$

Calculated ΔG values have been mentioned in Table 4.3, and these values were observed to become positive with the rise in drug amount and decrease with an increase in temperatures, depicting the unstable nature of the activated complex and the improbability of the formation of the activated complex.

c) Adsorption Isotherms

The isotherm gives the relationship between the extent of adsorption against the concentration at constant temperature. Isotherm provides basic information regarding the interaction between metal and the inhibitor. All the drugs act through surface adsorption at the interface between metal and aggressive solution to control corrosion. To find a suitable isotherm, data were fitted into various isothermic models. The data best fit various adsorption isothermic models such as Tempkin, Freundlich, El-Awady, and Langmuir adsorption isotherms. The most appropriate fit was observed with the Langmuir adsorption isotherm (Figure 4.9) with a correlation coefficient ($R^2 > 0.99$), as mentioned in Table 4.4. This indicates monolayer adsorption of Paroxetine in 1 M hydrochloric acid on the mild steel surface. The Langmuir isotherm for adsorption is given as:

$$\frac{C}{\theta} = \frac{1}{K_{ads}} + C$$

Where, K_{ads} is an equilibrium constant for adsorption process, C is inhibitor concentration and θ is degree of surface coverage

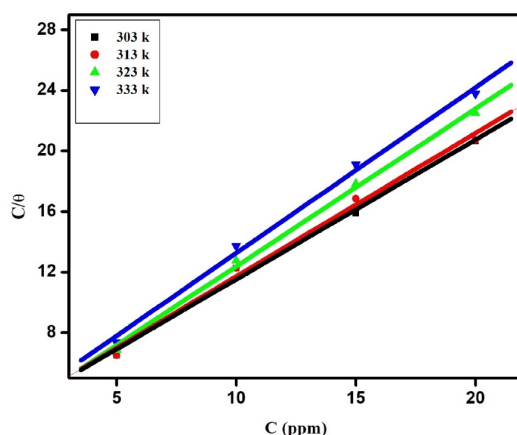


Figure 4.9: Adsorption isotherm of drug Paroxetine on mild steel surface in 1 M HCl at various temperatures.

The equilibrium constant and standard free energy can be related by the following equation:

$$K_{ads} = \frac{1}{10^6} \exp\left(-\frac{\Delta G_{ads}}{RT}\right)$$

where K_{ads} is Equilibrium adsorption constant, T is Temperature in Kelvin, ΔG_{ads} is standard free energy and R is molar gas constant.

Table 4.4: Parameters of adsorption computed from Langmuir isotherm of adsorption

Temp. (K)	Slope	R ²	K _{ads} × 10 ⁻³	ΔG _{ads} (kJ/mol)
303	0.95	0.98925	441.50	-37.47
313	1.10	0.99633	505.14	-37.13
323	1.05	0.99302	429.14	-37.55
333	1.07	0.99822	391.09	-37.78

4.3.3 Electrochemical Study

a) Analysis of Linear Polarization Measurements (LPR)

The polarization resistance (R_p) and inhibition efficiency in absence and with varied concentration of paroxetine in 1 M HCl for mild steel were calculated and enumerated in the Table 4.5. After close observation, it has been concluded that R_p at 20 ppm inhibitor concentration was maximum and it was increased from 22.51 of the uninhibited to 109.7, 147, 248.2 and 298.5 for varied concentration of inhibitor indicating increased effectiveness of paroxetine in corrosion inhibition with increasing concentration.

Table 4.5: Linear polarization resistance data for mild steel in blank and in the presence of Paroxetine inhibitor at various concentrations.

Conc. (ppm)	E _{corr} (mV(Ag/AgCl))	I _{corr} (μA/cm ²)	IE(%)	R _p (cm ²)	IE(%)
Blank	-754.1	1157	-	22.51	-
5	-443.1	273.5	76.36	109.7	79.48
10	-430.3	176.1	84.78	147	84.69
15	-438	105	90.92	248.2	90.93
20	-443.7	93.56	91.91	298.5	92.46

b) Analysis of Potentiodynamic Polarization Curves

The PDP curves provide information about the cathodic and anodic reactions of the metal in the solution. Iron (Fe) undergoes ionization at the anodic part, while at the cathodic part, H₂O is produced.

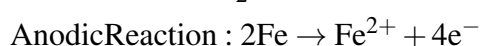
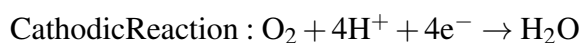


Figure 4.10 shows PDP curves of MS in acidic both in uninhibited and inhibited states using varied doses of paroxetine. To analyze the kinetic information of cathodic and anodic reactions in the corrosion process, Tafel curves were utilized to obtain corrosion current density, cathodic slope (β_c), anodic slope (β_a), corrosion potential (E_{corr}), and are enumerated in Table 4.6.

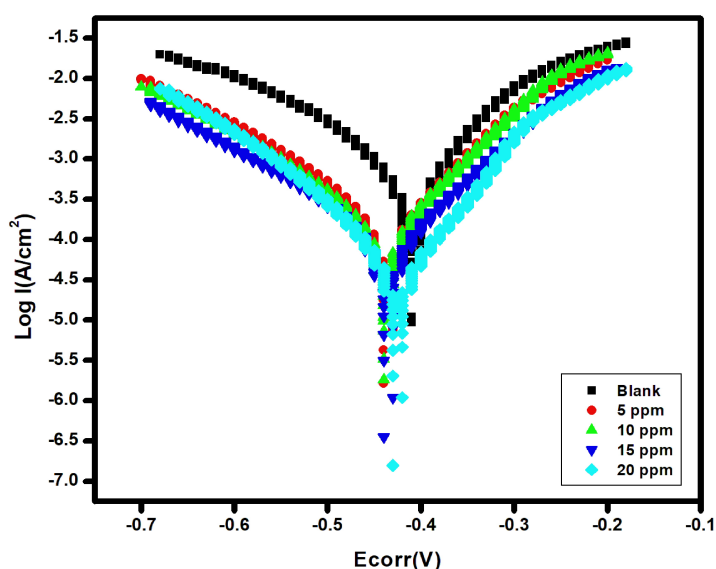


Figure 4.10: Tafel plot for mild steel in 1M HCl solution containing various Concentrations of Paroxetine

Table 4.6: Tafel polarization parameters of mild steel in the presence of Paroxetine in 1M HCl.

Potentiodynamic Polarisation Parameters					
Conc. (ppm)	β_a (mV/dec)	β_c (mV/dec)	$-E_{\text{corr}}$ (Ag/AgCl)	I_{corr} ($\mu\text{A}/\text{cm}^2$)	IE (%)
Blank	93	117.4	432	635	
5	104	115	435	146	77.01
10	102	117	431	126	80.16
15	50.9	47	422	31.5	95.04
20	58.2	49.1	424	23.5	96.30

After close scrutiny of Table 4.5, it is observed that as the doses of drug was increased from blank to 20 ppm, the E_{corr} value decreased. Since the E_{corr} value does not change significantly with the addition of the inhibitor, it indicates a mixed-type behavior of the inhibitor used. The inhibitor protects the metal by preventing the formation of water at the cathode and inhibiting the dissolution of the metal at the anode. I_{corr} value of

blank solution was decreased with the addition of inhibitor as well as with increase in concentration of paroxetine, which may be because of the development of a drug-bound coating over MS substrate, which shows that the drugs's ability to stop corrosion is becoming stronger as it is concentrated.

c) Electrochemical Impedance Spectroscopy

Electrochemical impedance spectroscopy provides information about the interface of metal and solution, indicating corrosion of the metal. Figure 4.11 shows the Nyquist plot of mild steel in blank and in variable concentrations of the inhibitor. Semicircle loops in the Nyquist plot for mild steel in 1 M HCl are observed, and the diameter of semicircles increased with an increase in the concentration of the inhibitor, showing enhancement of the inhibition efficiency of the inhibitor for controlling corrosion. Imperfections in semicircles indicate roughness in mild steel due to frequency distribution.

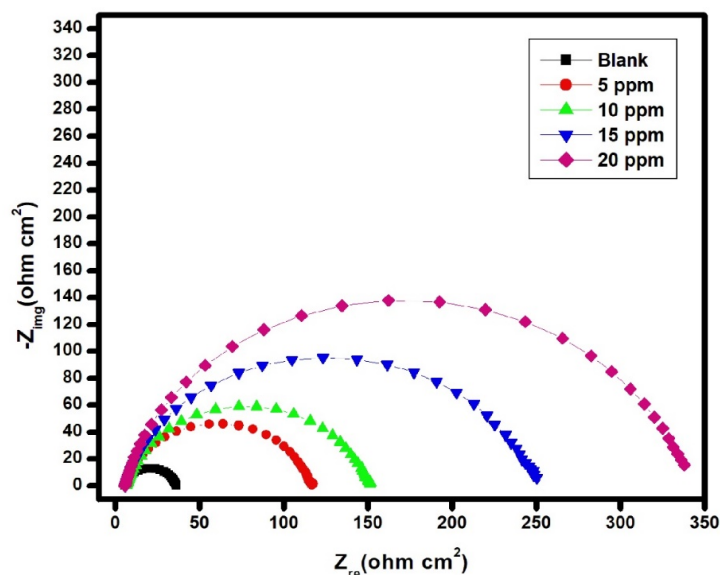


Figure 4.11: Nyquist plots for mild steel in 1M HCl solution with various concentrations of Paroxetine

Figure 4.12 represents the equivalent circuit of the electrochemical impedance spectra. The impedance of double layers changes with frequency, so C_{dl} is replaced by CPE (common phase element). The impedance of the constant phase element, Z_{CPE} , is calculated as follows.

$$Z_{CPE} = Y_0^{-1}(i\omega)^{-n}$$

Where; Y_0 - CPE constant, n is the CPE exponent (phase shift), ω is the angular frequency.

The double-layer capacitance was calculated by using the equation:

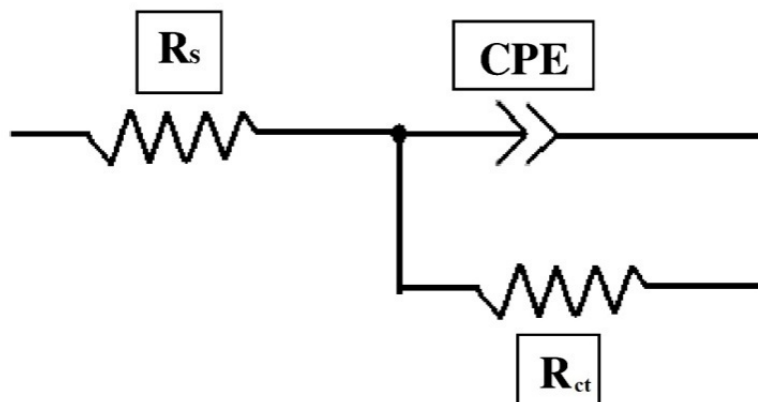


Figure 4.12: Equivalent Circuit Model of the EIS

$$C_{dl} = (Y_0 R_{ct}^{1-n})^{1/n}$$

Inhibition efficiency from electrochemical impedance data was calculated using charge transfer resistance (R_{ct}):

$$IE\% = \frac{100(R_{ct}' - R_{ct}^0)}{R_{ct}'}$$

Where, R_{ct}^0 is the charge transfer resistance in the blank solution; R_{ct}' is the charge transfer resistance with the inhibitor.

Table 4.7: Electrochemical Impedance Variables of Mild Steel in blank and in presence. of variable concentrations of Paroxetine

Conc. (ppm)	R_s ($\Omega \text{ cm}^2$)	R_{ct} ($\Omega \text{ cm}^2$)	Y_0 ($10^{-6} \Omega^{-1} \text{ cm}^2$)	n	C_{dl} ($\mu\text{F cm}^{-2}$)	I.E (%)
Blank	4.3	30.7	185.5	0.878	616.8	
5	6.2	110.6	80.7	0.859	359.2	72.24
10	6.6	144.7	72.4	0.863	314.7	78.79
15	5.9	244.3	67.3	0.879	256.1	87.43
20	5.7	332.1	51.2	0.886	179.3	90.76

Table 4.7 provides unambiguous evidence that an increase in the inhibitor concentration in the 1 M corrosive solution results in improved R_{ct} values and reduced C_{dl} values. The increase in R_{ct} values is likely linked to a slower extent of corrosion, possibly by the formation of a layer on the metal substrate. Conversely, the decrease in C_{dl} values might be attributed to either an increase in double-layer thickness or a reduction in dielectric constant, indicating the binding of drug molecules on MS. Electrochemical impedance spectroscopy data confirms that inhibition efficiency increases with greater

drug concentrations, supporting the idea that Paroxetine in an acidic environment is an effective agent for inhibiting MS corrosion. The results from EIS and PDP curves are in strong alignment.

4.3.4 Surface Study: Atomic Force Microscope (AFM)

Over the course of a 4-hour immersion period, a surface study of an MS specimen in 1 M corrosive solution and 20 ppm paroxetine solution in the corrosive medium was carried out using an AFM scan. The surface analysis determined the surface roughness on a $10\text{m} \times 10\text{m}$ area. The mean surface roughness of MS decreased from 220 nm in blank to 92 nm in the inhibitor solution (Figure 4.13). It is clear that the mild steel surfaces exposed to the corrosive medium were found to be shattered in the blank, but when an inhibitor was present, the surfaces were less likely to splinter because of protection from corrosion.

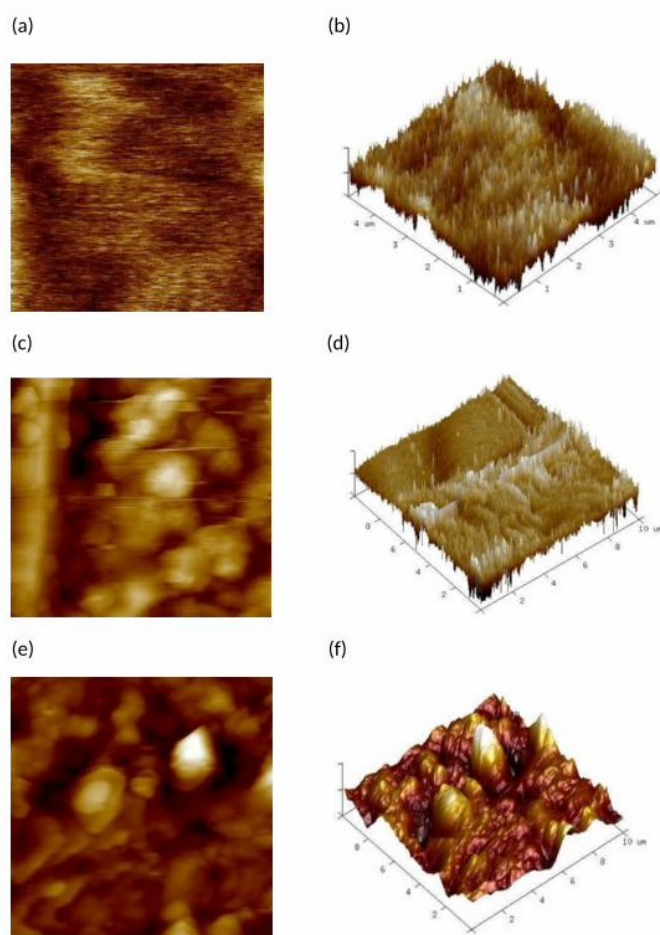


Figure 4.13: (a) and (b) are 2D and 3D scan of polished metal (reference), (c) and (d) are 2D and 3D scan of MS surface immersed in 1 M HCl (blank), (e) and (f) are 2D and 3D scan of MS immersed in 20 ppm Paroxetine in 1 M HCl.

4.3.5 Quantum Chemical Study

The E_{HOMO} signifies the tendency to provide electrons to electron-deficient species, while E_{LUMO} is the molecule's propensity to gain electrons. For a molecule to act as an efficient inhibitor, it should have higher E_{HOMO} and lower E_{LUMO} values with a small energy gap. The experimental compound has a higher E_{HOMO} and lower E_{LUMO} ($\Delta E = 8.84$), making it an efficient inhibitor.

The dipole moment gives the polarity, and a molecule with higher polarity has the tendency for dipole-dipole attraction. The dipole moment is related to inhibition efficiency. The number of electrons transferred (ΔN) provides information about electron acceptance or donation property. The positive and higher value of ΔN indicates its electron-donation property, while a negative and lower value indicates the electron-acceptance property of a compound. For the molecule, a fraction of transferred electrons (ΔN) less than 3.6 shows increased efficacy with a rise in electron-giving ability with MS. A larger fraction of transferred electrons is associated with increased inhibition efficiency, while the least value of the fraction of transferred electrons is associated with lower inhibition efficacy. For the present inhibitor, the ΔN value is less than 3.6, indicating its high electron-donation capacity, which makes it an efficient corrosion inhibitor.

Chemical hardness is an important factor to indicate the propensity of a compound to take electrons. A positive value of chemical hardness of paroxetine indicates its electron-donation characteristic resulting in lesser dissolution of the metal. The chemical hardness value for the compound agrees with experimental results. The various quantum chemical parameters for gas and aqueous phase paroxetine have been mentioned in Table 4.9, and the optimized structure and corresponding HOMO and LUMO for Paroxetine are shown in Fig 4.14.

Table 4.8: Quantum Chemical parameters for Paroxetine for gas and aqueous phase .

	E_{HOMO} (eV)	E_{LUMO} (eV)	I (eV)	A (eV)	χ (eV)	η (eV)	ΔE (eV)	μ (D)	ΔN
Gas	-7.23	1.61	7.23	-1.61	2.81	4.42	8.84	0.89	0.473
Aqueous	-7.35	1.66	7.35	-1.66	2.845	4.505	9.01	1.04	0.461

After the close observation, it can be said that the values of quantum chemical parameters for aqueous phase are greater than the gaseous phase paroxetine indicating protonation of the inhibitor and protonated inhibitors have greater tendency of donation of electrons and thereby increase adsorption capacity of a compound on metal surface. The higher dipole moment of the compound in aqueous phase than the gaseous phase makes it capable to interact with metal electrostatically due to protonation indicating physical adsorption[144]. Quantum chemical parameters support both physisorption and chemisorption of the drug on metal, which also supports experimental results. The

optimized structure, distribution of HOMO and LUMO of gaseous and aqueous phase paroxetine, have been given in Figure 4.14.

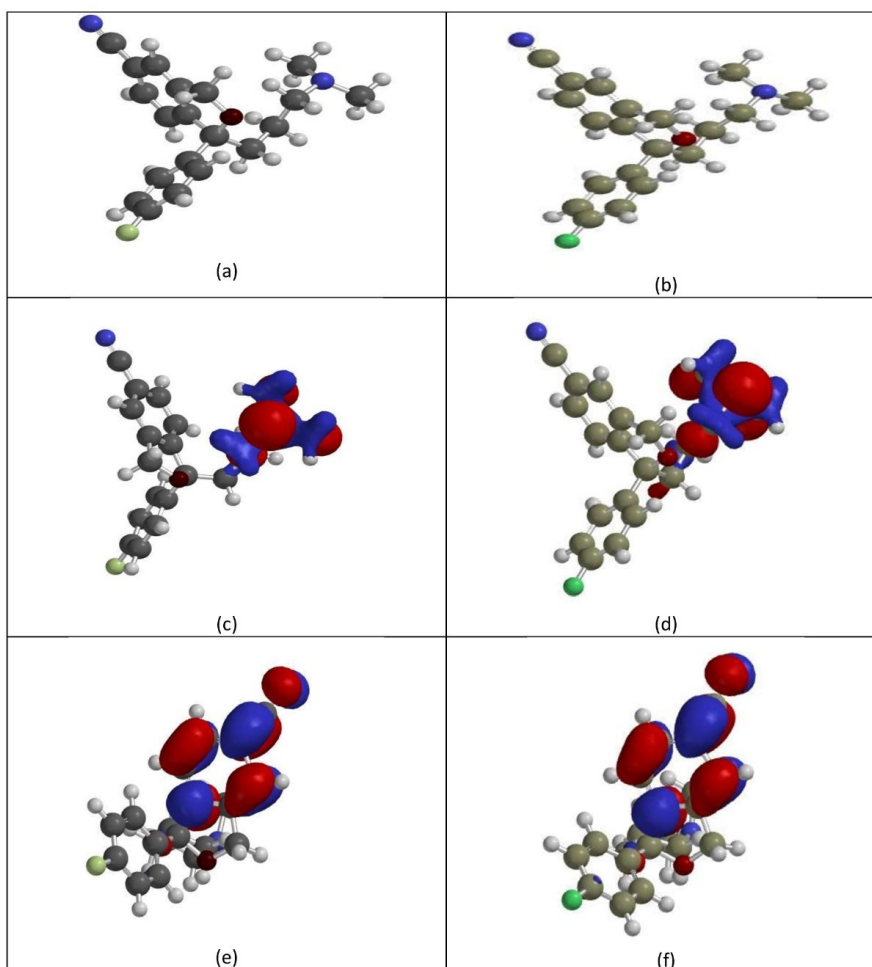


Figure 4.14: Optimized Structure and the corresponding HOMO and LUMO for Paroxetine in Gas (a,c,e) and Aqueous phase (b,d,f)

The Mulliken charges for gas and aqueous phase paroxetine as computed from quantum chemical study have been mentioned in the table 4.8. After close observation maximum charges were found on N1(-0.62), O1(-0.56), O2(-0.56) and O3(-.56) The charge present on the atoms indicate active centres for adsorption[144].

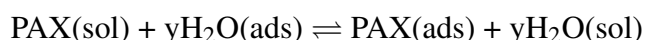
Table 4.9: Mulliken Charges for gas(g) and aqueous phase(aq) Paroxetine

Atom	Charge		Atom	Charge		Atom	Charge	
	Gas	Aqueous		Gas	Aqueous		Gas	Aqueous
C1	-0.28	-0.31	C18	-0.24	-0.26	H14	0.32	0.345
C2	0.339	0.333	C19	-0.25	-0.26	H15	0.164	0.174

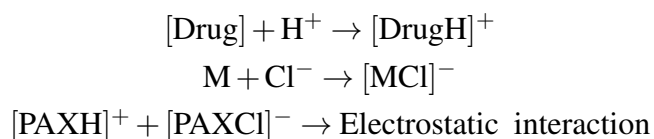
C3	0.32	0.314	C20	0.388	0.372	H16	0.14	0.138
C4	-0.23	-0.25	C21	-0.17	-0.17	H17	0.166	0.17
C5	-0.25	-0.27	F1	-0.31	-0.32	H18	0.159	0.173
C6	0.377	0.369	H1	0.193	0.211	H20	0.159	0.181
C7	0.167	0.149	H2	0.186	0.213	H22	0.17	0.195
C8	-0.07	-0.09	H4	0.201	0.192	H24	0.167	0.199
C10	-0.18	-0.18	H5	0.166	0.202	H26	0.186	0.21
C12	-0.17	-0.18	H6	0.152	0.18	H28	0.186	0.209
C13	-0.31	-0.32	H7	0.17	0.198	N1	-0.58	-0.62
C14	-0.21	-0.21	H8	0.186	0.216	O1	-0.54	-0.56
C15	0.142	0.129	H10	0.168	0.171	O2	-0.55	-0.56
C16	-0.21	-0.24	H11	0.137	0.15	O3	-0.54	-0.56
C17	-0.21	-0.23	H12	0.182	0.175			

4.4 MECHANISM OF INHIBITION

Corrosion inhibition mechanism of paroxetine on MS can be explained by thermodynamic, electrochemical, and quantum chemical studies in hydrochloric acid. Drug molecules get bonded on MS surface by dislodging H₂O molecules already adsorbed on the metal by a displacement reaction. Thermodynamic, electrochemical, and quantum chemical investigations may be used to learn about the working of paroxetine's inhibition nature on MS in hydrochloric acid. By dislodging water molecules that have previously been adsorbed on the metal via a displacement process, drug molecules are bonded over the MS surface.



Weight loss measurements justify physical adsorption mechanism of inhibition. The paroxetine molecules get protonated at active sites (N, O) having maximum charge density (Table 9) and generate charge in acidic medium. Chloride ions of hydrochloric acid gets adsorbed on charged metal surface to generate negative charge thereby causing electrostatic attraction between negatively charged metal and protonated inhibitor hence, physical adsorption.



Monolayer adsorption of the drug on the MS surface is defined by the Langmuir adsorption isotherm. Electrochemical calculations suggest a mixed-type behavior of the

drug for MS in an acidic atmosphere. The drug prevents corrosion at the anodic site by reducing the evolution of hydrogen as well as at the cathodic site by interacting directly on the MS surface and preventing oxidation. Quantum chemical study suggests the donation of electrons from the active site of the inhibitor to the metal, thereby proving a strong interaction between paroxetine and the metal surface.

4.5 CONCLUSION

1. The corrosion inhibitory performance of paroxetine on mild steel in 1 M HCl has been analyzed by weight loss, electrochemical techniques, quantum chemical study, and atomic force microscopy.
2. The studied medication proved to be an excellent corrosion inhibitor, and its efficacy improved with a rise in concentration and decreased as the temperature increased. The maximum efficacy of 96% was observed at a 20 ppm concentration and 303 K.
3. Langmuir Adsorption isotherm was obeyed with a regression coefficient of 0.99, which is quite near 1, showing the effectiveness of the compound.
4. The Tafel plot reveals mixed-type behavior of the inhibitor. The observations from weight loss study, potentiodynamic polarization, and electrochemical impedance are correlated with each other.
5. Decrease in average roughness of the surface also justifies surface protection by the inhibitor. Quantum chemical study reveals the donation of electrons from the active site of the inhibitor to the metal, thereby proving paroxetine as an efficient corrosion inhibitor.

CHAPTER 5

ANTI-DEPRESSANT DRUG ESCITALOPRAM AS EFFICIENT CORROSION INHIBITOR FOR MILD STEEL

5.1 INTRODUCTION

Mild steel (MS) holds paramount significance within engineering applications, occupying a pivotal role in critical sectors such as oil and gas refinement, extraction, boilers, process industries, water pipelines, and petrochemical domains. In these sectors, hydrochloric acid, either in isolation or within mixtures, is ubiquitously employed, wielded at varying concentrations to mitigate rust and corrosion-derived manifestations. Nonetheless, exposure to acidic media precipitates profound material deterioration, instigating consequential material, temporal, and fiscal detriments. In response to this formidable challenge, researchers have undertaken an exhaustive exploration of diverse corrosion inhibitors, poised to counteract the pernicious repercussions of corrosion. Corrosion inhibitors have emerged as an ecologically prudent panacea, stemming from their parsimonious usage requisites, facile accessibility, and remarkable efficacy in corrosion governance. These inhibitors evince an innate proclivity for substantial adsorption onto the metal substrate via physicochemical interactions, thereby potentiating their corrosion-mitigative prowess. Notably, so far untapped pharmaceutical agents are being repurposed to address solid waste containment exigencies, proffering ecocentric alternatives for corrosion abrogation. The economic outlay associated with the synthesis or conveyance of chemical inhibitors for corrosion prophylaxis approximates 7% of the aggregate expenditures earmarked for safeguarding metals and alloys against corrosive vicissitudes in the industrial milieu.

The investigation of pharmaceutical chemicals as potential corrosion inhibitors for metals exposed to corrosive environments has attracted significant attention in the academic community. This heightened attention stems from the fact that a predominant proportion of pharmaceutical agents encompass aromatic ring structures, heteroatomic moieties, and conjugated double bonds. Owing to the confluence of these intricate functional groups within the molecular architecture, pharmaceutical agents have garnered recognition as efficacious agents for corrosion inhibition[145].

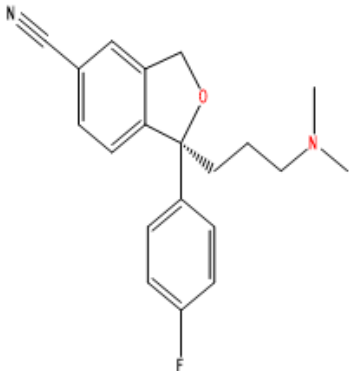
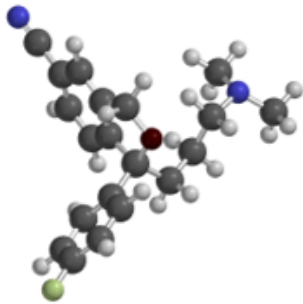
Drug name	Escitalopram
Drug category	Psychotherapeutic drug
Chemical Formula	C ₂₀ H ₂₁ FN ₂ O
IUPAC name	(1S)-1-[3-(dimethylamino)propyl]-1-(4-fluorophenyl)-3H-2bezofuran-5-carbonitrile
Structural formula	 <p>The 2D chemical structure shows a benzofuran ring system. At the 5-position of the benzofuran, there is a cyano group (-C≡N). At the 1-position, there is a chiral center (indicated by a wedge bond) attached to a 4-fluorophenyl group and a 3-(dimethylamino)propyl group. The 3-(dimethylamino)propyl group consists of a three-carbon chain with a dimethylamino group (-N(CH₃)₂) at the end.</p>
3 D structure	 <p>The 3D ball-and-stick model illustrates the spatial arrangement of the atoms in the Escitalopram molecule. Carbon atoms are shown in grey, hydrogen in white, nitrogen in blue, oxygen in red, and fluorine in green. The model highlights the three-dimensional nature of the chiral center and the spatial orientation of the various functional groups.</p>

Figure 5.1: Structural information of Escitalopram

Escitalopram is predominantly recommended for managing general anxiety disorder, which involves excessive and uncontrollable worry about various aspects of life, and severe depressive disorder, characterized by a chronically depressed attitude, a decline in interest or enjoyment, and other emotional and physical symptoms. It falls into the category of pharmaceuticals known as Selective Serotonin Reuptake Inhibitors (SSRIs). The mechanism of action for SSRIs involves elevating serotonin, a neurotransmitter, within the brain. This elevation can lead to mood enhancement, anxiety reduction, and the alleviation of specific symptoms associated with depression. Its function involves the inhibition of serotonin reuptake in the brain, resulting in heightened serotonin levels within the synaptic cleft, the gap between nerve cells. This heightened serotonin activity is believed to contribute to the therapeutic effects in treating depression and anxiety. Generally, drug molecules have become the focus of increased interest as potential corrosion inhibitors because of their capacity to create protective coatings on metal surfaces. These compounds possess unique chemical structures and functional groups that allow them to interact with metal surfaces, forming protective layers that

inhibit corrosive reactions. Extensive research is ongoing to explore the corrosion-inhibiting properties of various drugs, including their efficiency, mechanism of action and compatibility with different metal substrates. Using drugs as corrosion inhibitors holds promise in providing environmentally friendly and cost-effective solutions for corrosion protection in various industrial applications. However, further research and investigation are necessary to understand the mechanisms of drug-metal interactions fully and to tailor these compounds for specific corrosion protection applications. Nevertheless, this emerging field holds great promise for advancing corrosion inhibition techniques with the utilization of pharmaceutical compounds. The current investigation is centered around the evaluation of escitalopram, an antidepressant, as a potential alternative anticorrosive agent for mild steel. The assessment encompasses the utilization of weight loss measurement along with electrochemical methodologies to determine the degree of inhibition efficacy, rate of corrosion, and the underlying mechanism of action. Additionally, FT-IR technique and UV analysis have been performed to facilitate comprehensive characterization. The inquiry also delves into the impact of temperature on the inhibitive effectiveness of escitalopram. To gain deeper insights into the protective attributes of escitalopram on the surface of test metal, the morphological examination of the safeguarded metal is performed using atomic force microscopy. Furthermore, certain quantum chemical computations have been executed to elucidate the experimental findings derived from this investigation, thereby providing enhanced understanding into the inhibitory effectiveness of escitalopram on the surface of mild steel.

5.2 EXPERIMENTAL AND METHODS

5.2.1 Preparation of metal sample and test solutions

Identical mild steel specimens, each measuring 10 cm², were employed for the current experimental investigation. The mild steel samples underwent a systematic preparation process involving abrasion with emery papers of varying grades (200, 400, 600, and 800) to attain a polished and lustrous surface. Subsequently, they were carefully washed using double-distilled water, then subjected to a degreasing process with acetone, and ultimately dried using hot air. The mild steel's elemental composition was determined as follows: Carbon (C) of 0.17%, Silicon (Si) of 0.20%, Manganese (Mn) of 0.54%, Phosphorus (P) of 0.16%, and Iron (Fe) of 98.7%. A corrosive environment was established by preparing a 1M solution of an aggressive medium, hydrochloric acid (HCl), employing high-purity AR-grade 37% HCl dissolved in double-distilled water. Inhibitor solutions with varying concentrations ranging from 5 to 20 ppm were formulated by dissolving precise quantities of the inhibitor in the aggressive medium.

5.2.2 Weight Loss Study

The weight loss methodology stands as the most widely employed mode of assessment for examining inhibition in the context of temperature influence. To comprehensively explore the temperature effect on the efficacy of escitalopram in safeguarding mild steel against corrosive processes within a 1 M hydrochloric acid solution, a meticulous investigation was conducted. This entailed exposing mild steel samples to a range of temperatures, spanning from 303 K to 333 K, under different inhibitor concentrations (5 ppm to 20 ppm), both with and without inhibitors. Prior to experimentation, the mild steel samples underwent a series of thorough preparatory steps. These steps included the achievement of a polished mirror-like surface through the sequential utilization of emery papers with varying degrees of abrasiveness. Post-abrasion, the samples were subjected to a rigorous cleansing process involving acetone and double-distilled water, followed by thorough drying utilizing a hot air stream.

The evaluation of inhibitory efficiency, surface coverage, and corrosion rate was executed employing the subsequent formulations[146].

$$IE\% = \frac{W_o - W_i}{W_o} \times 100$$

$$\theta = \frac{W_o - W_i}{W_o}$$

$$C_r = \frac{534 \times W}{A \times t \times D}$$

Where, the notation employed is as follows: IE signifies the Inhibition Efficiency, the symbol θ represents the fraction of surface coverage, and C_r stands for the Corrosion Rate (expressed in mpy) . The parameters W_0 and W_i respectively stand for the Weight Loss of the metal sample with exclusion and inclusion of the drug. Here, W signifies the overall weight loss in milligrams, while 'A' pertains to the specimen surface area in cm^2 ; the symbol 't' represents the duration of immersion in hours, while 'D' stands for the density of the sample, measured in grams per cubic centimeter.

5.2.3 Electrochemical Study

Nyquist impedance curves and Tafel polarization curves were acquired through the employment of an Electrochemical Workstation Gamry Potentiostat, specifically the IFC-1010E model. The experimental setup included three electrodes: the working electrode of Mild steel sheet with an exposed area measuring 1 cm^2 ; reference electrode as Ag/AgCl electrode, and the platinum wire as a counter electrode. The procedure involved immersing the working electrode into diverse sample solutions. All electrochemical assessments were performed under steady-state conditions at a temperature of 303 K, utilizing 300 ml of electrolyte composed of 1 M hydrochloric acid (HCl). Before each PDP and EIS test, the working electrode experienced a corrosion phase,

during which its open circuit potential (OCP) was assessed. To attain Nyquist plots, EIS was accomplished with AC signals in a frequency range of 100 kHz to 0.2 Hz and an amplitude of 10 mV. Through the utilization of the furnished equation, the judgment of the effectiveness of the inhibitor was based on the values of charge transfer resistance (R_{ct}).

$$IE\% = \left(1 - \frac{R_{ct}^0}{R_{ct}'}\right) \times 100$$

Here, R_{ct} and R_{ct}' represent the charge transfer resistance when the inhibitor is excluded and when the inhibitor is included.

The PDP curves were systematically captured within a voltage range spanning from -250 to $+250$ mV vs. the standard electrode (Ag/AgCl), comparative to the measured OCP. A scanning rate of 1 mV/s was employed for these measurements. By exploiting current densities (I_{corr}), the inhibitory efficacy of the inhibitor was assessed through the application of the subsequent formula:

$$IE\% = \frac{I_{corr}^0 - I_{corr}'}{I_{corr}^0} \times 100$$

Where I_{corr}^0 and I_{corr}' are current density in the absence of inhibitor and at various concentrations of inhibitor, respectively.

The mean value of each parameter is reported after running the experiment in triplicate.

5.2.4 Quantum Chemical Study

Density Functional Theory (DFT) was made use of for analyzing various quantum molecular characteristics with the goal of establishing a connection between the effectiveness of inhibition and the molecular structure of the drug, while also investigating the mechanisms of inhibition. The optimized configuration and quantum chemical parameters of escitalopram were computed in both gaseous and aqueous phases through DFT calculations employing the ω B97X-D method and the basic set 6-31 G* within the Spartan 20 software platform. DFT has been recognized for furnishing dependable outcomes in describing a spectrum of molecular properties, including E_{LUMO} , E_{HOMO} and electronegativity. These attributes can be computed from the aforementioned parameters.

Ionization potential (I) characterizes the disposition of a chemical entity to give up electrons, and its relation with (E_{HOMO}) is elucidated by the equation:

$$I = -E_{HOMO}$$

Electron affinity (A) signifies a chemical species' propensity to acquire electrons, and its correspondence with E_{LUMO} is delineated through the equation:

$$A = -E_{LUMO}$$

Electronegativity is intrinsic inclination of an atom to allure electrons, and its quantification can be achieved utilizing the subsequent formula:

$$\chi = \frac{I+E}{2}$$

Chemical hardness (η) evaluates an atom's resistance to a transfer of charge and can be computed via the equation:

$$\eta = \frac{I-A}{2}$$

The equation expresses the proportion of electrons transferred in a chemical reaction.

$$\Delta N = \frac{\chi_{Fe} - \chi_{inh}}{2(\gamma_{Fe} + \gamma_{inh})}$$

Where χ_{Fe} –electronegativity of iron(7 eV/mol), γ_{Fe} – global hardness of iron(0).

5.2.5 Surface Study

To find out how the inhibitor affects the preservation of metals, an analysis of the surface was conducted subsequent to immersing the metal samples separately in the unaltered medium (1 M HCl) and a solution containing a 20 ppm inhibitor concentration for a duration of 4 hours. This investigation was facilitated through the utilization of an Atomic Force Microscope (specifically, the Bruker Atomic Force Microscope).

5.3 RESULT AND DISCUSSIONS

5.3.1 Characterization

a) UV-Vis Study

In order to carry out the characterization of the drug, a drug solution was meticulously prepared at a concentration of 100 mg/ml. Subsequently, the electronic spectra of the drug solution were obtained using a Shimadzu UV-Vis spectrophotometer (UV-3600 plus). The discerned outcome indicated a prominent peak of maximal absorption at a wavelength of 238 nm, a distinctive feature aligned with the spectral profile of escitalopram (Figure 5.2)[147]. **b) FT-IR Analysis**

To verify that specific groups really exist, in the experimental drug, Fourier Transform Infrared (FT-IR) spectroscopy was utilized, employing a Perkin Elmer Fourier Transform Infrared spectrophotometer. The spectral analysis revealed distinct peaks at specific wavenumbers: 3336 cm^{-1} for -N-H stretching, 2882 cm^{-1} denoting aliphatic -C-H stretching, 2249 cm^{-1} corresponding to -CN stretching, 1240 cm^{-1} indicative of -C-N stretching, 1102 cm^{-1} representing aliphatic -C=O deformation, 1022 cm^{-1} signifying -C-F stretching, and 766 cm^{-1} relating to -C=C bending. These observed spectral features align precisely with the characteristic vibrational patterns of Escitalopram (Figure 5.3)[147].

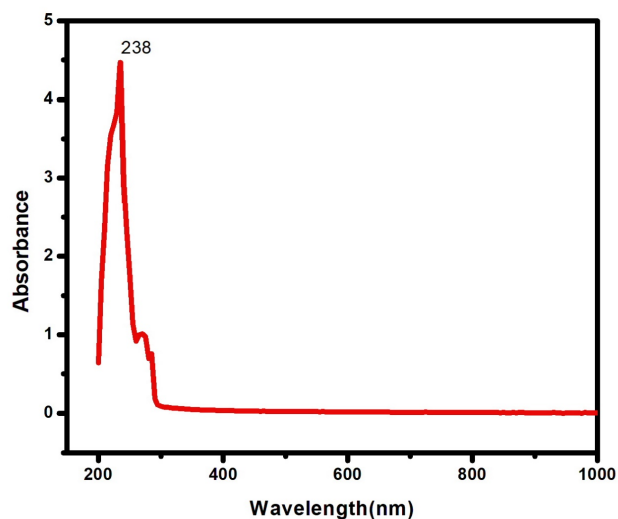


Figure 5.2: UV spectrum of Escitalopram

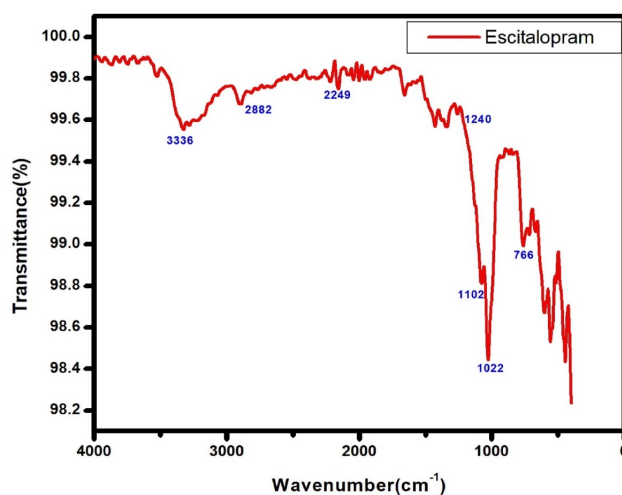


Figure 5.3: FT-IR Spectrum of Escitalopram

5.3.2 Weight Loss Study

a) Effect of inhibitor concentration on Corrosion rate and Inhibition efficiency

A comprehensive investigation through weight loss analysis was undertaken to evaluate variables like inhibition efficacy (IE), rate of corrosion (C_r), and surface coverage (θ). This examination entailed subjecting a mild steel specimen to an array of inhibitor concentrations spanning from 5 to 20 ppm within a corrosive medium, conducted over a temperature ranging from 303 K to 333 K. From the presented data of Table 5.1, 5.2 it has been concluded how the incorporation of the drug into the aggressive environment

yields a notable enhancement in inhibition efficiency along with a concurrent reduction in the magnitude of corrosion. Specifically, the IE% exhibited an escalation from 85.7% to 96% as the inhibitor concentration was augmented from its base value to 20 ppm. On the other hand, a decrease in effectiveness from 96% to 80.27% was seen when the drug dosage was maintained at 20 ppm at the elevated temperature of 333 K.

The binding of the drug onto the MS surface causes a rise in surface protection, which, in turn, causes a decline in the degree of corrosion and a rise in prevention efficacy. In contrast, with the enhancement of concentration, the corrosion rate declines (Figure 5.3), and inhibition efficiency increases (Figure 5.4), since the drug develops a layer of protection over the MS sample, reducing or eliminating the likelihood of corrosion. It's evident that as the inhibitor concentration rises, the surface protection by the studied drug also rises.

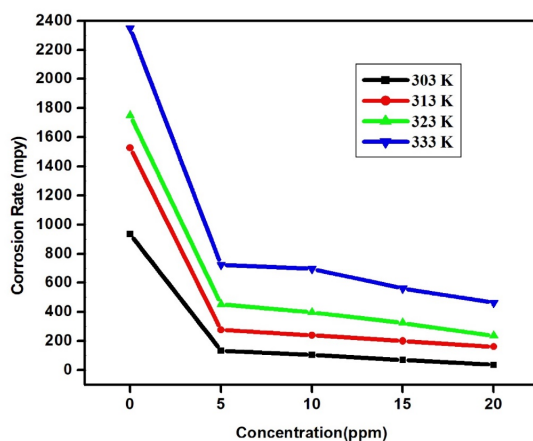


Figure 5.4: Rate of Corrosion of MS in 1M HCl with 5-20 ppm of EST at 303-333K

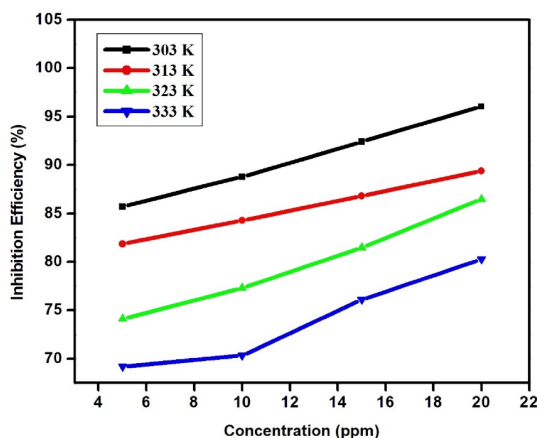


Figure 5.5: Inhibition Efficiency of Escitalopram for mild steel protection in 1 M HCl at 303-333K with 5-20 ppm of EST.

Table 5.1: IE, C_r , and θ of Escitalopram with mild steel at 303K and 313K temperature with different concentration range

Temp. (K)	303			313		
	C_r (mpy)	θ	I.E. (%)	C_r (mpy)	θ	I.E. (%)
0	934.57	-	-	1526.07	-	-
5	133.51	0.86	85.71	277.16	0.82	81.84
10	104.78	0.89	88.79	239.98	0.84	84.27
15	70.98	0.92	92.41	201.11	0.87	86.82
20	37.18	0.96	96.02	162.24	0.89	89.37

Table 5.2: IE, C_r , and θ of Escitalopram with mild steel at 323K and 333K temperature with different concentration range

Temp. (K)	323			333		
	C_r (mpy)	θ	I.E. (%)	C_r (mpy)	θ	I.E. (%)
0	1749.15	-	-	2347.41	-	-
5	452.92	0.74	74.11	723.32	0.69	69.19
10	397.15	0.77	77.29	696.28	0.7	70.34
15	324.48	0.81	81.45	561.08	0.76	76.1
20	236.6	0.86	86.47	463.06	0.8	80.27

b) Thermodynamic and Kinetic Parameters

Present investigation focused on the mild steel protection against corrosion, coupled with an examination of the temperature's influence, aiming to delineate the trends in inhibition efficiency and corrosion behavior across a temperature spectrum of 308 K to 338 K. This analysis was carried out within an acidic milieu comprising 1N hydrochloric acid (HCl), facilitated by the introduction of inhibitors. Fluctuations in temperature lead to various changes on the MS substrate, including processes such as adsorption, desorption, rearrangement, and dissociation of the drug. The influence of temperature holds a notable sway over corrosion phenomena, a facet that can be harnessed to elucidate the mechanisms underpinning corrosion inhibition. The connection between temperature and corrosion rate is understood by applying the principles of the Arrhenius equation[97].

$$\log C_r = -\frac{E_a}{2.303RT} + \log A$$

Where, E_a : Apparent effective activation energy,

R: Molar gas constant

A: Arrhenius pre-exponential factor.

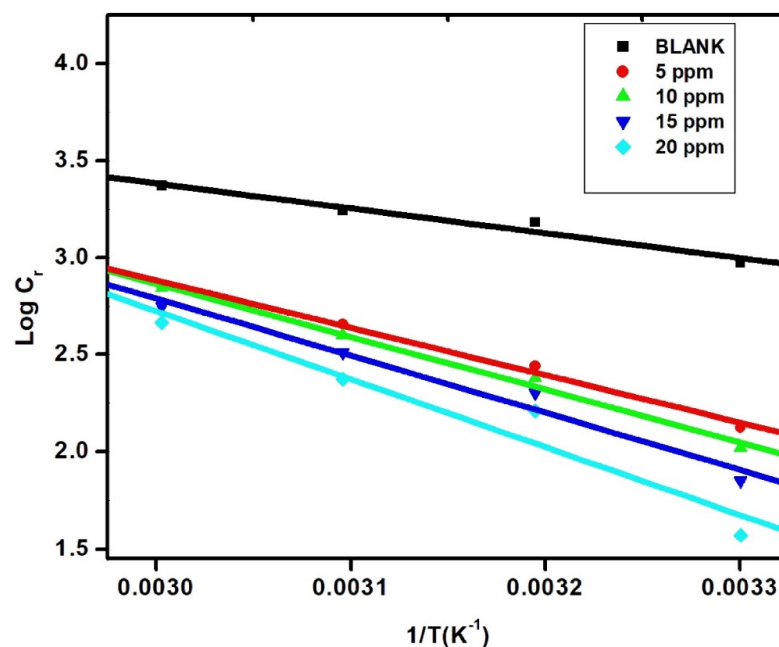


Figure 5.6: Arrhenius plot for $\log C_r$ vs $1/T$ for mild steel variable concentrations of Escitalopram.

The pre-exponential factor (A) was determined by finding the intersection point on the graph that illustrates the $\log C_r$ vs $1/T$ (Figure 5.5). On the other hand, E_a was found using the gradient or slope of this curve. The dataset presented in Table 5.3 demonstrates a conspicuous contrast in activation energy between the inhibited and uninhibited samples. This difference suggests that the inhibited sample demonstrates a significantly greater activation energy, indicating a substantial binding of drug onto the mild steel surface, which in turn leads to a decrease in the extent of corrosion.

Table 5.3: Kinetic and Thermodynamic parameters of Escitalopram with MS at different temperatures and inhibitor concentration range

Conc. (ppm)	E_a (kJ/mol)	A ($\times 10^3$)(Sec ⁻¹)	ΔH (kJ/mol)	$-\Delta S$ (kJ/mol/K)	ΔG (kJ/mol)			
					303 (K)	313 (K)	323 (K)	333 (K)
Blank	24.41	1.61×10^3	21.77	0.117	57.34	58.51	59.69	60.86
5	46.75	1.62×10^4	44.11	0.059	62.02	62.61	63.2	63.8
10	51.99	1.03×10^8	49.35	0.044	62.55	62.99	63.42	63.86
15	56.26	4.06×10^8	53.62	0.032	63.32	63.64	63.96	64.28
20	67.01	1.69×10^{10}	64.38	0.001	64.55	64.55	64.56	64.56

The transition state equation, an alternative representation of the Arrhenius equation, was employed to compute the remaining activation parameters[148].

$$C_r = \frac{RT}{Nh} \exp\left(\frac{\Delta S}{R}\right) \exp\left(-\frac{\Delta H}{RT}\right)$$

(h: Planck's constant; N: Avogadro's number)

Upon constructing the graph of the logarithm of corrosion rate ($\log C_r$) divided by temperature (T) against the reciprocal of temperature ($1/T$), a linear relationship was evident, as depicted in Figure 5.6. Through analysis of the intercept and slope of this straight line curve, the values of ΔH and ΔS were computed and subsequently documented in Table 5.2. The inhibitor's presence impedes the onset of corrosion, as evidenced by the observed increase in the ΔH value related to the phenomenon of corrosion. The presence of negative entropy of activation values suggests that as the reaction progressed with higher inhibitor concentrations, there was a reduced degree of disorder or entropy involved.

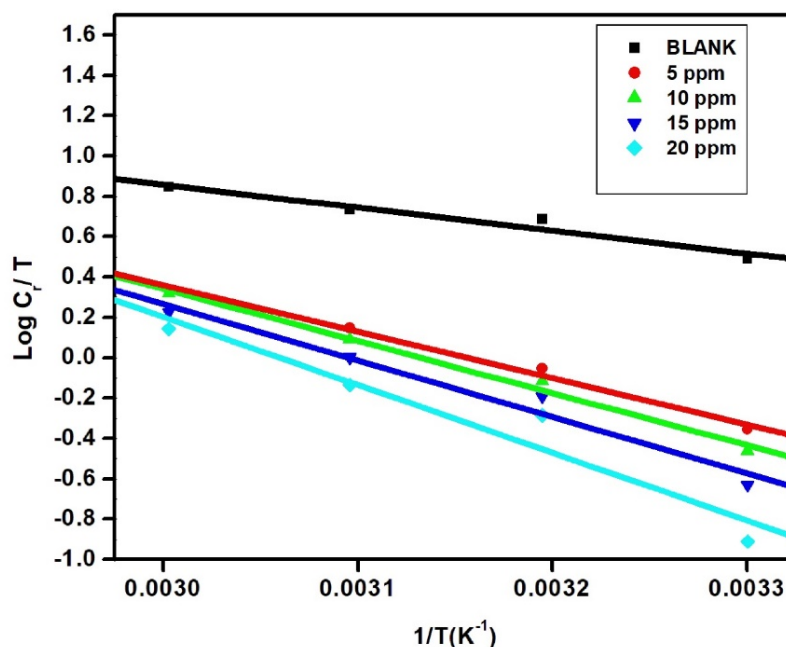


Figure 5.7: Transition state plot for mild steel protection in blank and at variable concentrations of Escitalopram in 1 M HCl.

From Figure 5.8, a discernible trend is evident where both activation energy and corrosion enthalpy exhibit an augmentation as the inhibitor concentration is heightened. This phenomenon can be ascribed to an amplified surface coverage stemming from the elevated propensity for inhibitor adsorption onto the metal surface.

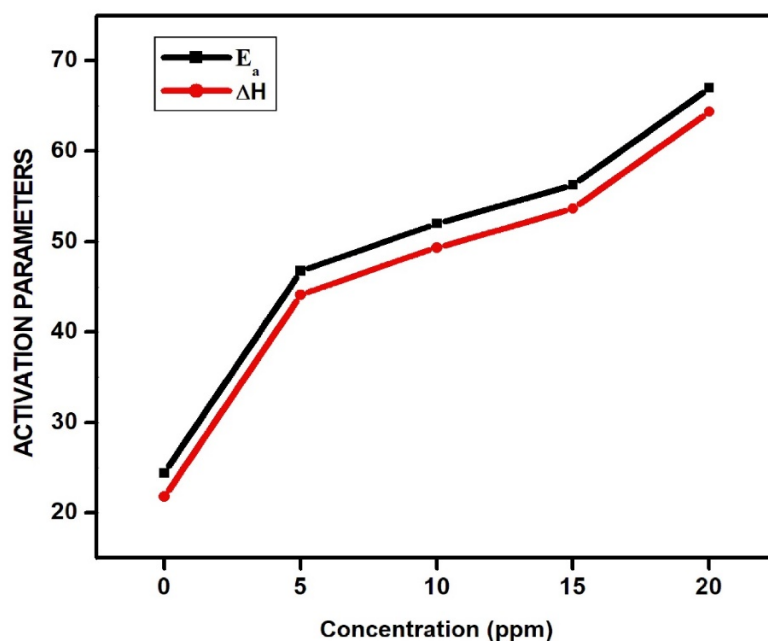


Figure 5.8: Variation of activation energy and enthalpy versus concentration of Escitalopram.

By using following formula, the free energy change of activation for corrosion phenomenon can be determined.

$$\Delta G = \Delta H - T\Delta S$$

The Gibbs free energy (ΔG) reflects the spontaneity of a chemical process. A positive ΔG indicates a non-spontaneous process, implying that energy input is required to initiate the reaction. As temperatures rise, the trend of ΔG values becoming more positive indicates a growing energy barrier for the reaction, implying a reduced likelihood of the reaction taking place. The Gibbs free energy for adsorption values, which are documented in Table 5.3, are characterized by their positive nature. Notably, there exists a subtle alteration in these values as temperatures are elevated, indicating a degree of instability associated with the activated complex.

Furthermore, when investigating the impact of increasing the inhibitor concentration, it is evident that the ΔG values undergo an increase. This upsurge in values signifies a reduced probability of the activated complex formation. The impact of the inhibitor's concentration on ΔG is significant. A higher ΔG value with a rise in dosages of the drug indicates that the presence of the drug reduces the spontaneity of the reaction, making it less likely to occur on its own. This supports the idea that the inhibitor is introducing an energy barrier, deterring the creation of the activated complex, and thus decreasing the likelihood of the corrosion process.

c) Adsorption Isotherms

The exploration of metal-inhibitor interactions is facilitated through the utilization of adsorption isotherms. Diverse sets of experimental adsorption data were subjected to several adsorption isotherm models, encompassing the Freundlich, Temkin, Langmuir, and El-Awady isotherms. Out of these models, the Langmuir adsorption isotherm displayed the highest degree of agreement, indicating the dominance of monolayer adsorption phenomena. This result emphasizes the tendency of the Escitalopram inhibitor to participate in monolayer adsorption on the MS substrate in acidic environment. The mathematical form of Langmuir isotherm for adsorption is given as:

$$\frac{C}{\theta} = \frac{1}{K_{ads}} + C$$

Where, K_{ads} : adsorption equilibrium constant, θ : degree of surface coverage, and C : Inhibitor concentration.

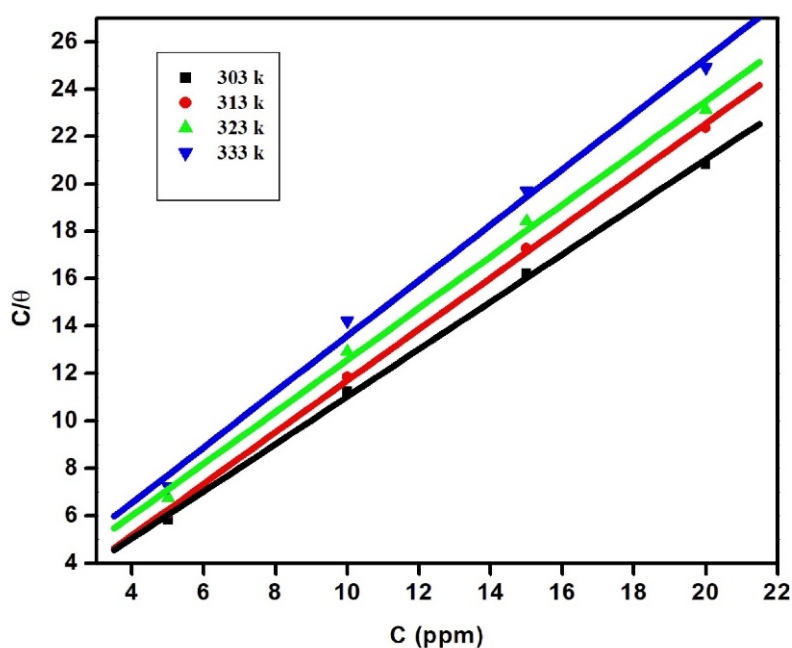


Figure 5.9: Langmuir Isotherm of adsorption for Escitalopram.

A plot of C/θ against C was constructed, revealing a slope that closely approximated unity across different experimental temperatures within the context of 1 M hydrochloric acid (HCl), as depicted in Figure 5.9. Subsequently, through the application of the isotherm model, both R^2 (the coefficient of determination) and values of ΔG_{ads} (Gibbs free energy of adsorption) pertinent to the current inhibitor were computed and cataloged in Table 5.3. The relationship of equilibrium constant with standard free energy is given as

$$K_{ads} = \frac{1}{1 \times 10^{-6}} \exp\left(-\frac{\Delta G_{ads}}{RT}\right)$$

Where K_{ads} : - Equilibrium adsorption constant, T: -Temperature in Kelvin, ΔG_{ads} : - standard free energy, R-molar gas constant.

Table 5.4: Parameters of adsorption as computed from Langmuir isotherm of adsorption.

Temp. (K)	Slope	R ²	$K_{ads} \times 10^3$	ΔG_{ads}
303	1.00	0.9993	952.032	-34.93
313	1.08	0.99964	1172.33	-35.54
323	1.01	0.99817	605.484	-38.45
333	1.07	0.99747	532.497	-40.00

The spontaneous nature of the adsorption phenomenon is quite obvious with the adsorption parameters presented in Table 5.4 yielding free energy with negative values, which is also indicative of the establishment of a stable adsorbed layer for the drug onto the surface of MS. The ΔG_{ads} values, below -20 kJ/mol, indicate a situation of physical adsorption, whereas values exceeding -40 kJ/mol imply chemical adsorption. In the context of the current investigation, the ΔG_{ads} values fall towards -40 kJ/mol, implying the chemical adsorption mechanisms for the escitalopram inhibitor on the substrate. The parameter K_{ads} represents the intensity of the binding between the MS and the drug. Higher positive K_{ads} values indicate a more effective binding between the substance being adsorbed and the surface it adheres to, ultimately leading to higher inhibition efficiency. Additionally, K_{ads} diminishes with escalating temperature, highlighting the reduced feasibility of the adsorption process under higher temperature conditions.

5.3.3 Electrochemical Study

a) Analysis of Linear Polarisation Measurements (LPR)

The linear polarization resistance method presents a straightforward and expeditious approach for swiftly determining corrosion rate, corrosion current, and polarization resistance, thus promptly assessing inhibition efficiency. Using this method, we determined the polarization resistance (R_p), corrosion current (I_{corr}), and inhibition rate in the inhibited solution of various concentrations of escitalopram in acidic media (HCl) for MS. These values are documented in Table 5.5. Upon meticulous analysis, it can be inferred that the R_p values exhibited an elevation while the corrosion current values registered a decline. These trends collectively underscore the heightened efficacy of escitalopram in terms of corrosion inhibition, a potency that strengthens as the concentration of the inhibitor increases.

Table 5.5: Linear polarization resistance characteristics of mild steel with Escitalopram.

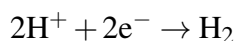
Conc. (ppm)	E_{corr} (mV (Ag/AgCl))	I_{corr} ($\mu\text{A}/\text{cm}^2$)	IE (%)	R_p ($\Omega \text{ cm}^2$)	IE (%)
Blank	-754	1157	-	38.11	-
5	-443.2	87.44	92.44	487.5	92.18
10	-439.1	67.43	94.17	617	93.82
10	-429.3	56.53	95.11	713.3	94.66
20	-436.9	41.99	96.37	930.9	95.91

b) Analysis of Potentiodynamic Polarization Curves

The potentiodynamic polarization curve, commonly known as a Tafel plot, illustrates the current response generated within an electrochemical cell as well as the electrode potential of a specific metal under controlled circumstances. This graphical representation, as depicted in Figure 5.10 furnishes insights into the corrosion potential and the ensuing current. Essentially, it elucidates the impact of corrosion on the metal under investigation. The phenomenon of corrosion is fundamentally the metal dissolution through oxidative breakdown at the metallic surface, concomitant with reduction reactions transpiring within an aqueous environment.

Anodic reaction- $M \rightarrow M^{n+} + ne^{-}$

Cathodic reaction- $H_2O + e^{-} \rightarrow H_2 + OH^{-}$



The Tafel parameters, denoted by β_a and β_b , alongside the corrosion current and corrosion potential, have been observed and documented in Table 5.6. A significant observation derived from the illustrated figure is the noticeable shift downward at all concentrations in the cathodic and anodic segments of the potential curves. Moreover, with the augmentation of inhibitor concentration, this shift towards lower current densities becomes more distinct. This trend substantiates the occurrence of inhibition, facilitated through the establishment of a layer adsorbed onto the metal surface. The corrosion potential values (E_{corr}) did not exhibit anomalous variations, signifying the mixed-type behavior for the Escitalopram inhibitor. The corrosion of the metal is clearly inhibited by its ability to impede both the anodic and cathodic processes, leading to a significant reduction in the rates of these processes[149].

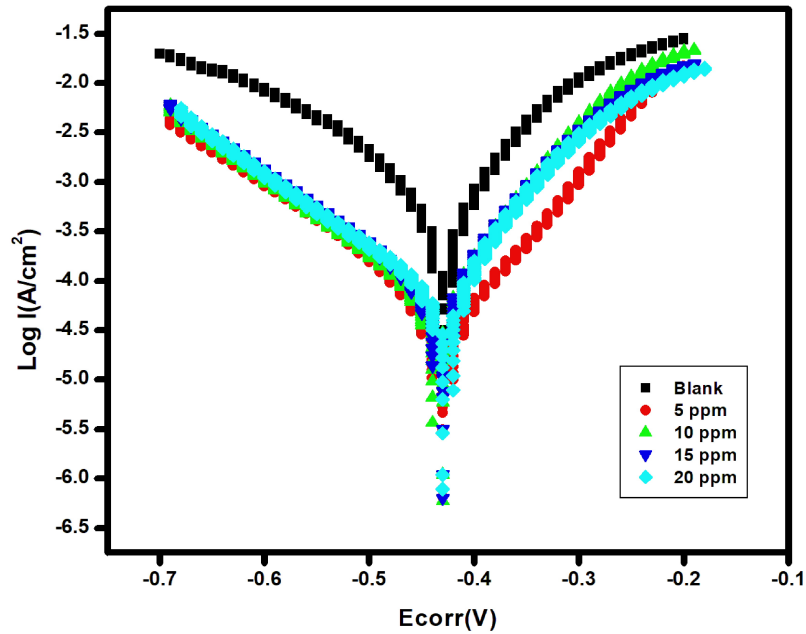


Figure 5.10: Tafel graph depicting mild steel in a 1M HCl with varying concentration of Escitalopram.

Table 5.6: Tafel polarization characteristics of mild steel when exposed to Escitalopram in a 1M HCl environment

Conc. (ppm)	β_a (mV/dec)	β_c (mV/dec)	E_{corr} (mV (Ag/AgCl))	I_{corr} ($\mu\text{A}/\text{cm}^2$)	IE (%)
Blank	93	117	-432	311	
5	126	119	-430	25.4	91.83
10	122.1	109.3	-427	23.2	92.54
15	166.7	139.9	-428	18.1	94.18
20	97.7	90	-420	11.6	96.27

c) Electrochemical Impedance Spectroscopy (EIS)

The EIS data was thoroughly examined in both 1 M HCl alone and when exposed to varying levels of escitalopram, specifically concerning mild steel corrosion. The Nyquist plot (depicted in Figure 5.11) distinctly illustrates how the resistance exhibited by mild steel against corrosion underwent modification upon the introduction of escitalopram. The impedance spectrum displays distinct capacitance semicircles, which are significantly enhanced by virtue of the presence of the inhibitor as compared to the blank solution. This enhancement in semicircle size is emblematic of the inhibitor's efficacy. As the inhibitor concentration escalates, the semicircles' dimensions mature,

indicative of an escalated proficiency for the inhibitor in governing the phenomenon of corrosion. The deviations within these semicircles are ascribed to frequency dispersion, stemming from the unevenness in MS surface influenced by the drugs binding[150]. At the interface between the MS and the aggressive medium, an electrical double layer is established, leading to the emergence of capacitance. This capacitance is subject to alteration in reaction to alternating current (AC).

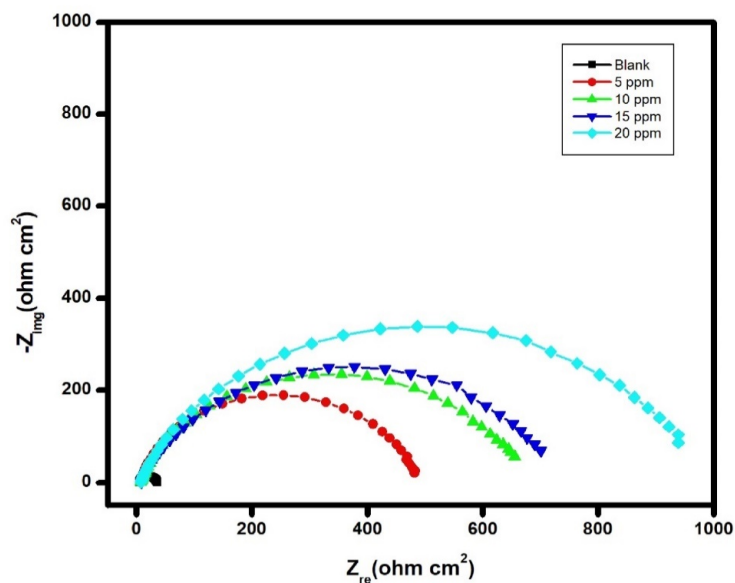


Figure 5.11: Nyquist Diagrams depicting mild steel in a 1 M HCl with varying concentration of Escitalopram.

As a result, the capacitive component (Cdl) has been replaced with a constant phase element (CPE). The representation of the electrochemical impedance spectra through an equivalent circuit is visually illustrated in Figure 5.12.

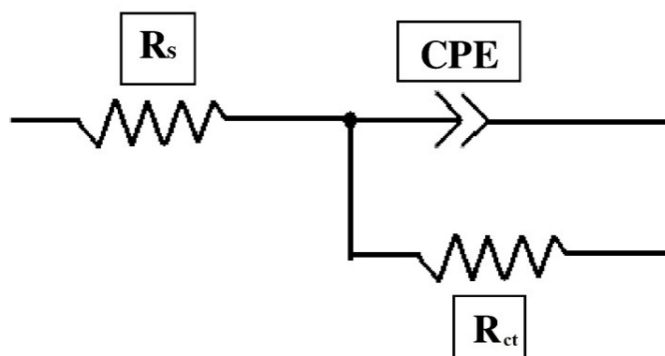


Figure 5.12: Equivalent Circuit model of the EIS

Where, CPE:-phase element, R_{ct} : charge transfer resistance and R_s : solution resistance and. The Z of CPE may be represented as

$$Z_{CPE} = Y_0^{-1}(j\omega)^{-n}$$

Where Y_0 is CPE constant, Ω represents angular frequency in rad s^{-1} , $i = (-1)^{1/2}$ and n is the represents phase shift, the measure of degree of irregularities in the metal surface. The calculation of double layer capacitance is done by using the equation;

$$C_{dl} = (Y_0 R_{ct}^{1-n})^{1/n}$$

The information in Table 5.7 makes it abundantly evident that as the drug's dosage rises in the aggressive medium, total impedance (R_{ct}) values rise while double layer capacitance (C_{dl}) values drop. The observed increase in (R_{ct}) values is probably explained by the development of a shielding layer on the exposed surface of the metal. Conversely, a rise in the double layer's thickness or a drop in the dielectric constant might be the cause of the (R_{dl}) values decline. Based on the insights gathered from the Electrochemical Impedance Spectroscopy data, there is a significant improvement in the rate of inhibition when the dosage of the drug is raised. This finding supports the assertion that escitalopram can function as an effective corrosion inhibitor against mild steel in an acidic medium. The outcomes of electrochemical impedance spectroscopy and potentiodynamic polarization are in good agreement, further confirming their consistency and reliability.

Table 5.7: EIS Characteristics of Mild Steel in the varying concentrations of Escitalopram

Conc. (ppm)	R_s ($\Omega \text{ cm}^2$)	R_{ct} ($\Omega \text{ cm}^2$)	Y_0 ($10^{-6} \Omega^{-1} \text{ cm}^{-2}$)	n	C_{dl} ($\mu \text{ F cm}^{-2}$)	I.E. (%)
Blank	4.34	30.70	186.00	0.88	618.74	-
5	6.64	475.45	82.30	0.87	383.26	93.54
10	7.39	582.29	74.60	0.88	315.64	94.73
15	8.04	692.22	69.50	0.89	266.57	95.56
20	7.77	930.32	54.20	0.89	203.16	96.70

5.3.4 Quantum Chemical Study

The Energy of HOMO (E_{HOMO}) represents a compound's tendency to provide electrons to electron-deficient species, whereas E_{LUMO} signifies the molecule's propensity to receive electrons. For a molecule to be an effective inhibitor, it should possess elevated E_{HOMO} and diminished E_{LUMO} values, alongside a narrow energy gap. The experimental compound under scrutiny exhibits higher E_{HOMO} and lower E_{LUMO} values, substantiating its efficacy as an efficient inhibitor.

The dipole moment of a molecule corresponds to its polarity, with higher polarity implying an inclination for dipole-dipole attractions. This attribute is intertwined with inhibition efficiency. The parameter ΔN gauges a molecule's capacity for electron acceptance or donation. A positively elevated ΔN value signifies electron donation propensity, whereas a negatively lower value indicates an electron-accepting nature. If the fraction of transferred electrons (ΔN) remains below 3.6, the compound demonstrates amplified efficacy with increasing electron donation towards the metal surface. A greater fraction of transferred electrons correlates with heightened inhibition efficiency, while a lower fraction corresponds to reduced inhibition efficacy.

In the case of the present inhibitor, the ΔN value lies below 3.6, highlighting its strong electron donation potential, a quality that contributes to its efficiency as a corrosion inhibitor. Computed ΔN values align with the experimental findings. Chemical hardness is a critical parameter indicating a molecule's readiness to accept electrons. Molecules with lower chemical hardness can serve as effective inhibitors. The calculated chemical hardness value for the compound concurs with experimental results. These evaluations have been made with a computational approach utilizing the Density Functional Theory (DFT), widely employed in quantum chemistry to predict molecular properties. DFT calculations for both the aqueous and gas phases of escitalopram are detailed in Table 5.8, elucidating the diverse quantum chemical parameters pertinent to the compound.

Table 5.8: Quantum Chemical parameters for Escitalopram for gas and aqueous phase

	E_{HOMO} (eV)	E_{LUMO} (eV)	I (eV)	A (eV)	χ (eV)	η (eV)	ΔE (eV)	μ (D)	ΔN
Gas	-7.6	0.28	7.6	-0.28	3.66	3.94	7.88	3.38	0.464467
Aqueous	-7.63	0.4	7.63	-0.4	3.615	4.015	8.03	4.3	0.465187

Upon thorough examination, it is evident that the quantum chemical parameters in the aqueous phase surpass those in the gaseous phase for escitalopram. This phenomenon suggests the occurrence of protonation, as protonated inhibitors tend to exhibit an augmented propensity for electron donation, thus enhancing the capability for the adsorption of the compound over the surface of the metal. The higher dipole moment observed for the compound in the aqueous phase signifies its capacity for electrostatic interaction with the metal, a trait attributed to protonation and indicating a form of physical adsorption. Quantum chemical parameters collectively corroborate the potential for both physisorption and chemisorption of the drug onto the metal substrate. This alignment between theoretical quantum insights and experimental outcomes underscores the validity of the findings. Figure 5.13 illustrates the optimized structural configuration, along with the distribution of HOMO and LUMO of both the gaseous as well as aqueous phases of escitalopram.

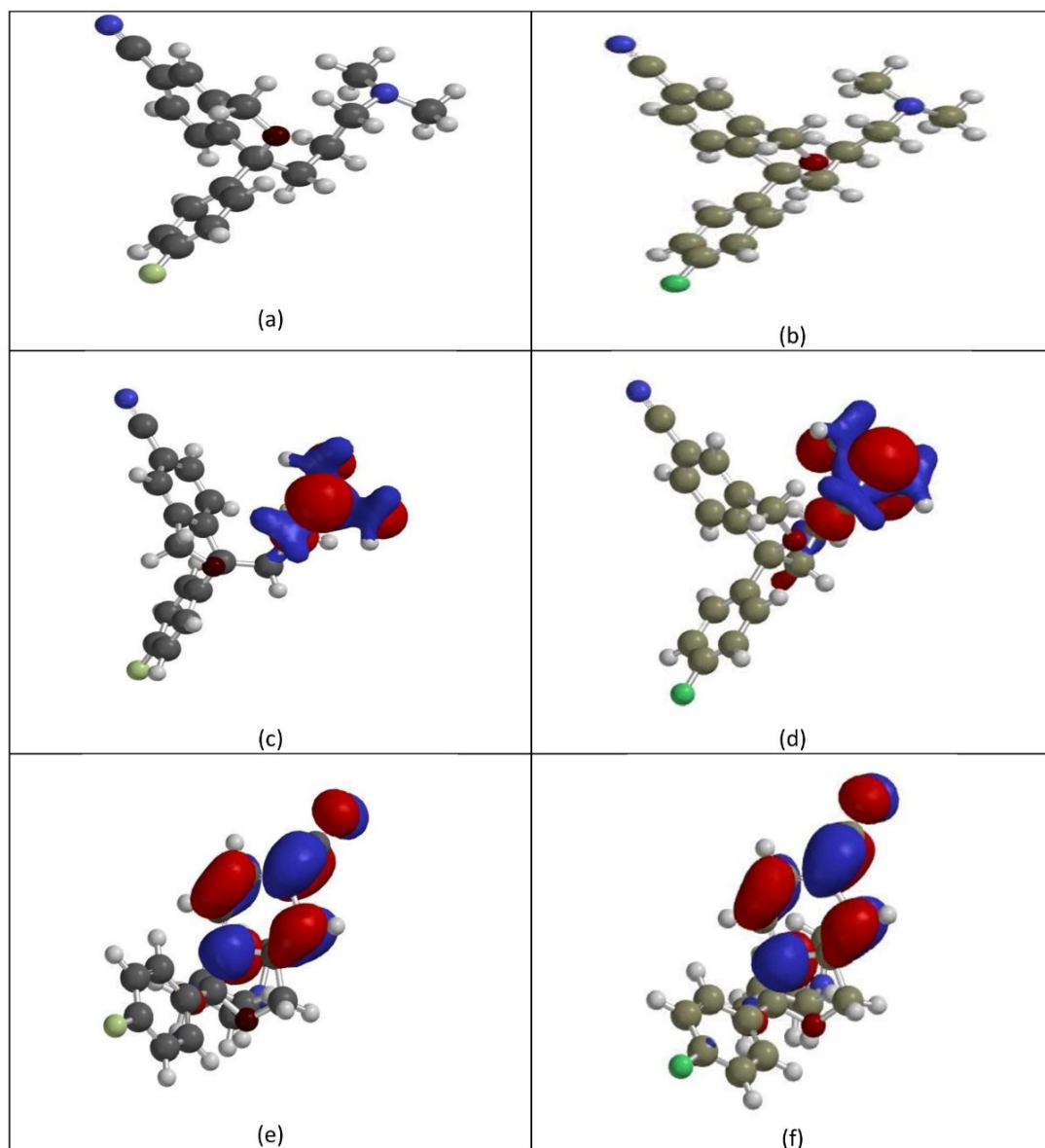


Figure 5.13: Optimized Structure and the corresponding HOMO and LUMO for Escitalopram in the Gas phase (a, c, e) and Aqueous phase (b, d, f).

The computed Mulliken charges for both gaseous and aqueous phases of escitalopram have been detailed in Table 5.9 through the quantum chemical investigation. A thorough scrutiny of these values reveals that the atoms N2 (-0.42), N3 (-0.54), and O1 (-0.56) exhibit the highest charges. These charged entities on specific atoms are indicative of active centers that hold significance for the adsorption process.

Table 5.9: Mulliken Charges for gas(g) and aqueous phase(aq) Escitalopram.

Atom	Charge		Atom	Charge		Atom	Charge	
	Gas	Aqueous		Gas	Aqueous		Gas	Aqueous
C1	-0.22	-0.22	C17	-0.15	-0.17	H14	0.132	0.145
C2	0.087	0.061	C18	-0.34	-0.36	H15	0.178	0.179
C3	-0.18	-0.18	C19	-0.34	-0.36	H16	0.16	0.179
C4	-0.23	-0.24	C20	0.247	0.278	H17	0.154	0.164
C5	0.101	0.091	C21	0.176	0.193	H18	0.161	0.171
C6	0.057	0.05	F1	-0.3	-0.32	H19	0.159	0.158
C7	-0.11	-0.12	H1	0.203	0.233	H20	0.154	0.164
C9	0.102	0.099	H2	0.186	0.225	H21	0.13	0.144
C10	0.393	0.377	H5	0.162	0.202	H22	0.169	0.174
C11	-0.19	-0.22	H6	0.203	0.229	H23	0.166	0.174
C12	-0.2	-0.22	H7	0.192	0.209	H24	0.166	0.175
C13	-0.24	-0.26	H8	0.181	0.197	H25	0.169	0.175
C14	-0.25	-0.26	H11	0.194	0.203	N2	-0.38	-0.42
C15	-0.3	-0.32	H12	0.189	0.212	N3	-0.46	-0.54
C16	-0.33	-0.33	H13	0.189	0.214	O1	-0.53	-0.56

5.3.5 Surface Study: Atomic Force Microscopy (AFM)

AFM was used to conduct a comprehensive surface characterization of a mild steel specimen under two different conditions: immersion in acid (HCl) and in the 20 ppm amount of the drug, over a 4-hour period. Within a $10 \mu\text{m} \times 10 \mu\text{m}$ area, the surface was meticulously examined to quantify the level of surface roughness. The computed mean surface roughness measurements for mild steel were found to be 224 nm when exposed to the corrosive environment and 39.88 nm when the inhibitor was present (Fig 5.14). Clearly, when inspecting the mild steel surfaces exposed to the corrosive environment without an inhibitor, they exhibited a fragmented appearance. In contrast, when the inhibitor was present, the surfaces showed reduced fragmentation, which can be supported by the protective effect of the drug effectively safeguarding the MS surface from degradation.

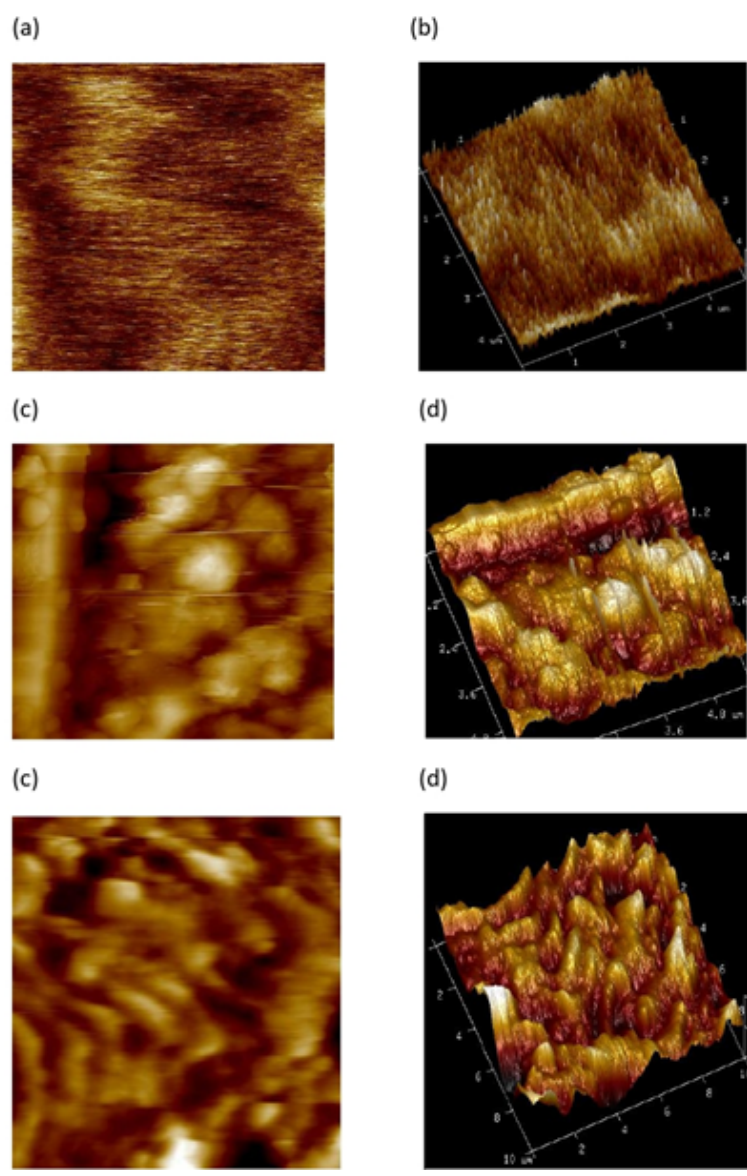
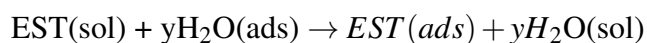


Figure 5.14: (a) & (b) are 2D and 3D scan of polished metal (reference), (c) & (d) are 2D and 3D scan of MS surface immersed in 1 M HCl(blank), (e) & (f) are 2D and 3D scan of MS immersed in 20 ppm Escitalopram in 1 M HCl

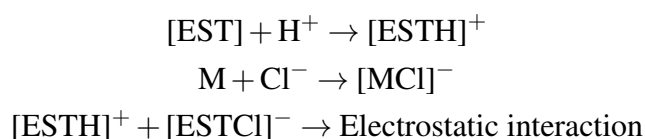
5.4 MECHANISM OF INHIBITION

It is possible to comprehend the mechanism by which escitalopram inhibits MS corrosion in acidic solution by doing a comprehensive analysis that includes thermodynamic, electrochemical, and quantum chemical investigations. This procedure involves the attachment of drug molecules to the substrate, achieved through a displacement reaction that replaces water molecules that had previously adhered to the metal surface.



The weight loss measurements substantiate the coexistence of mechanism of physisorption and chemisorption underlying the method of inhibition. Within this context, the es-

escitalopram molecules, upon interacting with active sites primarily located on nitrogen (N) and oxygen (O) atoms, undergo protonation, thereby attaining heightened charge density. Consequently, these protonated sites serve as docking points for chloride ions, thereby leading to a generation of charges within the acidic environment. In the presence of hydrochloric acid, chloride ions binds onto the charged metal surface, results in the formation of a negatively charged area. This situation promotes the electrostatic attraction between the protonated drug molecules and the negatively charged metal surface. This combined interaction mechanism leads to a type of physical adsorption, providing an explanation for the intricate interaction between charged species in the corrosive environment.



The monolayer adsorption process of the drug onto the MS surface is accurately explained by employing the Langmuir adsorption isotherm model. Electrochemical evaluations indicate a mixed-type behavior of the drug where the inhibitory effect is multifaceted, manifested both at the anodic zone where it curbs H₂ emission and at the cathodic zone where it directly adheres to the metal surface. Insights gathered from the quantum chemical study illuminate the mechanism of adsorption, where escitalopram participates in giving electron to vacant orbitals within the MS. This composed electron donation engenders strong chemical interactions, facilitating the formation of bonds between the metal surface and inhibitor molecule.

5.5 CONCLUSION

The effectiveness of Escitalopram as a corrosion inhibitor against mild steel in a 1M hydrochloric acid (HCl) environment was methodically assessed over a concentration range of 5-20 ppm and temperatures ranging from 303K to 333K. This comprehensive investigation encompassed weight loss analysis, electrochemical examinations, quantum chemical investigations, and surface analyses.

1. Increasing the inhibitor concentration resulted in a simultaneous enhancement of the effectiveness of inhibition and a decrease in the rate of corrosion. The peak of inhibition efficiency, registering at 96.02%, was achieved at a temperature of 303 K and an inhibitor concentration of 20 ppm.
2. The observed trend of activation energies increasing alongside increasing inhibitor concentration underscored the inhibitor's influence on the corrosion process. Notably, the rise in activation enthalpy with escalating temperature reaf-

firmed the inhibitory role of the compound, especially with higher inhibitor concentrations.

3. The observed adherence to the isotherm for Langmuir adsorption signified the occurrence of monolayer adsorption, reflecting a controlled surface interaction. A comprehensive examination of the thermodynamic characteristics related to the adsorption of the inhibitor on mild steel clarified that the adsorption process is spontaneous, encompassing aspects of both physical and chemical interactions.
4. Electrochemical analysis revealed Escitalopram's character as a mixed-type inhibitor, an insight that supported the multi-layered mode of inhibition observed experimentally.
5. Quantum chemical exploration revealed the involved electronic interaction between Escitalopram and the metal surface. Through the mechanism of electron donation, Escitalopram established a strong chemical interaction with the metal, reinforcing its inhibitory role through the formation of strong chemical bonds.

CHAPTER 6

CONCLUSION

In this study, effectiveness of Ethambutol, Sertraline, Paroxetine and Escitalopram as corrosion inhibitor for on mild steel (MS) protection in acidic media has been examined by Weight loss method, Linear Polarization Technique, Electrochemical Impedance method and Potentiodynamic Polarization study. Additionally, surface characteristics of mild steel was examined to assess corrosion inhibitory performance of experimental drugs to protect the metal. To gauge the significance of structural attributes and substantiate the experimental outcomes, theoretical quantum chemical calculations were executed. Here are the key and significant conclusions derived from this current study:

- i. In weight loss was measured at various concentrations of the drug in acidic media and at various temperatures. It was noticed that inhibition efficiency was enhanced, and the corrosion rate declined with an enhancement in drug concentration, but reverse behavior was observed with the rise of temperature. The highest inhibition effectiveness was noticed at the concentration of 1000 ppm, reaching an inhibition efficiency of 92.78% for the EBT drug in 0.5 M H₂SO₄, 93.3% at 50 ppm for Sertraline drug at 313 K, 96.4% at 20 ppm for Paroxetine, and Escitalopram exhibited an inhibition efficiency of 96.2% at a concentration of 20 ppm in 1 M HCl at a temperature of 303 K.
- ii. Based upon the thermodynamic study, it appears that E_a (activation energy of corrosion) values in the inhibited sample were found to be high as compared to uninhibited indicating a decrease in the corrosion rate when inhibitors were applied, and it was also observed that the corrosion rate increased as the concentration increased for all investigated drugs. The enthalpy change (ΔH) associated with the corrosion process exhibited a positive trend for all concentrations, signifying the endothermic nature of the corrosion process. Furthermore, these values demonstrated an upward trend as the inhibitor concentration increased, underscoring the corrosion rate reduction achieved through inhibitor usage. Change in free energy (ΔG) values for corrosion phenomenon were found to be +ve for inhibited as well as uninhibited sample indicating instability of activation complex formed during corrosion process.

- iii. The Adsorption Isotherm provides a comprehensive understanding of the inhibition activity of investigated drugs as corrosion inhibitor on the metal surface. It not only reveals the interaction between the interface of metal and corrosive medium but also offers valuable insights into corrosion inhibition. In the present research, various adsorption isotherms such as Langmuir, Freundlich, Frumkin, Flory-Huggins and Temkin were employed for the analyze of the adsorption behavior for all the investigated corrosion inhibitors. Among these, the Langmuir isotherm of adsorption, represented by a linear curve, was found to be best fitted on the experimental results. Langmuir isotherm of adsorption reveals monolayer adsorption of inhibitor on the surface of mild steel.
- iv. The Gibbs free energy values for adsorption of inhibitor on metal surface are negative as computed from Langmuir adsorption isotherm, indicating the stability and spontaneity of drug adsorption occurring at metal surface and corrosive media interface. The ΔG_{ads} values were found to be between -20 to -40 KJ/mole for all the drugs showing physical as well as chemical adsorption of drug on metal.
- v. The linear polarization resistance experiment was employed to calculate rate of corrosion, corrosion current and polarization resistance and thereby inhibition efficiency instantly. The polarization resistance (R_p), corrosion current (I_{corr}) and inhibition efficiency in absence and with variable concentration of drug in acidic medium for mild steel were computed and it was concluded that R_p values increased and corrosion current values decreased for all the drug inhibitors indicating improved efficacy of drug towards corrosion inhibition with rise in inhibitor concentration.
- vi. The electrochemical impedance behavior on the mild steel (MS) sample was studied in acidic solution both with and without various concentrations of each investigated drug inhibitor at 298 K. The impedance information was presented through Nyquist plots, where it was observed that the impedance plots formed single semicircles depicting that the mechanism of inhibition is not influenced by adding the inhibitor. The size of these semicircles expanded as the concentration of each corrosion inhibitor in the acidic solution rose, indicating an enhanced inhibitor effectiveness. Nonetheless, the loops exhibited deviations from perfect semicircular shapes because of the dispersion of interfacial impedance at various frequencies. This dispersion is linked to surface roughness, irregularities, and the adsorption behavior of the corrosion inhibitor on the metal surface. The findings from electrochemical impedance spectroscopy (EIS) suggested that as the inhibitor concentration increased, there was a corresponding rise in the charge transfer resistance (R_{ct}), effectively regulating the corrosion process. At the same

time, there was a reduction in the double-layer capacitance (C_{dl}), which signified the adsorption of corrosion inhibitors onto the surface of mild steel. The decline in C_{dl} as the inhibitor concentration rose implied either an expansion in the electrical double layer's thickness or a reduction in its dielectric constant. This observation suggested that each corrosion inhibitor molecule interacted with the MS surface through adsorption.

- vii. Polarization analysis has been employed to investigate the response of mild steel by behavior of all the drug inhibitors used, concerning both anodic and cathodic corrosion reactions. Basically, it was used to depict the effect of corrosion on metal and to determine kinetics of corrosion process. The results obtained from potentiodynamic polarization analysis (Tafel plot) demonstrate that all the studied corrosion inhibitors function as both anodic and cathodic inhibitors. Polarization measurements revealed that when corrosion inhibitors were introduced into the acidic solution, the cathodic plots shifted to more negative potential values, while the anodic plots shifted to more positive potential values compared to the solution without inhibitors. Consequently, the corrosion rate was significantly reduced. This can primarily be attributed to the adsorption of corrosion inhibitor molecules on the metal surface, where electrons are donated from the heteroatoms of the drug molecules. This confirms that the cathodic and anodic reactions are attenuated at various concentrations of all the examined corrosion inhibitors in an acidic environment, indicating that these drugs acted as mixed-type corrosion inhibitors. Moreover, as the drug concentration increased, the corrosion current densities shifted towards lower values, signifying that the studied drugs were adsorbed onto the MS surface and inhibited charge transfer reactions.
- viii. Quantum Chemical analysis was acknowledged for the substantial contribution in comprehending the reactivity of corrosion inhibitor molecules and their various connections to the metal surface. These analyses were performed to look into how the molecular makeup of each corrosion inhibitor impacted the extent of inhibition efficiency. The study reveals a strong interaction between metal and inhibitor molecule by the donation of electrons from the inhibitor to mild steel due to chemical adsorption.
- ix. Atomic Force Microscopic studies showed that surface roughness was reduced from 226.6 to 89.3 nm for EBT, 221 to 50 nm for Sertraline, 220 to 92 nm for paroxetine and 220 to 39.88 nm justifying protection of mild steel by drugs against corrosion. A decline in surface roughness indicates the drug's effectiveness in preventing corrosion.

Four medications, namely Ethambutol, Sertraline, Paroxetine, and Escitalopram, were

found to be effective in inhibiting corrosion due to the presence of atoms with non-bonded electrons and conjugated pi electrons. This resulted in the transferring of electrons from the inhibitor to the unfilled orbital of the metal, creating a strong interaction between them. As a result, a coating of inhibitor layer formed on the MS surface. Among the four inhibitors, inhibition efficiency was found to be maximum for Paroxetine due to the presence of a large number of heteroatoms along with an aromatic ring. The inhibition efficacy, corrosion rate, and corresponding concentration and temperature have been mentioned in Table 6.1 and figure 6.1.

Table 6.1: Effectiveness of experimental drugs against corrosion

Name of the drug	Concentration (ppm)	Optimum temperature(K)	Corrosion rate (mpy)	% Inhibition efficacy
EBT	1000	313	74.36	92.78
Sertraline	50	313	170.69	93.3
Paroxetine	20	303	30.42	96.4
Escitalopram	20	303	37.4	96

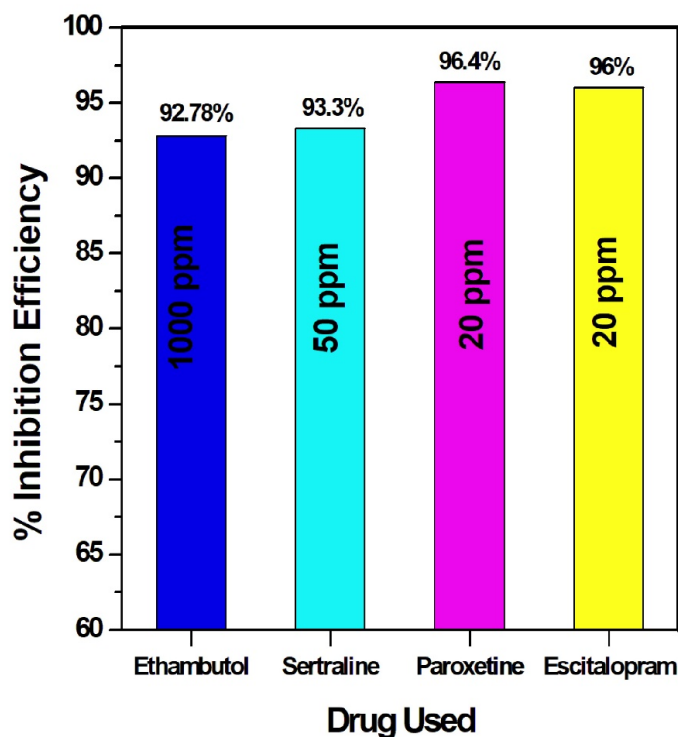


Figure 6.1: Plot showing % Inhibition efficiency versus drug used under study

Future scope of work

The work reported in the thesis may be further extended in the future to study the following points:

- i. The comparative study of experimental drugs for their inhibitory performance can be done.
- ii. The expired drugs as corrosion inhibitor can be compared with fresh drugs.
- iii. The derivatives of the drugs can be synthesized, and the derivatives of these drugs can be researched for their potential as corrosion inhibitors.
- iv. The corrosion phenomenon can be explored in different aggressive environments.
- v. To study the drugs for other materials like aluminum, copper, nickel, brass, and stainless steel.
- vi. Additional surface analysis methods, including XRD (X-ray diffraction), SEM (Scanning Electron Microscopy), and TEM (Transmission Electron Microscopy), can be utilized to evaluate how these corrosion inhibitors interact with the surface of mild steel (MS).

BRIEF PROFILE OF RESEARCH SCHOLAR

Rajni Narang is presently working as Assistant Professor in B. S. Anangpuria Institute of Technology and Management, Faridabad. She has obtained Master's degree in Chemistry from Maharshi Dayanand University, Rohtak in 2001. She has qualified National Eligibility Test(NET). She is having 22 years of teaching experience. She is pursuing Ph.D. under the guidance of Dr. Bindu Mangla, Associate Professor, Department of Chemistry, J.C. Bose University of Science and Technology, YMCA, Faridabad.

LIST OF PUBLICATIONS

List of Published Papers

Sr. No	Title of Paper	Journal	No	Volume & Issue	Year	Pages
1	Electrochemical and surface study of an antibiotic drug as sustainable corrosion inhibitor on mild steel in 0.5 M H ₂ SO ₄	Journal of Molecular Liquids (Elsevier)	10.1016/j.molliq.2023.122277	Vol.384 & Issue. April	2023	122277
2	Applicability of drugs as sustainable corrosion inhibitors	Advanced Material Letters (Elsevier)	10.5185/amlett.2023.041732	Issue. April	2023	1-13
3	Thermodynamic and electrochemical investigation of inhibition efficiency of green corrosion inhibitor and its comparison with synthetic dyes on MS in acidic medium	Journal of Molecular Liquids (Elsevier)	10.1016/j.molliq.2022.120042	Vol. 365	2022	120042
4	Efficacy of biomass derived nanocomposites as promising material as corrosion inhibitor(Book Chapter)	Antiviral and Antimicrobial coatings Based on Functionalized Nanomaterials (Elsevier)	10.1016/B978-0-323-91783-4.00007-3	ISBN: 9780323917834	2023	285-303

5	Experimental and Computational studies of novel metal oxide nanoparticles/conducting polymer nanocomposite (TiO ₂ /PVP) as corrosion inhibitor on low carbon steel in diprotic acidic medium	Industrial and Engineering Chemistry Research (ACS)	10.1021/acs.iecr.3c00099	Issue.62	2023	10982-11000
6	Low carbon steel corrosion inhibition using environment-friendly Solanum Lycopersicum extract in monoprotic and diprotic acidic medium.	Chemical Engineering Communications (Taylor & Francis)	10.1080/00986445.2023.2255545	ISSN: 5635201	2023	1-20

List of Accepted Papers

Sr. No.	Title of Paper	Journal	No:	Volume Issue	Year
1	Experimental and Quantum Chemical Investigation of Corrosion inhibitive action of Sertraline on Mild Steel in Acidic Medium	Chemistry Africa (Springer)	CHAF-D-23-00711R4	-	2023
2	Protection of Mild steel by Novel Chitosan/ C_eO_2 Nanocomposite in aggressive chloride media: Experimental and Computational Studies	Corrosion Communication (Elsevier)	CORCOM-D-25-00058R1	-	2023
3	Experimental investigation of Sustainable corrosion inhibitor Albumin on low-carbon steel in 1N HCl and 1N H_2SO_4	Surfaces and Interfaces (Elsevier)	RSURFI-D-23-00110R2	-	2023

REFERENCES

- [1] A. A. Al-Amiery A. Kadhim. "Corrosion inhibitors. a review". *International Journal of Corrosion and Scale Inhibition*, 10(1):54–67, 2021.
- [2] Z. Petrovic. "Catastrophes caused by corrosion". *Vojnotehnički glasnik*, 64(4): 1048–1064, 2016.
- [3] F. Khan E. Shekari and S. Ahmed. "Economic risk analysis of pitting corrosion in process facilities". *International Journal of Pressure Vessels and Piping*, 157: 51–62, 2017.
- [4] G. Koch. "*Cost of Corrosion*". Elsevier Ltd, 2017.
- [5] H. Bairagi S. K. Shukla R. Narang, P. Vashishth and B. Mangla. " Applicability of drugs as sustainable corrosion inhibitors". *Advanced Materials Letters*, pages 1–13, 2023.
- [6] Martin Matula, Ludmila Hyspecka, Milan Svoboda, Vlastimil Vodarek, Catherine Dagbert, Jacques Galland, Zuzana Stonawska, and Ludek Tuma. "Intergranular corrosion of AISI 316L steel". *Materials characterization*, 46(2-3):203–210, 2001.
- [7] J. R. Gabriel G. J. Schafer and P. K. Foster. "On the role of the oxygen concentration cell in crevice corrosion and pitting". *J. electrochem. Soc.*, 107(12): 1002–1004, 1960.
- [8] A. J. Betts and L. H. Boulton. "Crevice corrosion: review of mechanisms, modelling, and mitigation". *British corrosion journal*, 28(4):279–296, 1993.
- [9] KV Akpanyung and RT Loto. Pitting corrosion evaluation: a review. In *Journal of Physics: Conference Series*, volume 1378, page 022088. IOP Publishing, 2019.
- [10] I. K. Marshakov. "Anodic dissolution and selective corrosion of alloys". *Protection of metals*, 38:118–123, 2002.
- [11] M. Jones and R. J. Llewellyn. "Erosion–corrosion assessment of materials for use in the resources industry". *Wear*, 267(11):2003–2009, 2009.

- [12] T Jebakumar Immanuel Edison and MG Sethuraman. "Electrochemical investigation on adsorption of fluconazole at mild steel/hcl acid interface as corrosion inhibitor". *International Scholarly Research Notices*, 2013, 2013.
- [13] M. G. Ferreira A. C. Bastos and A. M. Simões. "Corrosion inhibition by chromate and phosphate extracts for iron substrates studied by EIS and SVET". *Corrosion Science*, 48(6):1500–1512, 2006.
- [14] M. RashvandAvei S. Rameshkumar, I. Danaee and M. Vijayan. "Quantum chemical and experimental investigations on equipotent effects of (+) r and (-) s enantiomers of racemic amisulpride as eco-friendly corrosion inhibitors for mild steel in acidic solution". *Journal of Molecular Liquids*, 212:168–186, 2015.
- [15] O. Lopez-Garrity and G. S. Frankel. "Corrosion inhibition of AA2024-T3 by sodium silicate". *Electrochimica Acta*, 130:9–21, 2014.
- [16] M. A. Diab A. S. Fouda and S. Fathy. "Role of some organic compounds as corrosion inhibitors for 316l stainless steel in 1 M HCl". *Int. J. Electrochem. Sci*, 12:347–362, 2017.
- [17] M. Abou-Krishna R. K. Hussein and T. A. Yousef. "Theoretical and experimental studies of different amine compounds as corrosion inhibitors for aluminum in hydrochloric acid". *Biointerface Res. Appl. Chem*, 11(2):9772, 2021.
- [18] M. A. Quraishi N. K. Gupta, C. Verma and A. K. Mukherjee. "Schiff's bases derived from l-lysine and aromatic aldehydes as green corrosion inhibitors for mild steel: experimental and theoretical studies". *Journal of Molecular Liquids*, 215:47–57, 2016.
- [19] E. Cano D. M. Bastidas and E. M. Mora. "Volatile corrosion inhibitors: A review". *Anti-Corrosion Methods and Materials*, 52(2):71–77, 2005.
- [20] Chandrabhan Verma, Dakeshwar K Verma, Eno E Ebenso, and Mumtaz A Quraishi. "Sulfur and phosphorus heteroatom-containing compounds as corrosion inhibitors: An overview". *Heteroatom Chemistry*, 29(4):e21437, 2018.
- [21] C. B. P. Kumar and K. N. Mohana. "Corrosion inhibition efficiency and adsorption characteristics of some schiff bases at mild steel/hydrochloric acid interface". *Journal of the Taiwan Institute of Chemical Engineers*, 45(3):1031–1042, 2014.
- [22] SA Umoren and MM Solomon. "Recent developments on the use of polymers as corrosion inhibitors-a review". *The Open Materials Science Journal*, 8(1), 2014.

- [23] M. Gopiraman D. Kesavan and N. Sulochana. "Green inhibitors for corrosion of metals: a review". *Chem. Sci. Rev. Lett*, 1(1):1–8, 2012.
- [24] E. E. Ebenso G. Ji, S. K. Shukla and R. Prakash. "Argemone mexicana leaf extract for inhibition of mild steel corrosion in sulfuric acid solutions". *Int. J. Electrochem. Sci.*, 8(8):10878–10889, 2013.
- [25] Akhil Saxena, Dwarika Prasad, Rajesh Haldhar, Gurmeet Singh, and Akshay Kumar. "Use of saraca ashoka extract as green corrosion inhibitor for mild steel in 0.5 M H₂SO₄". *Journal of Molecular Liquids*, 258:89–97, 2018.
- [26] R. Haldhar G. Singh A. Saxena, D. Prasad and A. Kumar. "Use of *Sida cordifolia* extract as green corrosion inhibitor for mild steel in 0.5 M H₂SO₄". *J. Environ. Chem. Eng.*, 6(1):694–700, 2018.
- [27] B. Tan Y. Qiang, S. Zhang and S. Chen. "Evaluation of ginkgo leaf extract as an eco-friendly corrosion inhibitor of X 70 steel in HCl solution". *Corrosion Science*, 133:6–16, 2018.
- [28] Gopal Ji, Sudhish Kumar Shukla, Priyanka Dwivedi, Shanthi Sundaram, Eno E Ebenso, and Rajiv Prakash. "Parthenium hysterophorus plant extract as an efficient green corrosion inhibitor for mild steel in acidic environment". *International Journal of Electrochemical Science*, 7(10):9933–9945, 2012.
- [29] A. N. Abd A. A. Khadom and N. A. Ahmed. "Xanthium strumarium leaves extracts as a friendly corrosion inhibitor of low carbon steel in hydrochloric acid: Kinetics and mathematical studies". *South African J. Chem. Eng.*, 25:13–21, 2018.
- [30] Mohammad Mobin, Megha Basik, and Jeenat Aslam. "Pineapple stem extract (bromelain) as an environmental friendly novel corrosion inhibitor for low carbon steel in 1 m HCl". *Measurement*, 134:595–605, 2019.
- [31] G. Y. El-Awady A. S. Fouda and W. T. El Behairy. "*Prosopis juliflora* plant extract as potential corrosion inhibitor for low-carbon steel in 1 m HCl solution". *J. Bio-Tribo-Corrosion*, 4(1):1–12, 2018.
- [32] V. S. Vasantha T. K. Bhuvanewari and C. Jeyaprabha. "*Pongamia Pinnata* as a green corrosion inhibitor for mild steel in 1n sulfuric acid medium". *Silicon*, 10(5):1793–1807, 2018.
- [33] N Ammouchi, H Allal, E Zouaoui, K Dob, D Zouied, and M Bououdina. "Extracts of *Ruta Chalepensis* as green corrosion inhibitor 8 for copper CDA 110 in

- 3% NaCl medium: Experimental 9 and theoretical studies 10". *J. Anal. Bioanal. Electrochem.*, 2019.
- [34] V. N. B. Tokala. "Corrosion inhibition of *Ocimum tenuiflorum* (tulsi) leaves extract as a green inhibitor for zinc in H_2SO_4 ". *J. Chem. Chem. Sci.*, 8(1):1–9, 2018.
- [35] S Chaithra, Apeksha Gupta, R Manivannan, and S Noyel Victoria. "Studies on corrosion inhibitory action of ocimum sanctum (tulsi) leaves extract in mild steel corrosion induced by desulfovibrio desulfuricans". 2018.
- [36] A. Chaturvedi N. Kumpawat and R. K. Upadhyay. "Comparative study of corrosion inhibition efficiency of naturally occurring ecofriendly varieties of holy basil (tulsi) for tin in HNO_3 solution". *Open Journal of Metal*, 2(03):68–73, 2012.
- [37] Mohammad Asaduzzaman Chowdhury, Nayem Hossain, Md Mir Shakib Ahmed, Mohammad Aminul Islam, Safiul Islam, and Md Masud Rana. "Green tea and tulsi extracts as efficient green corrosion inhibitor for aluminum alloy in alkaline medium". *Heliyon*, 9(6504), 2023.
- [38] G. A. El-Mahdy A. M. Atta and H. A. Al-Lohedan. "Corrosion inhibition efficiency of modified silver nanoparticles for carbon steel in 1 M HCl". *Int. J. Electrochem. Sci.*, 8(4):4873–4885, 2013.
- [39] N. Renevier-I. Sherrington W. Shao, D. Nabb and J. K. Luo. "Mechanical and corrosion resistance properties of tio_2 nanoparticles reinforced ni coating by electrodeposition". *IOP Conf. Ser. Mater. Sci. Eng.*, 40(1), 2012.
- [40] M Mahmood and MA" Maleque. "Anodized nano-coating of copper material for thermal efficiency enhancement". *The Mattingley Publishing Co., Inc. Test Eng. Manag*, 83:1430–1437, 2020.
- [41] H. Norita J. N. Hasnidawani, H. N. Azlina and N. Samat. "Zno nanoparticles for anti-corrosion nanocoating of carbon steel". *Materials Science Forum*, 894: 76–80, 2017.
- [42] Sara Lopez de Armentia, Mariola Pantoja, Juana Abenojar, and Miguel Angel Martinez. "Development of silane-based coatings with zirconia nanoparticles combining wetting, tribological, and aesthetical properties". *Coatings*, 8(10): 368, 2018.

- [43] X. F. Zhang L. K. Wu and J. M. Hu. "Corrosion protection of mild steel by one-step electrodeposition of superhydrophobic silica film". *Corrosion Science*, 85: 482–487, 2014.
- [44] G. K. Dey S. K. Ghosh, A. K. Grover and A. K. Suri. "Synthesis of corrosion-resistant nanocrystalline nickel-copper alloy coatings by pulse-plating technique". *Defence Science Journal*, 55(1):63–74, 2005.
- [45] Donald R Paul and Lloyd M Robeson. "Polymer nanotechnology: nanocomposites". *Polymer*, 49(15):3187–3204, 2008.
- [46] L. P. Sung et al. "Scratch behavior of nano-alumina/polyurethane coatings". *Journal of Coatings Technology and Research*, 5:419–430, 2008.
- [47] C. Li T. Huang, G. Lai and M. Tsai. "Advanced anti-corrosion coatings prepared from α -zirconium phosphate/polyurethane nanocomposites". *RSC advances*, 7 (16):9908–9913, 2017.
- [48] D. A. Al-Enezi L. A. Al Juhaiman and W. K. Mekhamer. "Polystyrene/organoclay nanocomposites as anticorrosive coatings of c-steel". *Int. J. Electrochem. Sci*, 11:5618–5630, 2016.
- [49] R. Rajalakshmi M. Srimathi and S. Subhashini. "Polyvinyl alcohol–sulphanilic acid water soluble composite as corrosion inhibitor for mild steel in hydrochloric acid medium". *Arabian Journal of Chemistry*, 7(5):647–656, 2014.
- [50] Niteen Jadhav and Victoria Gelling. "Titanium dioxide/conducting polymers composite pigments for corrosion protection of cold rolled steel". *Journal of Coatings Technology and Research*, 12:137–152, 2015.
- [51] Edidiong A Essien, Doga Kavaz, Ekemini B Ituen, and Saviour A Umoren. "Synthesis, characterization and anticorrosion property of olive leaves extract-titanium nanoparticles composite". *Journal of adhesion science and technology*, 32(16):1773–1794, 2018.
- [52] A. H. Abu-Nawwas R. S. Abdel Hameed, E. A. Ismail and H. I. Al-Shafey. "Expired voltaren drugs as corrosion inhibitor for aluminium in hydrochloric acid". *International Journal of Electrochemical Science*, 10(3):2098–2109, 2015.
- [53] H. Lgaz I. M. Chung A. Singh S. Bashir, V. Sharma and A. Kumar. "The inhibition action of analgin on the corrosion of mild steel in acidic medium: A combined theoretical and experimental approach". *Journal of Molecular Liquids*, 263:454–462, 2018.

- [54] M. H. Abdulmajeed S. A. Naser R. A. Anae, I. H. R. Tomi and M. M. Kathem. "Expired etoricoxib as a corrosion inhibitor for steel in acidic solution". *Journal of Molecular Liquids*, 279:594–602, 2019.
- [55] A. S. Fouda and Y. M. Abdallah. "Corrosion inhibition of aluminum–silicon alloy in 1 m hcl solution using phenazone and aminophenazone". *Arabian Journal for Science and Engineering*, 39:5363–5371, 2014.
- [56] M. Sobhi J. H. Al-Fahemi M. Abdallah, E. A. M. Gad and M. M. Alfakeer. "Performance of tramadol drug as a safe inhibitor for aluminum corrosion in 1.0 M HCl solution and understanding mechanism of inhibition using DFT". *Egyptian Journal of Petroleum*, 28(2):173–181, 2019.
- [57] S. K. Shukla and M. A. Quraishi. "Cefotaxime sodium: a new and efficient corrosion inhibitor for mild steel in hydrochloric acid solution". *Corrosion Science*, 51(5):1007–1011, 2009.
- [58] IA Akpan and NO" Offiong. "A modiaquine drug as a corrosion inhibitor for mild steel in 0.1 M HCl solution. *Chemistry of metals and alloys*, (7,№ 3-4): 149–153, 2014.
- [59] B. U. Ugi and M. E. Obeten. "Inhibition of localized corrosion in 2205 duplex stainless steel by expired myambutol (ethambutol hydrochloride) drug in acid catalyzed environment". *Intl. J. Innov. Sc. Res. Tech*, 4(11):752–760, 2019.
- [60] A. Kumar and S. Bashir. "Ethambutol: A new and effective corrosion inhibitor of mildsteel in acidic medium". *Russian Journal of Applied Chemistry*, 89:1158–1163, 2016.
- [61] Shefali Dahiya, Nisha Saini, Naveen Dahiya, Hassane Lgaz, Rachid Salghi, Shehdeh Jodeh, and Suman Lata. Corrosion inhibition activity of an expired antibacterial drug in acidic media amid elucidate DFT and MD simulations. *Portugaliae Electrochimica Acta*, 36(3):213–230, 2018.
- [62] M. Eissa A. S. Fouda and A. El-Hossiany. "Ciprofloxacin as eco-friendly corrosion inhibitor for carbon steel in hydrochloric acid solution". *International Journal of Electrochemical Science*, 13(11):11096–11112, 2018.
- [63] N. O. Obi-egbedi I. B. Obot and S. A. Umoren. "Antifungal drugs as corrosion inhibitors for aluminium in 0.1 M HCl". *Corrosion Science*, 51(8):1868–1875, 2009.
- [64] N. O. Obi-Egbedi I. B. Obot and S. A. Umoren. "Adsorption characteristics and corrosion inhibitive properties of clotrimazole for aluminium corrosion in

- hydrochloric acid". *International Journal of Electrochemical Science*, 4(6):863–877, 2009.
- [65] Imran Reza, Ejaz Ahmad, and Farhan Kareem. "Corrosion inhibition mechanism of piperacillin sodium for mild steel protection in acidic media". *Afinidad*, 69 (557), 2012.
- [66] I. Ahamad S. K. Shukla, A. K. Singh and M. A. Quraishi. "Streptomycin: A commercially available drug as corrosion inhibitor for mild steel in hydrochloric acid solution". *Materials Letters*, 63(9-10):819–822, 2009.
- [67] S. K. Shukla and M. A. Quraishi. "The effects of pharmaceutically active compound doxycycline on the corrosion of mild steel in hydrochloric acid solution". *Corrosion Science*, 52(2):314–321, 2010.
- [68] Z. M. Anwar M. M. Kamel, Q. Mohsen and M. A. Sherif. "An expired cef-tazidime antibiotic as an inhibitor for disintegration of copper metal in pickling HCl media". *Journal of Materials Research and Technology*, 11:875–886, 2021.
- [69] M. Kamel A. S. Fouda, S. M. Rashwan and A. A. Badawy. "Unused meropenem drug as corrosion inhibitor for copper in acidic medium; experimental and theoretical studies". *Int. J. Electrochem. Sci*, 11:9745–9761, 2016.
- [70] A. K. Singh et al. "Eco-friendly disposal of expired anti-tuberculosis drug isoniazid and its role in the protection of metal". *Journal of Environmental Chemical Engineering*, 7(2):102971, 2019.
- [71] O. S. I. Fayomi A. A. Ayoola and S. O. Ogunkanmbi". "Data on inhibitive performance of chlorphenicol drug on A315 mild steel in acidic medium". *Data in brief*, 19:804–809, 2018.
- [72] D. C. Akintayo C. U. Ibeji and I. A. Adejoro. "The efficiency of chloroquine as corrosion inhibitor for aluminium in 1M HCl solution: Experimental and DFT study". *Jordan Journal of Chemistry*, 11(1):38–49, 2016.
- [73] E. E. Ebenso K. K. Singh M. J. Reddy, C. B. Verma and M. A. Quaraishi. "Nitrofurantoin as effective corrosion inhibitor for mild steel in 1M hydrochloric acid solution". *International Journal of Electrochemical Science*, 9(9):4884–4899, 2014.
- [74] M Abdallah, IA Zaaferany, and BA" Al Jahdaly. "Corrosion inhibition of zinc in hydrochloric acid using some antibiotic drugs". *J Mater Environ Sci*, 7(4): 1107–1118, 2016.

- [75] M. N. El-Haddad A. S. Fouda and Y. M. Abdallah. "Septazole: antibacterial drug as a green corrosion inhibitor for copper in hydrochloric acid solutions". *IJIRSET*, 2(12):7073, 2013.
- [76] Samar T Hameed, Taghried A Salman, and Shatha F Al-Saidi. "The inhibition effect of ampicillin on corrosion of pure aluminium in 3.5% NaCl aqueous solution". *Al-Nahrain Journal of Science*, 18(3):50–61, 2015.
- [77] S. Hari Kumar and S. Karthikeyan. "Inhibition of mild steel corrosion in hydrochloric acid solution by cloxacillin drug". *J. Mater. Environ. Sci*, 3(5):925–934, 2012.
- [78] "Potentiodynamic polarization studies of cefadroxil and dicloxacillin drugs on the corrosion susceptibility of aluminium AA6063 in 0.5 M nitric acid", author=O. S. I. Fayomi, I. G. Akande, A. P. I. Popoola, and H. Molifi, journal=Journal of Materials Research and Technology, volume=8, number=3, pages=3088–3096, year=2019, publisher=Elsevier.
- [79] K. N. Manonmani N. Kavitha S. M. Megalai, P. Manjula and N. Baby. "Metronidazole: A corrosion inhibitor for mild steel in aqueous environment". *Portuguese Electrochimica Acta*, 30(6):395–403, 2012.
- [80] N. Johar A. Kalra. "Evaluation of norfloxacin and ofloxacin as corrosion inhibitors for mild steel in different acids: Weight loss data". *Journal Name*, 6(1): 2320–2882, 2018.
- [81] H. Yang X. Wang and F. Wang. "An investigation of benzimidazole derivative as corrosion inhibitor for mild steel in different concentration HCl solutions". *Corrosion Science*, 53(1):113–121, 2011.
- [82] M. Romero-Romo J. Aldana-González, A. Espinoza-Vázquez. "Electrochemical evaluation of cephalothin as corrosion inhibitor for API 5L X52 steel immersed in an acid medium". *Arabian Journal of Chemistry*, 12(8):3244–3253, 2019.
- [83] A. Srinivasulu and P. K. Kasthuri. "Study of inhibition and adsorption properties of mild steel corrosion by expired pharmaceutical gentamicin drug in hydrochloric acid media". *Oriental Journal of Chemistry*, 33(5):2616–2624, 2017.
- [84] B. Tutunaru R. Grecu C. Tigae A. Samide, G. E. Iacobescu and C. Spînu. "Inhibitory properties of neomycin thin film formed on carbon steel in sulfuric acid solution: Electrochemical and AFM investigation". *Coatings*, 7(11), 2017.

- [85] K. Shalabi A. S. Fouda and A. E-Hossiany. "Moxifloxacin antibiotic as green corrosion inhibitor for carbon steel in 1 M HCl". *Journal of Bio- and Tribo-Corrosion*, 2(3):1–13, 2016.
- [86] E. E. Ebenso I. Ahamad, R. Prasad and M. A. Quraishi. "Electrochemical and quantum chemical study of albendazole as corrosion inhibitor for mild steel in hydrochloric acid solution". *International Journal of Electrochemical Science*, 7(4):3436–3452, 2012.
- [87] J. Ishwara Bhat and V. D. P. Alva. "A study of aluminium corrosion inhibition in acid medium by an antiemetic drug". *Transactions of the Indian Institute of Metals*, 64(4–5):377–384, 2011.
- [88] Ying Lu, Ling Zhou, Bochuan Tan, Bin Xiang, Shengtao Zhang, Shicheng Wei, Bo Wang, and Qiong Yao. "Two common antihistamine drugs as high-efficiency corrosion inhibitors for copper in 0.5 M H₂SO₄". *Journal of the Taiwan Institute of Chemical Engineers*, 123:11–20, 2021.
- [89] R. Prasad I. Ahamad and M. A. Quraishi. "Experimental and theoretical investigations of adsorption of fexofenadine at mild steel/hydrochloric acid interface as corrosion inhibitor". *Journal of Solid State Electrochemistry*, 14(11):2095–2105, 2010.
- [90] M. Shahraki M. Dehdab and S. M. Habibi-Khorassani. "Theoretical study of inhibition efficiencies of some amino acids on corrosion of carbon steel in acidic media: green corrosion inhibitors". *Amino acids*, 48(1):291–306, 2016.
- [91] J Ishwara Bhat and Vijaya DP Alva. "A study of aluminium corrosion inhibition in acid medium by an antiemetic drug". *Transactions of the Indian Institute of Metals*, 64:377–384, 2011.
- [92] R. Prasad I. Ahamad and M. A. Quraishi. "Inhibition of mild steel corrosion in acid solution by pheniramine drug: Experimental and theoretical study". *Corrosion Science*, 52(9):3033–3041, 2010.
- [93] I. G. Akande M. A. Fajobi, O. S. I. Fayomi and O. A. Odunlami. "Inhibitive performance of ibuprofen drug on mild steel in 0.5 M of H₂SO₄ acid". *Journal of Bio- and Tribo-Corrosion*, 5(3):0–5, 2019.
- [94] I. G. Akande O. A. Odunlami M. A. Fajobi, O. S. I. Fayomi and O. O. Oluwole. "Evaluation of the inhibitive effect of ibuprofen drug on the acidic corrosion of aluminium 6063 alloy". *Key Engineering Materials*, 886:133–142, 2021.

- [95] A. P. I. Popoola O. Sanni, O. S. I. Fayomi and O. Agboola. "Data on the effect of ibuprofen drug derivative on 430 T1 stainless steel in acid solutions". *IOP Conference Series: Materials Science and Engineering*, 1107(1):012074, 2021.
- [96] M. Mihajlović Z. Tasić. "Ibuprofen as a corrosion inhibitor for copper in synthetic acid rain solution". *Nature*, 9(1):14710, 2019.
- [97] Žaklina Z Tasić, Marija B Petrović Mihajlović, Milan B Radovanović, Ana T Simonović, and Milan M Antonijević. "Experimental and theoretical studies of paracetamol as a copper corrosion inhibitor". *Journal of Molecular Liquids*, 327: 114817, 2021.
- [98] Arej S Al-Gorair and M Abdallah. "Expired paracetamol as corrosion inhibitor for low carbon steel in sulfuric acid. electrochemical, kinetics and thermodynamics investigation". *Int J Electrochem Sci*, 16(7):1–16, 2021.
- [99] M. L. Dan D. A. Duca and N. Vaszilcsin. "Expired domestic drug - paracetamol - as corrosion inhibitor for carbon steel in acid media". *IOP Conference Series: Materials Science and Engineering*, 416(1), 2018.
- [100] N. Hebbar T. V. Venkatesha H. C. Tandon B. M. Prasanna, B. M. Praveen and S. B. Abd Hamid. "Electrochemical study on inhibitory effect of aspirin on mild steel in 1 M hydrochloric acid". *Journal of the Association of Arab Universities for Basic and Applied Sciences*, 22:62–69, 2017.
- [101] Alexander I Ikeuba, Omang B John, Victoria M Bassey, Hitler Louis, Augustine U Agobi, Joseph E Ntibi, and Fredrick C Asogwa. "Experimental and theoretical evaluation of aspirin as a green corrosion inhibitor for mild steel in acidic medium". *Results in Chemistry*, 4:100543, 2022.
- [102] S. Sagdinc F. Kayadibi and S. Zor. "Theoretical and experimental study of the acid corrosion inhibition of copper by aspirin (acetylsalicylic acid)". *Protection of Metals and Physical Chemistry of Surfaces*, 56(1):202–213, 2020.
- [103] N. Raghavendra. "Application of expired alprazolam drug as corrosion inhibitor for aluminum in 3 M HCl environment". *Journal of Science, Engineering, and Technology*, 6(1):35–42, 2018.
- [104] I. I. I. M. Chung S. Bashir, H. Lgaz and A. Kumar. "Potential of venlafaxine in the inhibition of mild steel corrosion in HCl: insights from experimental and computational studies". *Chemical Papers*, 73(9):2255–2264, 2019.

- [105] W. Niouri et al. "Electrochemical and chemical studies of some benzodiazepine molecules as corrosion inhibitors for mild steel in 1 M HCl". *International Journal of Electrochemical Science*, 9(12):8283–8298, 2014.
- [106] N. Raghavendra. "Expired lorazepam drug: A medicinal compound as green corrosion inhibitor for mild steel in hydrochloric acid system". *Chemistry Africa*, 2(3):463–470, 2019.
- [107] Narayana Hebbar, BM Praveen, BM Prasanna, and T Venkatarangaiah Venkatesha. "Corrosion inhibition behavior of ketosulfone for zinc in acidic medium". *Journal of Fundamental and Applied Sciences*, 7(2):271–289, 2015.
- [108] G. Kardaş M. Özcan, R. Solmaz and I. Dehri. "Adsorption properties of barbiturates as green corrosion inhibitors on mild steel in phosphoric acid". *Colloids and Surfaces A: Physicochemical and Engineering Aspects*, 325(1-2):57–63, 2008.
- [109] R. Hameed H. Al-Shafey. "Effect of expired drugs as corrosion inhibitors for carbon steel in 1m hcl solution". *International Journal of Pharmaceutical Sciences and Research*, 5(11):4643–4646, 2014.
- [110] Dahiya N Lgaz H Salghi R Jodeh S Lata S Dahiya S, Saini N. "Corrosion inhibition activity of an expired antibacterial drug in acidic media amid elucidate DFT and MD simulations". *Portugaliae Electrochimica Acta*, 36(3):213–230, 2018.
- [111] Somya Tanwer and Sudhish Kumar Shukla. "Recent advances in the applicability of drugs as corrosion inhibitor on metal surface: A review". *Current Research in Green and Sustainable Chemistry*, 5:100227, 2022.
- [112] M. K. Pavithra, T. V. Venkatesha, M. K. Punith Kumar, and K. Manjunatha. "Investigation of the inhibition effect of ibuprofen triazole against mild steel corrosion in an acidic environment". *Research on Chemical Intermediates*, 41(10):7163–7177, 2015.
- [113] V. Ordodi N. Vaszilcsin and A. Borza. "Corrosion inhibitors from expired drugs". *International Journal of Pharmaceutics*, 431(1–2):241–244, 2012.
- [114] M. Dehdab, M. Shahraki, and S. M. Habibi-Khorassani. "Theoretical study of inhibition efficiencies of some amino acids on corrosion of carbon steel in acidic media: Green corrosion inhibitors". *Amino Acids*, 48(1):291–306, 2016.
- [115] M. K. Pavithra, T. V. Venkatesha, K. Vathsala, and K. O. Nayana. "Synergistic effect of halide ions on improving corrosion inhibition behaviour of benzisothiazole-3-piperazine hydrochloride on mild steel in 0.5 M H₂SO₄ medium". *Corros Sci*, 52(11):3811–3819, 2010.

- [116] Umoren SA Obot IB, Obi-egbedi NO. "Antifungal drugs as corrosion inhibitors for aluminium in 0.1 M HCl". *Corrosion Science*, 51(8):1868–1875, 2009.
- [117] Alazawi R Al-Ghezi MKS Abass RH Kadhim A, Al-Amiery AA. "Corrosion inhibitors. a review". *International Journal of Corrosion and Scale Inhibition*, 10(1):54–67, 2021.
- [118] Sulochana N Kesavan D, Gopiraman M. "Green inhibitors for corrosion of metals: a review". *Chem. Sci. Rev. Lett*, 1(1):1–8, 2012.
- [119] Ebenso EE Shukla SK. "Corrosion inhibition, adsorption behavior and thermodynamic properties of streptomycin on mild steel in hydrochloric acid medium". *Int. J. Electrochem. Sci*, 6(8):3277–3291, 2011.
- [120] Borza A Vaszilcsin N, Ordodi V. "Corrosion inhibitors from expired drugs". *International journal of pharmaceutics*, 431(1-2):241–244, 2012.
- [121] Hussin I Al-Shafey, RS Abdel Hameed, FA Ali, Abd El-Aleem S Aboul-Magd, and M Salah. "Effect of expired drugs as corrosion inhibitors for carbon steel in 1m hcl solution". *Int. J. Pharm. Sci. Rev. Res*, 27(1):146–152, 2014.
- [122] Ramezanzadeh B Hossein A, Bahlakeh G. "A comprehensive electronic-scale dft modeling, atomic-level mc/md simulation, and electrochemical/surface exploration of active nature-inspired phytochemicals based on heracleum persicum seeds phytoextract for effective retardation of the acidic-induced corrosion of mild steel". *Journal of Molecular Liquids*, 331:115764, 2021.
- [123] Arej S Al-Gorair and M Abdallah. "Expired paracetamol as corrosion inhibitor for low carbon steel in sulfuric acid. electrochemical, kinetics and thermodynamics investigation". *Int J Electrochem Sci*, 16(7):1–16, 2021.
- [124] Leasure C Suzuki BM-Robinson KJ Currey H Wangchuk P Eichenberger RM Saxton AD Bird TD Kraemer BC Loukas A Hawdon JM Caffrey CR Liachko NF Weeks JC, Roberts WM. "Sertraline, paroxetine, and chlorpromazine are rapidly acting anthelmintic drugs capable of clinical repurposing". *Scientific reports*, 8(1):975, 2018.
- [125] Corradini MG Peleg M, Normand MD. "The arrhenius equation revisited". *Critical reviews in food science and nutrition*, 52(9):830–851, 2012.
- [126] R. Narang SK Shukla P. Vashishth, H. Bairagi and B. Mangla. "Electrochemical and surface study of an antibiotic drug as sustainable corrosion inhibitor on mild steel in 0.5 M H₂SO₄". *Journal of Molecular Liquids*, 384:122277, 2023.

- [127] Channar PA Shehzadi SA-Ahmed MN Siddiq M Arshad I, Saeed A. "Bis-schiff bases of 2, 2-dibromobenzidine as efficient corrosion inhibitors for mild steel in acidic medium". *RSC advances*, 10(8):4499–4511, 2020.
- [128] Ambrish Singh and Eno E Ebenso. "Use of glutamine as a new and effective corrosion inhibitor for mild steel in 1 m hcl solution". *Int. J. Electrochem. Sci*, 8: 12874–12883, 2013.
- [129] Quraishi MA Sudheer. "Electrochemical and theoretical investigation of triazole derivatives on corrosion inhibition behavior of copper in hydrochloric acid medium". *Corrosion science*, 70:161–169, 2013.
- [130] Gong Y Huang H-Ma Y Xie H Li H Zhang S Gao F Jing C, Wang Z. "Photo and thermally stable branched corrosion inhibitors containing two benzotriazole groups for copper in 3.5 wt% sodium chloride solution". *Corrosion Science*, 138: 353–371, 2018.
- [131] Ramanath Prabhu, B Roopashree, T Jeevananda, Srilatha Rao, Kakarla Raghava Reddy, and Anjanapura V Raghu. "Synthesis and corrosion resistance properties of novel conjugated polymer-Cu₂C14L3 composites". *Materials Science for Energy Technologies*, 4:92–99, 2021.
- [132] Shukla SK Kabanda MM-Ebenso EE Murulana LC, Singh AK. "Experimental and quantum chemical studies of some bis (trifluoromethyl-sulfonyl) imide imidazolium-based ionic liquids as corrosion inhibitors for mild steel in hydrochloric acid solution". *Industrial & Engineering Chemistry Research*, 51(40): 13282–13299, 2012.
- [133] Himanshi Bairagi, Priya Vashishth, Rajni Narang, Sudhish Kumar Shukla, and Bindu Mangla. "Experimental and computational studies of a novel metal oxide nanoparticle/conducting polymer nanocomposite (TiO₂/PVP) as a corrosion inhibitor on low-carbon steel in diprotic acidic medium". *Industrial & Engineering Chemistry Research*, 62(28):10982–11000, 2023.
- [134] Salghi R Shubhalaxmi-Jodeh S Algarra M Hammouti B Ali IH Essamri A Lgaz H, Subrahmanya Bhat K. "Insights into corrosion inhibition behavior of three chalcone derivatives for mild steel in hydrochloric acid solution". *Journal of Molecular Liquids*, 238:71–83, 2017.
- [135] A. Suhasaria P. Banerjee S. Satpati, S. K. Saha and D. Sukul. "Adsorption and anti-corrosion characteristics of vanillin schiff bases on mild steel in 1 M HCl: experimental and theoretical study". *RSC advances*, 10(16):9258–9273, 2020.

- [136] Ambrish Singh and Eno E Ebenso. "Use of glutamine as a new and effective corrosion inhibitor for mild steel in 1 M HCl solution". *Int. J. Electrochem. Sci.*, 8: 12874–12883, 2013.
- [137] Michel Bourin, Pierre Chue, and Yannick Guillon. "Paroxetine: a review". *CNS drug reviews*, 7(1):25–47, 2001.
- [138] Ashish K Singh, Sudhish K Shukla, MA Quraishi, and Eno E Ebenso. "Investigation of adsorption characteristics of n, n-[(methylimino) dimethylidene] di-2, 4-xylidine as corrosion inhibitor at mild steel/sulphuric acid interface". *Journal of the Taiwan Institute of Chemical Engineers*, 43(3):463–472, 2012.
- [139] RS Abdel Hameed, Gh MS Aleid, A Khaled, D Mohammad, Enas H Aljuhani, Saedah R Al-Mhyawi, Freaah Alshammary, and M Abdallah. "Expired dulcolax drug as corrosion inhibitor for low carbon steel in acidic environment". *International Journal of Electrochemical Science*, 17(6):220655, 2022.
- [140] A Ahmed, E Nazeer, and R Fouda. "Expired drug theophylline as potential corrosion inhibitor for 7075 aluminium alloy in 1M NaOH solution". *Chem. Intermed.*, 39:921, 2013.
- [141] G. Kishore Babu P. Ravisankar, C. Roja and K. Sai Rahul. "Validated UV spectrophotometric method for quantitative analysis of paroxetine in bulk and pharmaceutical dosage form". *Der Pharm. Lett.*, 8(3):254–260, 2016.
- [142] David Germann, George Ma, Feixue Han, and Anna Tikhomirova. "Paroxetine hydrochloride". *Profiles of Drug Substances, Excipients and Related Methodology*, 38:367–406, 2013.
- [143] B. Tan Y. Qiang, S. Zhang and S. Chen. "Evaluation of ginkgo leaf extract as an eco-friendly corrosion inhibitor of X70 steel in HCl solution". *Corrosion Science*, 133:6–16, 2018.
- [144] EM Attia. "Expired farcolin drugs as corrosion inhibitor for carbon steel in 1 M HCl solution". *Journal of Basic and Applied Chemistry*, 5(1):1–15, 2015.
- [145] F. E. Heakal A. S. Fouda and M. S. Radwan. "Role of some thiadiazole derivatives as inhibitors for the corrosion of C-steel in 1 M H₂SO₄". *Journal of applied electrochemistry*, 39:391–402, 2009.
- [146] V. Ramesh Saliyan and A. V. Adhikari. "Inhibition of corrosion of mild steel in acid media by N-benzylidene-3-(quinolin-4-ylthio) propanohydrazide". *Bulletin of Materials Science*, 31(4):699–711, 2008.

- [147] Khairia Mohammed Al-Ahmary et al. "Spectrophotometric determination of escitalopram in pharmaceuticals". *International Journal of Pharmaceutical Chemistry*, 2(4):121–125, 2012.
- [148] Priya Vashishth, Himanshi Bairagi, Rajni Narang, Sudhish K Shukla, and Bindu Mangla. "Thermodynamic and electrochemical investigation of inhibition efficiency of green corrosion inhibitor and its comparison with synthetic dyes on ms in acidic medium". *Journal of Molecular Liquids*, 365:120042, 2022.
- [149] Micha Peleg, Mark D Normand, and Maria G Corradini. "The arrhenius equation revisited". *Critical reviews in food science and nutrition*, 52(9):830–851, 2012.
- [150] Naresh Hiraram Choudhary, Manoj Shivaji Kumbhar, Deepak Annasheb Dighe, riti S Mujgond, and Meera Chandradatt Singh. "Solubility enhancement of escitalopram oxalate using hydrotrope". *International Journal of Pharmacy and Pharmaceutical Sciences*, 5(1):121–125, 2013.